Appendix A
Sediment Transport Technical Memoranda

A1 Coarse Sediment Transport Technical Memorandum

TECHNICAL MEMORANDUM

Date: July 9, 2024
To: Matt Dillin, Chehalis River Basin Flood Control Zone District
From: Paul DeVries, PhD, PE, CFP and Robert Schomp, MS, EIT, Kleinschmidt Associates
Cc: MaryLouise Keefe, PhD and Jason Kent, PE, PMP, Kleinschmidt Associates
Re: Evaluation of Potential Coarse Sediment Transport Impacts of FRE Operations on Chinook Salmon Spawning Habitat

Preface

Following the release of Draft Environmental Impact Statements (DEISs) by the Washington Department of Ecology and the United States Army Corp of Engineers for the proposed Flood Reduction Expandable Facility, the project's proponent, the Chehalis Flood Control Zone District (District) has undertaken more detailed technical studies to better understand the nature of potential project impacts to environmental resources. These studies have been undertaken to provide the basis for development of avoidance, minimization, and mitigation measures for the project. The transport of sediments within the Chehalis River was identified among potentially affected resources in the DEISs that could affect aquatic habitat. This technical memorandum describes a more detailed analysis of coarse sediment transport processes performed for the District than was available in the DEISs. It is a companion to separate technical memoranda that address fine sediment transport processes, salmonid spawning habitat availability, and salmonid spawning habitat scour risk. These technical memoranda are necessary for developing an understanding of the mechanisms affecting sediment transport and aquatic habitat sufficient for the District to formulate appropriate avoidance, minimization, and mitigation measures for the proposed project. These measures will be fully described in the District's forthcoming mitigation plan, which will incorporate the memoranda as technical appendices.

Executive Summary

This technical memorandum describes sediment transport analyses performed to improve understanding of coarse bedload erosion, transport, and deposition processes operating at reach scales in the upper Chehalis River basin, both with and without the proposed Flood Reduction Expandable (FRE) facility. This information is necessary to understand the feasibility of species and life-stage specific mitigation actions that would compensate for any impacts associated with effects of the facility on coarse sediment transport processes. Further, because of the limited habitat available for them in the upper river basin, the primary focus of the analyses described herein is on reach level dynamics that would affect the feasibility, location and potential sustainability of spawning habitat mitigation actions for Chinook salmon, and particularly for the spring run population.

Previous modeling completed as part of the National and State Environmental Policy Acts DEISs analyses relied on a one-dimensional (1D) Hydrologic Engineering Center River Analysis System (HEC-RAS) sediment transport model of long-term changes in the longitudinal riverbed profile. Impacts in the DEISs were qualified based on model output in terms of broad level effects of predicted aggradation of sediments associated with FRE operations. Sediments were evaluated as a total load, without distinguishing quantitatively between coarse and fine sediment deposition volumes, bedload and suspended load, or short-term vs. long-term effects. The resulting data was informative but not sufficient for developing species and reach-specific mitigation to potential operational impacts in terms of quantities and distribution of spawning gravels, or of entombment of existing spawning habitat. In addition, the DEISs' modeling framework involved a set of assumptions regarding sediment transport mechanics, the amount of sediment delivered to the channel network annually, and other aspects affecting predicted hydraulics and transport modeling. The nature of the assumptions applied in the DEISs' sediment transport modeling affected predictions of both long- and short-term aggradation and degradation. Interpretations of likely effects to Chinook salmon spawning habitat in the DEISs were accordingly constrained by the analysis' assumptions. To address this constraint, the District undertook extensive analyses identifying effects of FRE operations more specifically with respect to coarse sediments. The results of the analyses can then be used to determine appropriate avoidance, minimization, and mitigation requirements with respect to effects to Chinook salmon spawning habitat availability.

As part of the corresponding analyses undertaken by the District, the same HEC-RAS model and hydrology used in preparing the DEISs was applied in the following four ways:

1. Using the model's hydraulic predictions to characterize conditions when and where along the length of river different grain sizes are mobilized based on an incipient motion criterion;
2. Using the model's hydraulic predictions as input to an independent bedload transport equation (as opposed to the total load equation used in the DEISs' modeling) developed specifically for gravel bed rivers to evaluate sediment transport capacity along the length of river;

3. Repeating the same DEIS' framework for morphodynamic modeling of long-term changes in bed elevation along the length of river, but using different assumptions and parameterizations to evaluate sensitivity of the model predictions of bed elevation changes to the conditions imposed on it; and
4. Using the independent bedload transport equation to characterize upstream-downstream variation in sediment trapping efficiency in terms of net overall sediment transport rate imbalances between successive cross-sections (as opposed to predicting bed elevation changes over time as was performed for the DEISs).

Prior to performing these analyses, various features of the HEC-RAS model affecting hydraulic predictions were modified to better simulate flood hydraulics at smaller sub-reach (i.e., with respect to bankfull width) scales than were needed originally to predict larger scale flood extents below the proposed FRE facility. This included modifying channel roughness coefficients in the steeper, confined reaches upstream to be more representative of typical hydraulics in such channels, and distribution of velocities between the floodplain and channel in alluvial and unconfined reaches at smaller sub-reach scales.

The results of the additional modeling analyses indicated the following:

1. Review of the longitudinal elevation profile in the model indicates that the locations most likely to be associated with long-term deposition of spawning substrates is immediately below the large-scale slope break below Fisk Falls, and below the slope break at the head of the Pe Ell valley. These locations coincide with where greatest densities of Chinook salmon spawning have been noted historically, both in prior documentation and in more recent WDFW redd survey data. Consistent with this, the modeling results indicated reduced bedload transport capacity and greater stability of substrate sizes suitable for Chinook salmon spawning in the reaches below each slope break location.
2. Changing assumptions and parameterization of the DEISs' sediment transport model substantially changed predicted outcomes in terms of aggradation and degradation. Notable changes were predicted based on the sediment transport equation used, the amount of annual sediment loading, and whether and where degradation limits are specified. The HEC-RAS model formulation itself leads to predicting aggradation when sediment is added to the model, and even when it is not.
3. Over the large scale, the bedload transport capacity of the Chehalis River upstream of Elk Creek, where most Chinook salmon spawning occurs, is predicted to be sufficient along the length of the river to transport substrates suitable for spawning at the 2-year and other low magnitude, frequent flood levels, including substrates that may be temporarily deposited during FRE operations. When summed over a 100-year period, the 2-year flood peak transports cumulatively more sediment than the 100- and 10-year flood peaks combined. The risk of

starving spawning areas downstream of gravel supplied from upstream of the FRE inundation zone consequently appears to be low.

4. At smaller scales, bedload transport capacity is predicted to be extremely high upstream of Fisk Falls, in the vicinity of the proposed FRE facility location, and in the canyon reach downstream to the Pe Ell valley. These reaches were predicted following the DEISs' modeling framework to also have the greatest risk of aggradation both with and without FRE operations, which appears counterintuitive. The high sediment transport capacity is also associated with risk of scouring for redds that are constructed in those reaches under existing conditions.
5. Some simulation scenarios resulted in predicting less aggradation under the with-FRE condition than under current conditions, which stands in contrast with DEISs' conclusions regarding potential impacts.
6. Also counterintuitive, the DEISs' modeling framework predicted smaller and less variable aggradation in the two major spawning reaches (i) extending approximately 2.5 miles below Fisk Falls, and (ii) within the approximately 5-mile reach of the Pe Ell Valley, compared with their respective steeper reaches upstream.
7. Differences in long-term aggradation rates predicted following the DEISs' modeling framework were negligible for sand-sized particles between the with- and without-FRE operations scenarios. More aggradation was predicted under the with-FRE scenario for gravel-sized substrates in the next two miles downstream of the 2.5-mile key spawning reach below Fisk Falls, which could lead to increases in spawning habitat availability.
8. Aggradation was predicted to increase slightly over time in the upper Chehalis River overall for the climate change scenarios evaluated in the DEISs, and the with-FRE scenario was associated with less aggradation than the without-FRE scenario.

These results led to the following inferences:

1. The DEISs' modeling of potential effects of FRE operations to coarse sediment transport and deposition patterns in the mainstem was constrained by the selected model architecture, assumptions, and parameterization. Interpretations based on the HEC–RAS model developed for the DEISs could lead to incorrect conclusions about sediment impacts. There will be greater confidence identifying species and site-specific impacts, and appropriate mitigation based on multiple independent, consistent lines of evidence.
2. The lines of evidence based on the additional analyses performed here suggest that potential effects of FRE operations on coarse sediment transport processes may manifest most significantly via deposition within the HEC-RAS model's river mile (RM) 110-112 reach within the inundation zone. Changes in sediment transport dynamics do not appear significant in the vicinity of or downstream of the proposed FRE location, or upstream of Fisk Falls.
3. Given the high shear stresses and corresponding large sediment transport volumes during high flows, and the negligible difference predicted for long-term sand aggradation whether or not the FRE is operated, the river appears to have more than sufficient capacity to move all fine

sediments that may accumulate in the channel within the inundation zone downstream after an operation event.

4. Long-term distribution and availability of mainstem spawning habitat within the inundation zone and downstream may be controlled overall by infrequent, large magnitude hydrologic events triggering extensive landslide activity throughout the basin, followed by evacuation of in-channel deposits downstream.
5. Survival to emergence may be limited by scour at larger peak flows as controlled by size of gravel deposit, location in the channel, and the temporal balance between episodic sediment supply and transport.

Background

The Chehalis Basin Flood Control Zone District (District) is proposing to construct a Flood Reduction Expandable (FRE) facility to reduce the risk of flood damage along the mainstem Chehalis River. The proposed FRE facility is located approximately 1.7 miles upstream from the city of Pe Ell, Washington in the upper Chehalis River watershed (Figure 1). The primary purpose of the FRE facility is to reduce flooding coming from the Willapa Hills by storing floodwaters in a temporary reservoir during extreme flood events. In 2020, the two draft Environmental Impact Statements (DEISs) released for this project (the Washington Department of Ecology's [Ecology] under the State's Environmental Policy Act and the United States Army Corps of Engineers' [Corps] under the National Environmental Policy Act) projected that by temporarily storing peak flows during major or catastrophic flood events, the FRE facility operations would alter sediment transport and deposition processes and thereby impact channel forming processes and spawning habitat quantity and quality. This, in turn, was hypothesized to impact reproductive success of fish species relying on spawning habitat within the potential reservoir footprint and downstream (Ecology 2020; Corps 2020). Impacts were generally represented as occurring upstream of Elk Creek (around river mile [RM] 100).

While fall Chinook salmon (*Oncorhynchus tshawytscha*), coho salmon (*O. kisutch*), and steelhead (*O. mykiss*) are all found in the basin and have segments of their populations that are mainstem spawners, the DEISs expected spring Chinook salmon populations to suffer the greatest potential impact on spawning habitat. This was largely due to their restricted distribution as compared to other salmonid species in the basin. In the upper Chehalis basin, both spring and fall Chinook salmon spawn predominantly in the mainstem, with greatest concentrations of redds noted in the first two miles below Fisk Falls and within a four-mile reach of the Pe Ell valley reach below where the river exits the Willapa Hills (Washington Department of Fish and Wildlife [WDFW] electronic data for 2015-2021 received from Ecology; Phinney et al. 1975; WG and Anchor 2017; Ferguson et al. 2017; Ronne et al. 2020; Figure 2). There are few tributaries large enough in the basin with sufficient gravel deposits to provide spawning habitat for Chinook salmon and they are primarily located downstream of the proposed location of the FRE. Steelhead and coho salmon spawn more extensively than Chinook salmon in tributary habitats most of which would not be influenced by FRE operations (Ronne et al. 2020). In addition, there would likely be more locations and opportunities to mitigate for impacts to those two species by providing access to disconnected spawning habitats than there would be for Chinook salmon. Thus, the focus for mitigation of sediment impacts to mainstem spawning habitat will be most important with respect to Chinook salmon.

Figure 1
Map of Chehalis River Study Reach, Including Location of Important Landmarks Indicated in This Technical Memorandum.

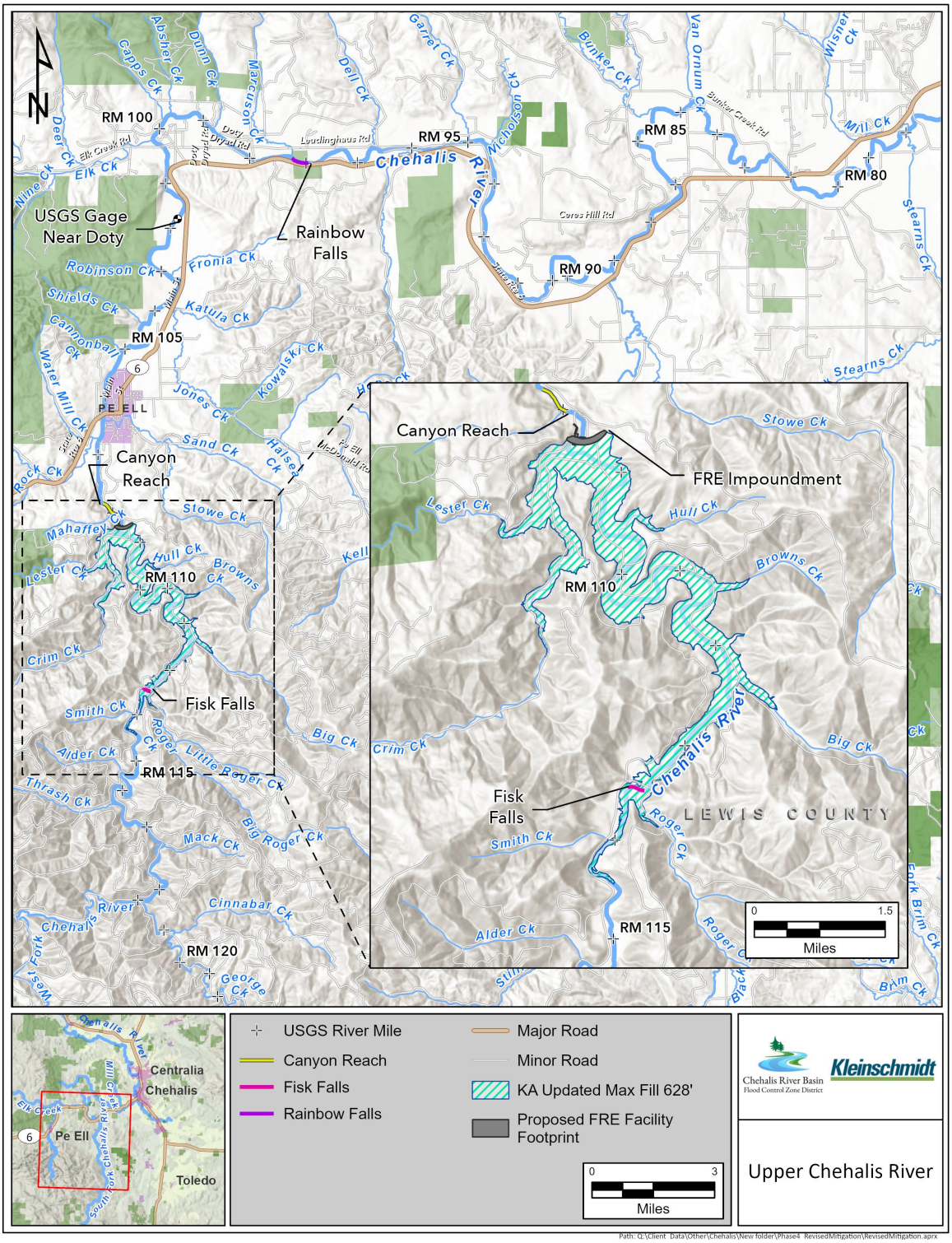

Figure 2
Redd Numbers Counted in Four Reaches of the Mainstem Chehalis River Between the Newaukum River and the West Fork-East Fork Confluence Each Year from 2017-2020. Data Were Not Collected Downstream of RM 103 in 2019 and 2020 ("ND").

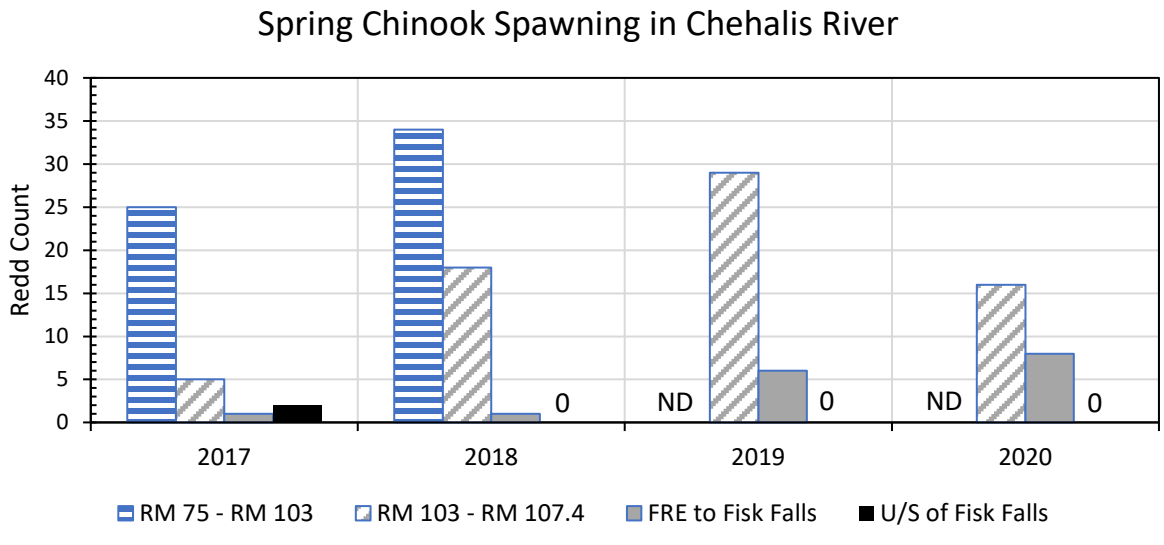

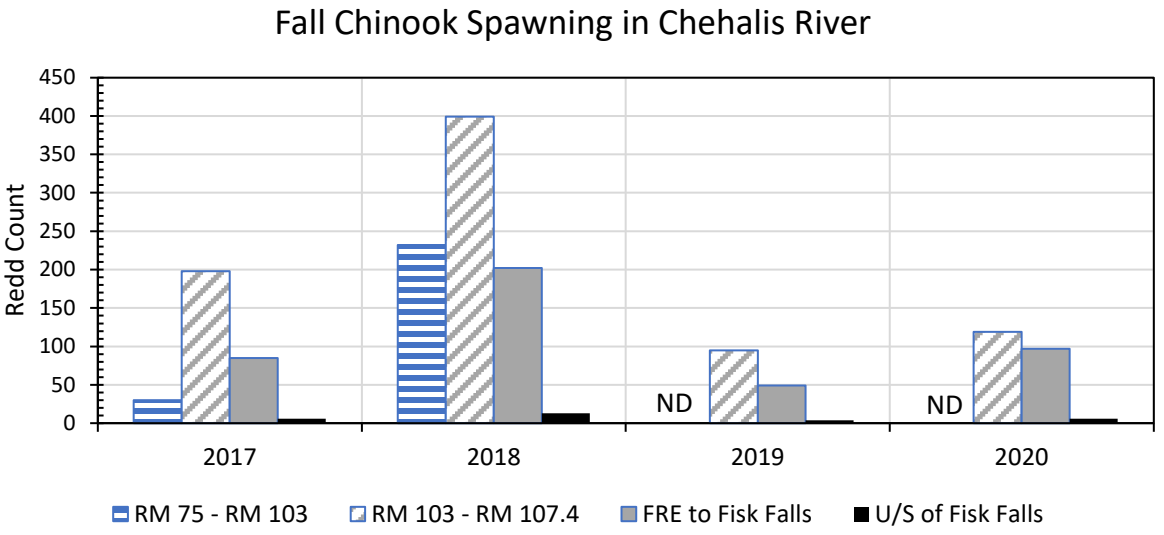

The DEISs indicated a potential for changes to sediment transport rates and grain size within and downstream of the facility to have direct impacts on Chinook salmon spawning, but provided limited descriptions of relevant mechanisms and context. The DEISs' simulation results were interpreted as predicting a net increase in total coarse and fine sediment stored upstream of the facility and a net decrease downstream, with potential impacts identified primarily upstream of Elk Creek. The amount of sediment accumulated within the inundation zone was projected to increase in the downstream

direction after major flood events. These modeled changes in sediment storage were then taken to represent significant adverse impacts.

Specificity was missing in terms of the DEISs' analysis of aquatic habitat changes associated with coarse vs. fine sediment deposition and transport, and how each size fraction may affect spawning habitat suitability. In the case of coarse sediments, the most direct implication inferred from the DEISs is that in years when the FRE operates, spawning habitat availability would be reduced overall because suitably sized gravel and cobble transported as bedload during extreme flood events would be trapped in excess near the head of the temporary reservoir, and prevented from resupplying suitably sized gravels and cobbles in spawning habitat downstream of the FRE.

The Ecology (2020) DEIS also projected that "cobble, gravel, and coarse sand would be deposited in the reservoir area where the mainstem Chehalis River meets Crim Creek, Lester Creek, Big Creek, Roger Creek, and Thrash Creek." This statement suggests that the tributaries are supplying gravel and cobble substrates that are currently transported downstream instead of forming localized deposits at each confluence. The importance of this was not explained in the DEIS, but it is inferred here that the concern is that such deposits might form temporarily, and if used by spawning salmon after the reservoir drops again, be scoured out if a smaller, successive competent flood flow occurs during the incubation period. Smith and Wenger (2001) noted that spawning gravels were limited in quantity in these tributaries, however. The degree of impact of coarse sediment deposition to spawning success may thus be negligible because the quantities deposited are likely to be small in most years except in years following major landslide events (see Section 4).

There were various attributes of the DEISs' sediment transport model that confound drawing definitive conclusions regarding impacts based on the results of the model. For example, the Hydrologic Engineering Center's River Analysis System (HEC-RAS) model used for the DEISs involves specific algorithms, options, and assumptions regarding input loading, transport rates, routing of bulk vs. specific grain sizes, and the evolution of cross-section profiles that result in highly uncertain predictions that may not resemble what would likely occur. The model output can also be difficult to interpret with respect to discerning an impact. For example, the size of material deposited was calculated to vary widely within the reservoir footprint, coarsening at some locations and fining at others without a clear spatial pattern or trend evident.

More detailed and diverse analyses were needed in the context of a physical and biological process-based, weight of evidence approach before the appropriate level of mitigation and locations for such measures could be ascertained. This includes examining model capabilities and limitations. It will be particularly important to distinguish between whether FRE operation will have a certain physical effect, and whether that effect translates at a sufficient level to an impact on salmon or their habitat through a specific mechanism. In other words, just because an effect has the potential to occur does not automatically equate to it being likely to adversely affect salmon spawning habitat.

The HEC-RAS model used in the DEISs was accordingly revisited. The input data, hydraulic predictions, and behavior of the sediment transport module programmed into the model were reviewed. The model was re-run and the output analyzed in alternative ways to better evaluate the weight of evidence. The same HEC-RAS model and hydrology used in preparing the DEISs was applied in the following four ways:

1. Characterizing conditions when and where along the length of river different grain sizes are mobilized based on an incipient motion criterion;
2. Using an independent bedload transport equation (as opposed to the total load equation used in the DEISs' modeling) developed specifically for gravel bed rivers to evaluate sediment transport capacity along the length of river;
3. Using different assumptions and parameterizations in the DEISs' model to evaluate sensitivity of the model predictions of bed elevation changes to the conditions imposed on it; and
4. Characterizing upstream-downstream variation in sediment trapping efficiency (as opposed to predicting bed elevation changes over time as was performed for the DEISs).

This memorandum describes these analyses and synthesizes the results in an independent assessment of potential effects and impacts on spawning habitat availability.

Methods

The following four analytical approaches were taken to evaluate and identify sediment transport and deposition patterns that might be associated with FRE operations, with a primary focus on characterizing the likely fate and disposition of coarse sediments used by spawning Chinook salmon in the mainstem Chehalis River:

- Calculating incipient motion conditions for grain sizes used for spawning and characterizing spatial variation in substrate stability from upstream to downstream;
- Calculating sediment transport capacity at the 2-, 10-, and 100-year flood levels, characterizing spatial variation in capacity from upstream to downstream, and evaluating effective capacity in the sense of Wolman and Miller (1960);
- Repeating and expanding on the same type of analysis and 30-year hydrograph forming the basis of the DEISs' conclusions, and evaluating the sensitivity of the model to different assumptions and model options involving sediment loading, bed scour simulation, and sediment size; and
- Evaluating upstream to downstream variation in reach scale aggradation-degradation tendency as represented by sediment trapping efficiency summed over a 50-year period, using a bedload transport equation developed specifically for gravel-sized material.

Each of these approaches provided an alternative indication of the extent to which operation of the FRE would be likely to materially affect the long-term availability of spawning habitat. Potential short-term effects may be inferred from the results as well. All four approaches necessitated first reviewing the model geometry, hydrology, and parameterization. Some modifications were made to the model

parameterization based on hydraulic engineering judgment. In addition, selected new cross-sections were interpolated between existing cross-sections, or inserted using new field survey data. Methodological details are provided in the following sections regarding model review and modification, and the four analysis approaches.

HEC-RAS Model Review and Modification

For consistency, the same one-dimensional (1D) version 5.0.7 HEC-RAS hydraulic and sediment transport model, peak flow hydrology, and grain size distribution data developed and analyzed for the DEISs were used. Electronic copies of the most recent model geometry, hydrologic, and hydraulic files used for the DEISs and described in WG and Anchor QEA (2017) and Ecology (2020) were provided by Anchor QEA in 2022. Model review and modification involved the following elements:

1. Refining inflow hydrology, including inspecting the 30-year daily flow time series evaluated in the DEISs and extracting numbers from the unsteady flow files provided with the model to create steady flow files for modeling selected flow duration quantiles and flood recurrence intervals;
2. Reviewing how the DEISs' proposed operation of the FRE facility influenced flow levels downstream and water levels upstream;
3. Inserting additional surveyed and interpolated cross-sections to the model;
4. Adjusting hydraulic parameters, such as Manning's *n* roughness coefficients and ineffective flow area specifications to improve model hydraulics; and
5. Reviewing grain size distributions specified in the model.

These elements are each described below.

Inflow Hydrology

Streamflow has been measured at a long-term United States Geological Survey Gaging Station (USGS #12020000, Chehalis River near Doty, Washington) located near RM 101.8[1] in the DEISs' HEC-RAS model. This location corresponds approximately to the expected downstream extent of gravel transport-related effects of FRE operations in the DEISs, and is downstream of the majority of Chinook salmon spawning activity. It is thus conveniently located for verifying and refining hydrology estimates needed for this analysis. The USGS gage downstream (Station #12027500, Chehalis River near Grand Mound, Washington) relied on for initiating operations of the FRE facility is influenced also by flows from the

[1] RM references in this report are as defined in the HEC-RAS model relied on by the DEIS. The value given may differ from RMs determined by USGS that Kleinschmidt has generally followed.

South Fork Chehalis, Skookumchuck, and Newaukum rivers, which can have peak flows that are not always synchronized with sediment transporting peak flows in the upper Chehalis River.

We relied primarily on hydrology determined previously for the DEISs and contained in the HEC-RAS model flow files. The model was originally calibrated using data from five USGS stream gaging stations in the upper Chehalis River basin (Hill and Karpack 2019). Flow files that came with the model included the following:

- A 30-year flow record was created for the DEISs' model using historical data from the Chehalis River basin from October 1, 1988 through September 30, 2018. Flow was divided into 24 different input locations based on respective drainage areas. The input inflows represented inflow at the upstream ends of the reaches, point source inflows at tributary junctions, and local accretion flow which was simulated as a uniform line source. A 1-day time step was used for lower flow conditions (approximately less than 2,000 cubic feet per second [cfs] at the Doty gage), and a 1-hour time step for higher flows. Results from a reservoir simulation model were used in the original model development to obtain hourly reservoir inflow, outflow, and reservoir water surface elevations for each event in the 30-year time series when the FRE facility would have operated and impounded water. These data were used to anticipate the necessary gate openings to calculate the proposed reservoir elevation at each time step, and to assess the effects of water impoundment or release on the flow downstream of the FRE facility (Hill and Karpack 2019).
- The 2009 flood event was selected in the DEISs to represent a major flood scenario where the FRE facility would be operated as proposed. A major flood was defined as a flow of 38,800 cfs or greater in the mainstem Chehalis River as measured at the Grand Mound gage. In the DEISs, the 2009 flood event was considered a 7-year flood event at the Grand Mound gage under current conditions, 5-year flood event under mid-century (2030-2060) conditions, and 4-year flood event under late-century (2060-2080) conditions.

Steady flow files were also developed specifically for this analysis from the unsteady flow files contained within the provided HEC-RAS model, by extracting and apportioning flow data from point sources (upstream boundary flow hydrographs and lateral inflow hydrographs) and distributed sources (uniform lateral inflows). Two sets of steady flows were developed as follows:

- Peak flow magnitudes were derived approximately for the 2-, 10-, and 100-year flood frequency events for evaluating incipient motion conditions and sediment transport capacity. A time step was identified in the DEISs' 30-year time series flow file when the flow at a model cross-section at the Doty gage corresponded approximately to the respective flood frequency estimates developed for the DEISs. The resulting flows were used to evaluate incipient motion and sediment transport capacity.
- Steady flows were also developed for use in evaluating upstream-downstream variation in sediment trapping efficiency, where the daily flow duration curve was approximated by a series

of incremental steps with a given duration for each flow level over a 50-year period. Discharge rates were specified to cover the range over which most bedload transport occurs, between the 5% exceedance flow, which approximates the onset of substantial bedload transport in gravel bed rivers (e.g., Richards 1982; Schmidt and Potyondy 2004), to the 50-year flood event. This range is considered representative of the main geomorphically effective natural flow regime (Wolman and Miller 1960). The 2-, 10- and 100-year flood peak flow estimates were used to interpolate peak flows at other intervening recurrence intervals. Mean daily exceedance flows were also computed from the period of record for the USGS gaging station at Doty. Eleven representative flow magnitudes were developed (Figure 3; Table 1). Each flow was assigned a representative duration over the 50-year period such that the number of days added up to 913 (equivalent to ~5% of a 50-year period). Because the DEISs' hydrology does not fully match the mean daily flow statistics at the Doty gage, the number of days for each level was determined iteratively while attempting to match the cumulative flow volume underneath the curve and resemble the shape of the flow duration curve at the Doty gage approximately.

The HEC-RAS model also included flows that were developed for the DEISs to represent potential future conditions in 2030-2060 and 2060-2080 pending climate change. Those flows were simulated as well as part of the evaluation of model sensitivity.

Figure 3
Eleven Cumulative Steady Flows Along the Mainstem Chehalis River for the 50-year Bedload Transport Sediment Trapping Efficiency Calculations.

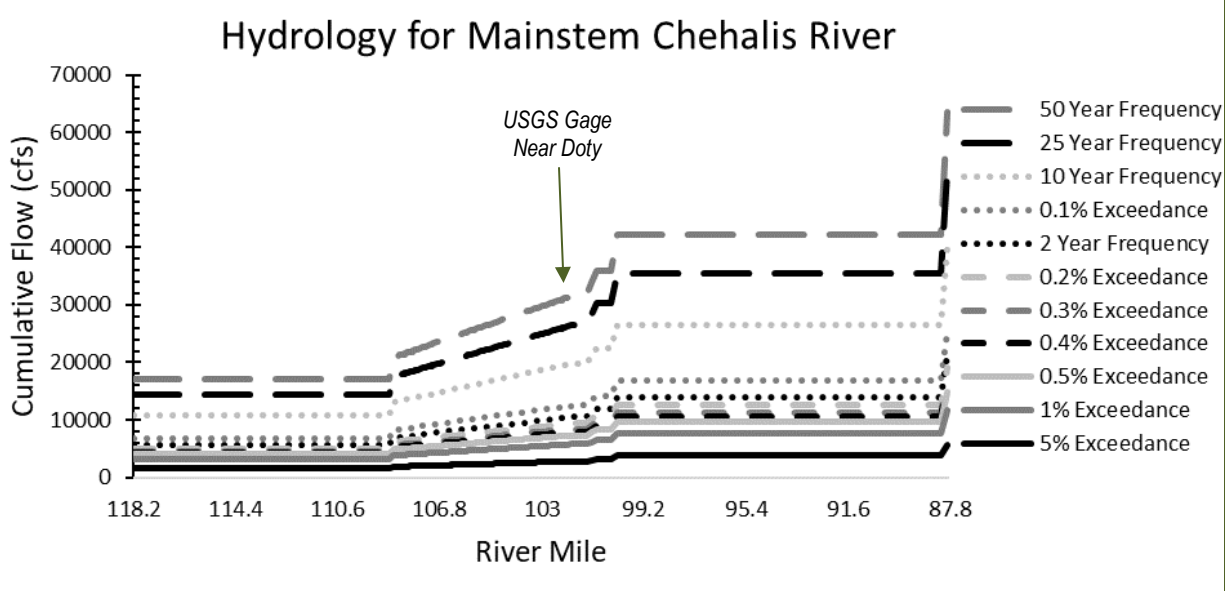

Table 1

Simulation Flows for Which Shear Stresses Were Computed in the Sediment Transport Analysis. The Flows Were Derived Using Data Extracted from the DEISs' HEC-RAS Model, Not Gage Data. The Resulting Predicted Total Transport Rate Over the Active Channel Bottom Was Multiplied by the Duration and Summed Across Flows.

HEC-RAS PROFILE NAME	PERCENT EXCEEDANCE	DURATION (DAYS)	MODEL FLOW (CFS)			
			PROPOSED FRE FACILITY	HWY 6 BRIDGE IN PE ELL	DOTY USGS STREAM GAGE	S. FK CHEHALIS CONFLUENCE
PF1	5	467	1,857	2,145	2,791	5,656
PF2	1	293	3,833	4,426	5,760	11,672
PF3	0.5	59	4,862	5,616	7,308	14,808
PF4	0.4	37	5,242	6,054	7,879	15,965
PF5	0.3	20	5,597	6,464	8,412	17,045
PF6	0.2	14	6,238	7,205	9,376	18,999
PF7	0.14 (~2-yr flood)	10	6,976	8,057	10,485	21,246
PF8	0.1	7	8,328	9,619	12,517	25,341
PF9	~0.03 (10-yr flood)	4	13,167	15,207	19,790	39,994
PF10	~0.01 (25-yr flood)	1	17,645	20,378	26,520	53,444
PF11	~0.005 (50-yr flood)	1	21,032	24,290	31,611	63,618

Simulating FRE Facility Operations

In repeating and expanding on the simulations relied on by the DEISs, it was necessary to simulate gate operations at the FRE facility controlling flows downstream and water levels upstream. The same initial conceptual set of operation rules applied in the DEISs were followed (Figure 4), where the FRE facility would operate when a major or greater flood is predicted, filling the temporary reservoir approximately 48 hours before the predicted flow rate reached 38,800 cfs at the Grand Mound gage (USGS Station #12027500). Flow through the FRE facility gate opening would be reduced to 300 cfs until the peak flood level is reached. Once the flood risk has passed, the drawdown process would begin over an approximately 32-day period when filled to maximum capacity. The proposed maximum outflow during drawdown would be limited to 5,000 to 6,500 cfs, which correspond to roughly the 0.4 and 0.2 percent exceedance flows, respectively, and approximate the annual flood.

Within the HEC-RAS model, the reservoir water surface elevation is controlled by simulating the FRE facility's gate opening height to match target reservoir water surface elevations. Drawdown is continued in the model until the temporary reservoir is emptied, whereupon the Chehalis River is effectively returned to a free-flowing state. In the development of the DEISs, the model was run for several time periods around peak flow events in 1990, 1991, 1996, 2007, and 2009 to check for model stability and calibrate gate openings to target reservoir elevations at each time step (WG and Anchor 2017). The model contained gate opening time series specific to each flow time series that were calibrated to fill the reservoir to a targeted water surface elevation for each timestep. As an artifact of the HEC-RAS model's internal workings, the calibrated gate openings necessitated manual editing of the flow files that involved artificially 'removing' flow from the model just downstream of the FRE facility to ensure that flow released from the gated opening was consistent with the proposed reservoir operation rules. The years when the FRE was simulated as operational are depicted in Figure 5. Figure 6 depicts the corresponding effect of gate operation simulated downstream of the FRE facility as represented by flows at the USGS Doty gage, using the HEC-RAS model to simulate the 2009 flood event. Figure 7 depicts representative changes in the water surface profile within the vicinity of the FRE and impounded reach for the simulated January 2009 event, with the reservoir filling and emptying at rates emulating the proposed operations in Figure 4.

Figure 4
FRE Facility Operations Proposed in the DEISs (figure from Ecology 2020).

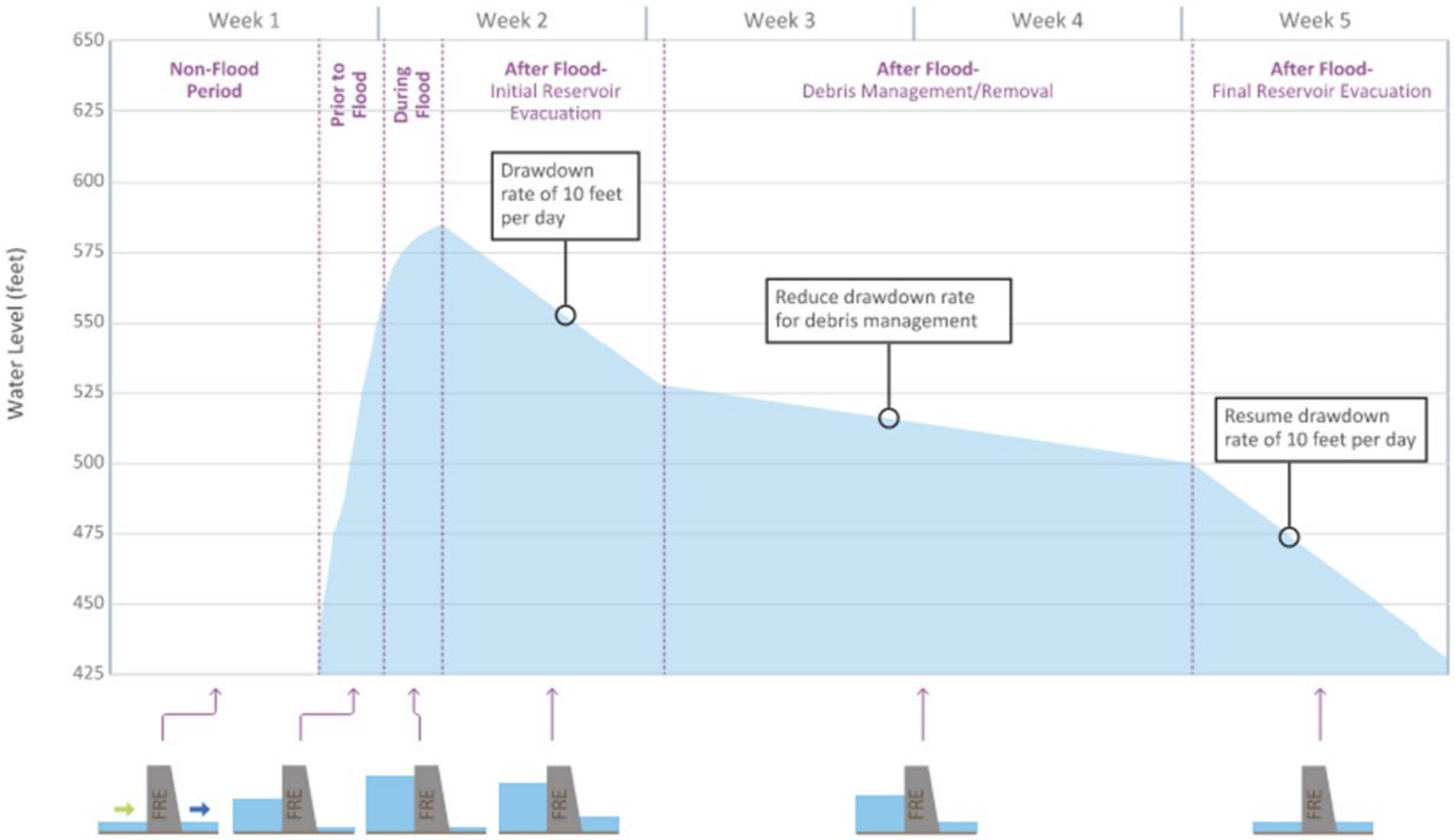

Figure 5
Comparison of Modeled Hydrographs of the 30-year Flow Time Series, with- vs. without-FRE Operation As Depicted in Figure 4.

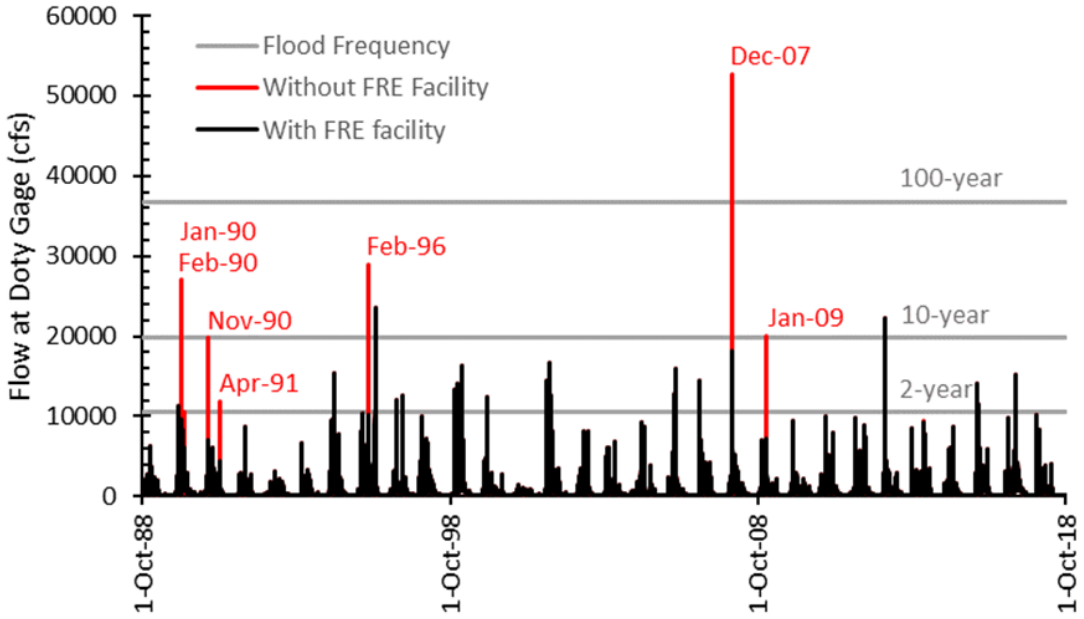

Figure 6
Comparison of Modeled Hydrographs of the January 2009 Flood Event, with- vs. without-FRE Operation As Depicted in Figure 4.

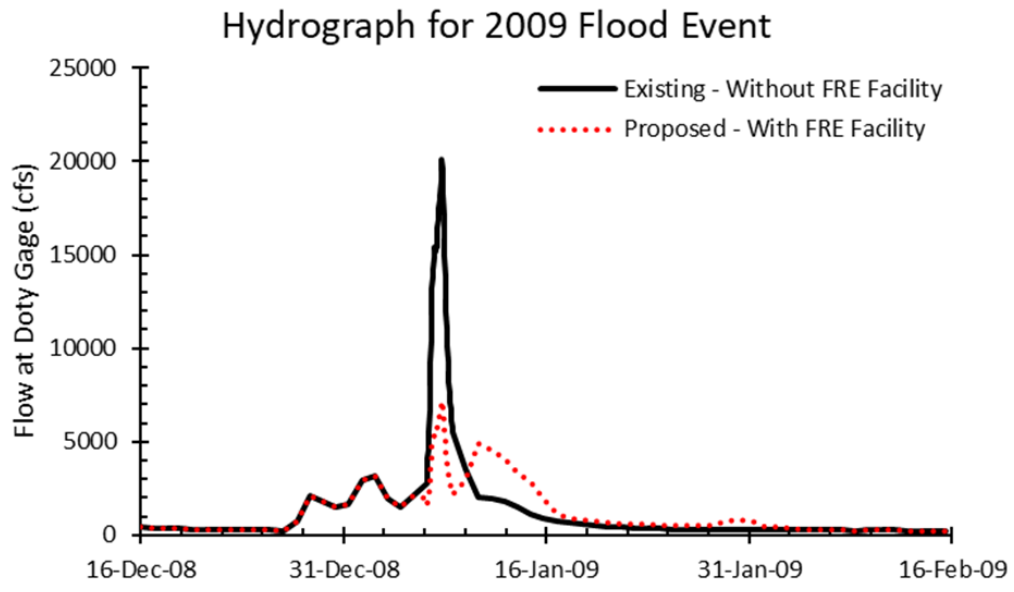

Figure 7
Simulated Water Surface Elevations (WSEs; blue line) in the Vicinity of the FRE and Impounded Reach During the January 2009 Event, Starting Approximately Two Days Before a Predicted Major Flood at Grand Mound Gage (USGS Station #12027500). Gate Begins to Close and Flow Reduced to 300 cfs, Reservoir Fills with Continued 300 cfs Release, Followed by Draining After Peak Passes.

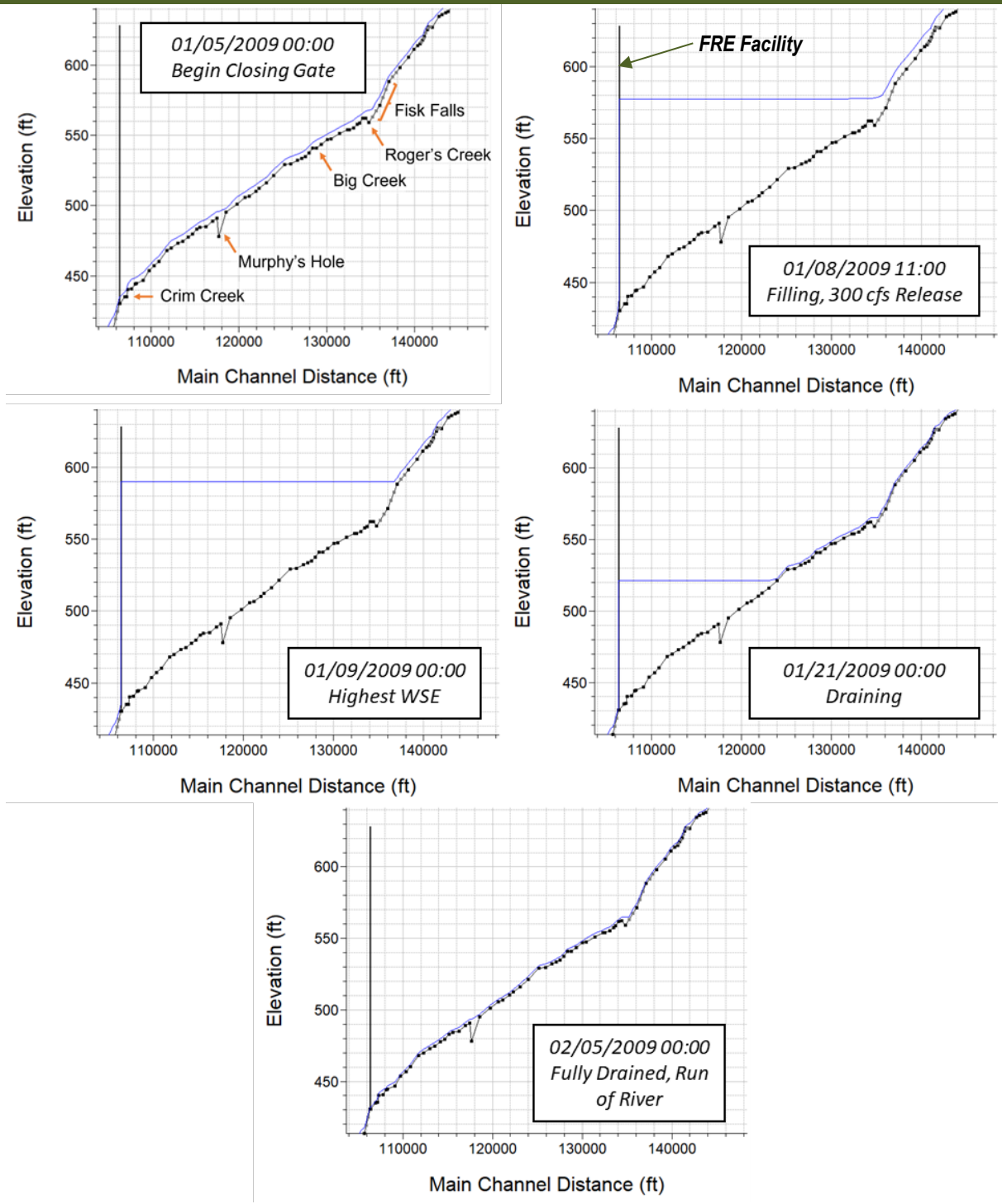

Inserting Surveyed and Interpolated Cross-Sections

The spatial resolution of the HEC-RAS model was first increased at selected locations where cross-section spacing was considered relatively large by adding interpolated cross-sections in the mainstem Chehalis River (Figure 8). This helped improve the model's computational stability by decreasing energy losses between more closely-spaced cross-sections. Cross-section bathymetry was also surveyed at selected locations as part of other field data collection efforts in 2022 using a combination of real time kinetic global positioning satellite and a total station in the vicinity of RMs 89, 102.2, and 102.4 (Figure 8). Cross-sections were also surveyed using a total station in the vicinity of RM 89.6 and their approximate locations were judged visually in the model geometry in relation to landmarks on georeferenced aerial photographs; The bathymetry data were supplemented with floodplain topography cut from the terrain in the HEC-RAS model using RAS-Mapper.

Adjusting Hydraulic Parameters

Bank and Sediment Bed Station Adjustments

The HEC-RAS model relied on by the DEISs had left and right bank station breaks specified near the top of bank. This is a common practice in HEC-RAS hydraulic modeling and is done to reflect locations where Manning's *n* roughness coefficients typically change between channel and floodplain. For sediment transport analyses outside of the HEC-RAS program, however, it is more convenient for post-processing to define the left and right bank stations to correspond approximately to the edges of the active bedload transport zone (Figure 9). These edges were previously defined in HEC-RAS's sediment transport module for the DEISs' simulations, and so the same values were used for parameterizing the cross-section geometry. HEC-RAS then would automatically calculate average channel bottom shear stress over the active bed width for use in calculating incipient motion, transport capacity, and aggradation-degradation tendency over the same area of stream bottom as the sediment transport modeling that was performed for the DEISs.

Figure 8
Map of Cross-section Locations in the HEC-RAS Model, with Different Colors Distinguishing Between Those That Were Originally in the DEISs' Simulations (green), and Those That Were Interpolated (pink) or Surveyed Later in 2022 by Kleinschmidt (red).

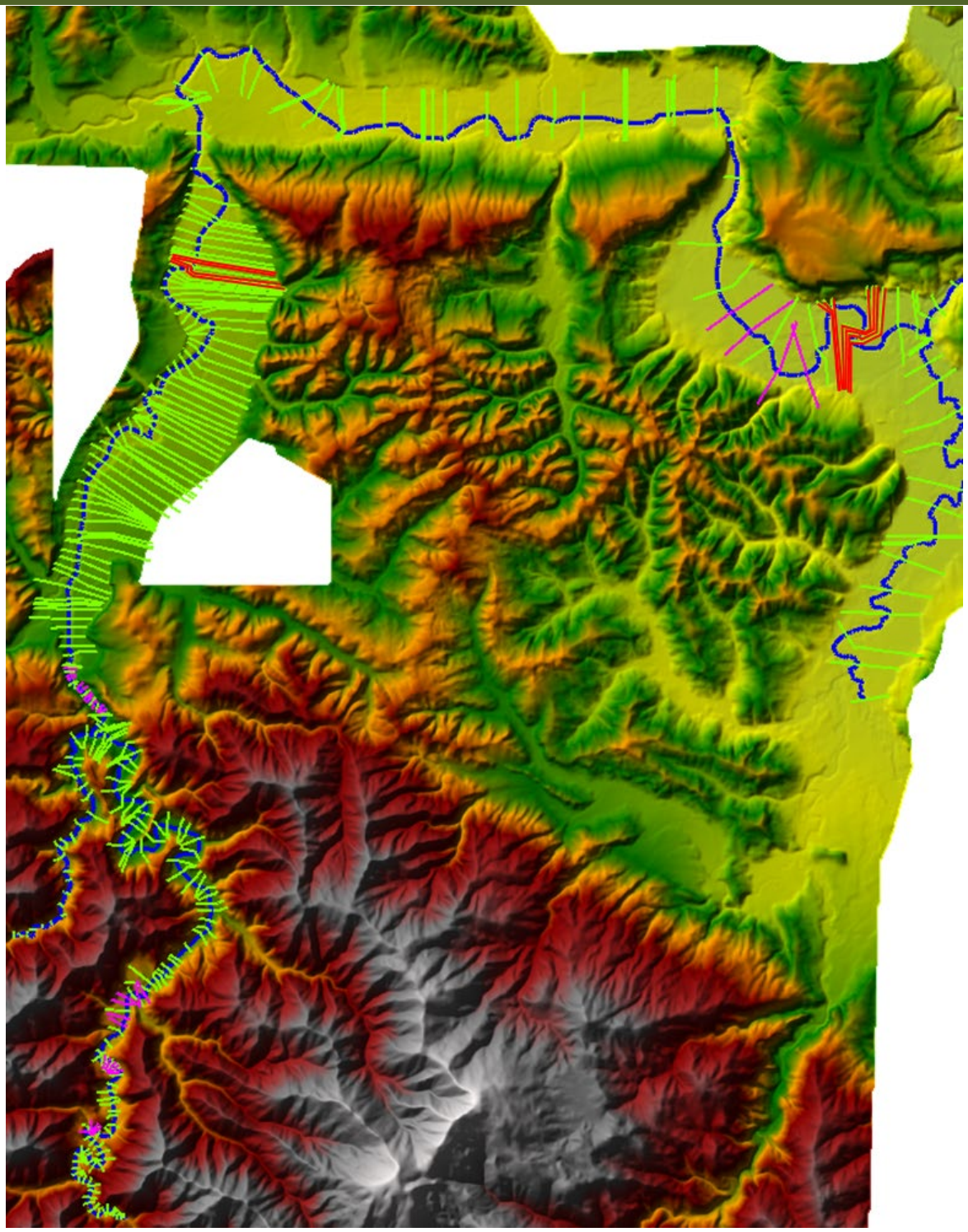

Figure 9
Schematic Depiction of Shifting of Left and Right Bank Station Locations in the HEC-RAS Model to Delimit the Width of Active Riverbed Where Coarse Bedload Transport Was Simulated to Occur.

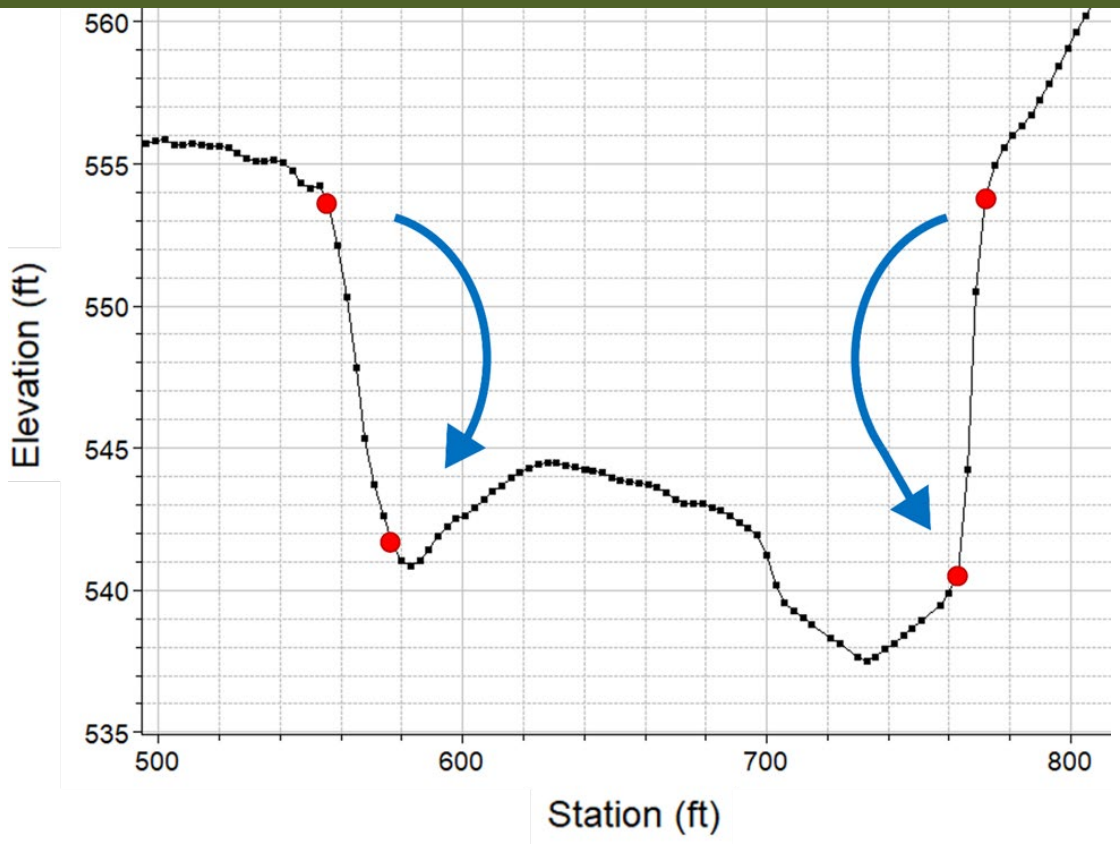

Manning's n Roughness Coefficients

Values of the Manning's *n* roughness coefficient in the HEC-RAS model provided to Kleinschmidt, which control predicted water levels, had been calibrated by comparing simulated water surface elevations to observed high water mark data, in which prediction errors were approximately normally distributed about a zero mean, with roughly 95 percent of errors distributed within +/- 3 feet (Elliot and Karpack 2014). A Manning's *n* value of 0.035 was used between RM 110.18 and RM 113.89 where the bed material was predominantly mobile, and the bed slope was generally flatter. A Manning's *n* value of 0.045 was used elsewhere between RM 108 and RM 118 based on the mixed bedrock/alluvial reaches being generally steeper. Manning's *n* was set to 0.05 from RM 107.33 to RM 100.43 and 0.045 elsewhere between the FRE facility and the confluence with the South Fork Chehalis River.

Our review of model velocities and Froude numbers indicated that mainstem Manning's *n* values were too low in the vicinity of and upstream of the FRE. Predicted Froude numbers were higher and closer to the transition between sub- and supercritical flow depths, with correspondingly high frequency spatial fluctuations in the predicted flood water surface elevation profiles that are symptomatic of unstable

conditions near critical depth. The resulting revised Manning's *n* roughness coefficients varied from 0.045 to 0.07 along the mainstem of the Chehalis River from its source to where it meets the South Fork. The changes resulted in predicting smoother water surface elevation profiles in the upper reach, and Froude numbers closer to typical values published in the geomorphic literature (e.g., Wohl et al. 1999; Wilcox and Wohl 2007; Comiti et al. 2007).

The mainstem Manning's *n* values downstream of the FRE to the Newaukum River confluence were also simplified where the cross-channel distribution of Manning's *n* values was reduced to fewer breaks particularly in the overbank regions (see example given in Figure 10). Manning's *n* values were assigned to different land cover types as follows: 0.08 for forested or logged areas, 0.025 for dirt/improved roads, 0.06 for the Chehalis River channel upstream of the FRE facility, 0.07 for the Chehalis River channel just downstream of the FRE facility in the steep canyon section, 0.045 for the Chehalis River channel below Pe Ell, 0.05-0.06 for fields/grassland which deviates from Chow 1959, and 0.09-0.11 for areas with buildings/structures. The use of a higher Manning's *n* value for fields/grassland accounted for roughness effects of small structures, low rock walls, sporadic trees, farming equipment, and structures.

Tables are presented in Attachment 1 that compare the specified Manning's *n* values of the DEISs' and modified models.

Ineffective Flow Areas

Ineffective flow area assignments were reviewed and adjusted at cross-sections where the model appeared to be underpredicting velocities in the main channel during the 100-year flood. The cause was determined to be an over-estimation of floodplain flow capacity at extreme flood levels, which is typically an artifact of using one-dimensional models to simulate overbank flows across more complex floodplains where the flow direction is not necessarily perpendicular to the cross-section and there are various impediments to flow between cross-sections that are not captured by the model geometry. In such instances, actual floodplain conveyance can be reduced substantially by flow impediments and changing topography between cross-sections. One way to model the reduced overbank conveyance is to specify ineffective flow areas, which is an option within 1-D HEC-RAS models. Ineffective flow areas are specified to represent portions of the wetted cross-section area in which water will pond with a velocity that is substantially less than if the water were flowing freely from upstream, such that this water is not included in calculations of the active flow area. Many alluvial floodplain areas of the Chehalis River appear to effectively pond water locally because of topographic high points between the main channel banks and the ponded area of the floodplain, or have a reduced volume of water flowing over them than would otherwise be calculated by HEC-RAS because the portion of upstream cross-section(s) with water routed towards them have less conveyance. Both cases result in a lower volumetric flow rate over the floodplain at a cross-section than would be predicted if the ineffective flow option is not used or is specified in a way that does not sufficiently represent the effects of reduced overall flow over the floodplain. As a result, predicted main channel velocities can be underestimated. Cross-sections where

this appeared to be occurring were compared against the LiDAR terrain topography, and the ineffective flow geometry was modified accordingly.

Tables are also presented in Attachment 1 that compare the resulting ineffective flow geometries with those specified in the DEISs' model.

Figure 10
Example of Cross-section Distribution of Manning's *n* Roughness Coefficients in Original (top) and Modified (bottom) HEC-RAS Model for a Transect at RM 109.87. Transect Includes Forested Areas (0.08), a Maintained Dirt Road (0.025), and the Mainstem Chehalis River Channel Bed (0.06). This Transect Is Located Approximately 1.5 Miles Upstream from the proposed FRE Facility Site.

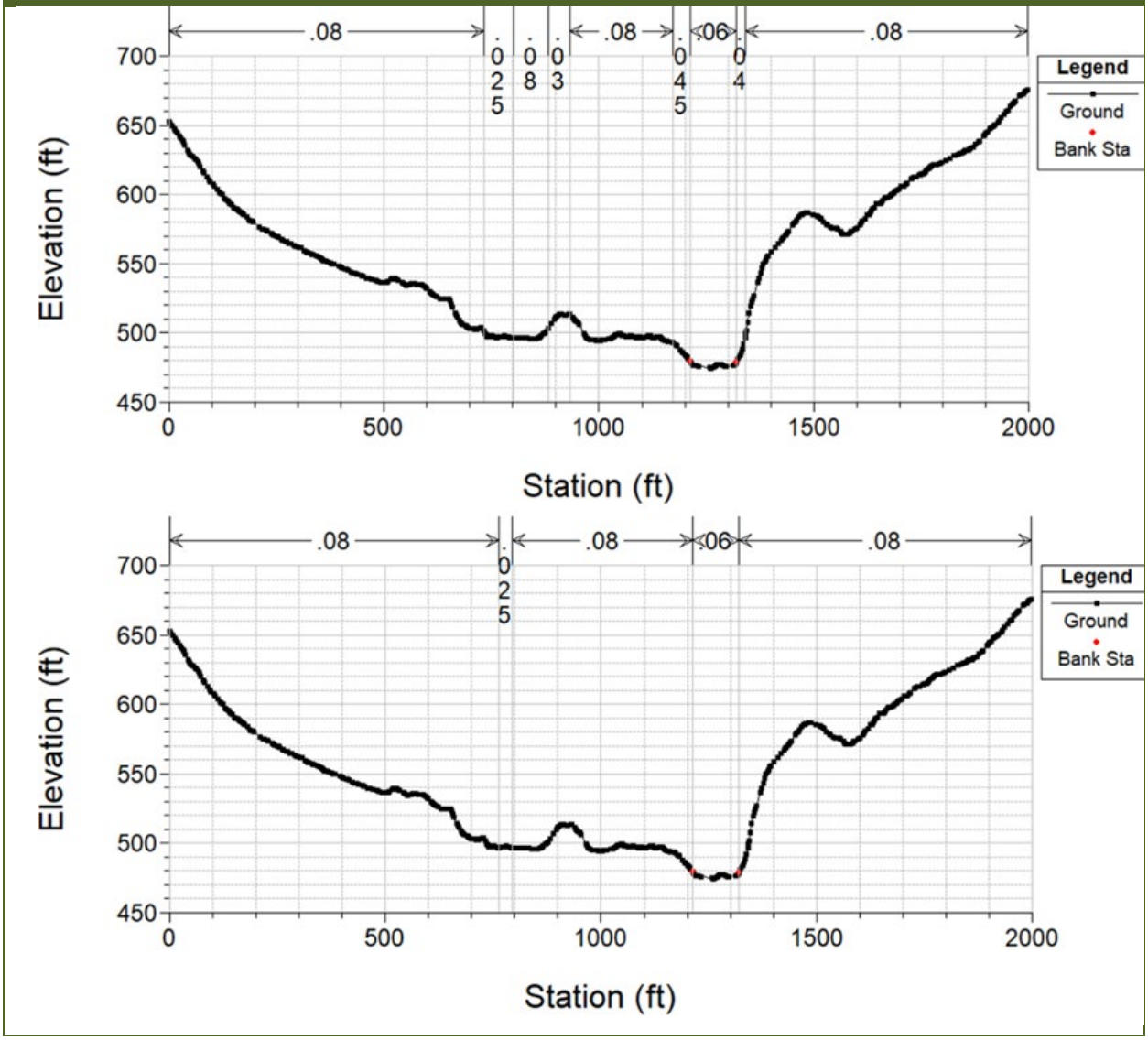

Grain Size Distribution Parameterization

Sediment grain size distributions were specified for every cross-section in the DEISs' HEC-RAS model based on grain size data collected in the study area in 2010, 2015, and 2018 (Corps 2020). Sample locations were selected on gravel and cobble bars in the Chehalis River and select tributaries. It was inferred from the assignments that pebble count results were applied directly to cross-sections proximal to the sampling location. Bedrock-boulder sections were characterized as mostly very coarse, and various non-sampled cross-sections were assigned grain size distributions that were interpolated between sample locations.

The same grain size distributions assigned for the DEISs' simulations were retained for the sensitivity analyses based on running the 30-year flow time series. For the sediment transport capacity and sediment trapping assessments, all non-interpolated, unique grain size distributions corresponding to gravel-cobble bedload deposits where the maximum particle size was smaller than 512 millimeters (mm) were averaged for (i) model cross-sections upstream of the FRE facility (DEISs' model Reach 0) and (ii) model cross-sections within the first 20.3 miles downstream of the FRE facility (DEISs' model Reach 1). While the two reach-average distributions were not substantially different, the downstream average distribution was finer than the upstream distribution, consistent with a lower overall river gradient downstream (Figure 11). Two independent pebble counts performed by Kleinschmidt of a more sorted channel bed at RM 102.4 and side bar deposit at RM 102.2 yielded distributions that were not substantially different from the smaller half of the average distribution computed for Reach 1 (Figure 11).

HEC-RAS Model Limitations

The sediment transport HEC-RAS version 5.0.7 model cannot be run in a mixed-flow regime, only the subcritical regime. However, there are sections of the Chehalis River where flows are likely to be supercritical during flood flows, including at Fisk Falls and just downstream of the FRE facility in the steeper bedrock canyon. Given high flows in most of the river are expected to be subcritical (e.g., Wohl et al. 1999; Wilcox and Wohl 2007; Comiti et al. 2007), the model was run in the sub-critical flow regime. Where critical depth is reached in the simulation, the model would default to the critical depth condition, whereas a supercritical flow-based solution would be more accurate. This can cause errors leading to spikes in shear stress, velocity, etc. which can result in a large amount of scour in a single time step. The potential for this was reduced during model modification by increasing the Manning's *n* roughness coefficient, but was determined to have still occurred at some locations.

The cross-section profiles in the model includes elevation data from various sources collected over multiple years before and after the 2007 flood event, which was associated with significant morphologic changes to the channel. The 30-year flow time series includes the calibrated flow series of the 2007 event, so the model simulates the sediment transport effects of the 2007 flood event on transects that were potentially surveyed before or after that.

Figure 11
Average Grain Size Distributions Upstream and Downstream of the FRE Facility in Reaches Where Spawning Habitat Is More Likely to Be Found.

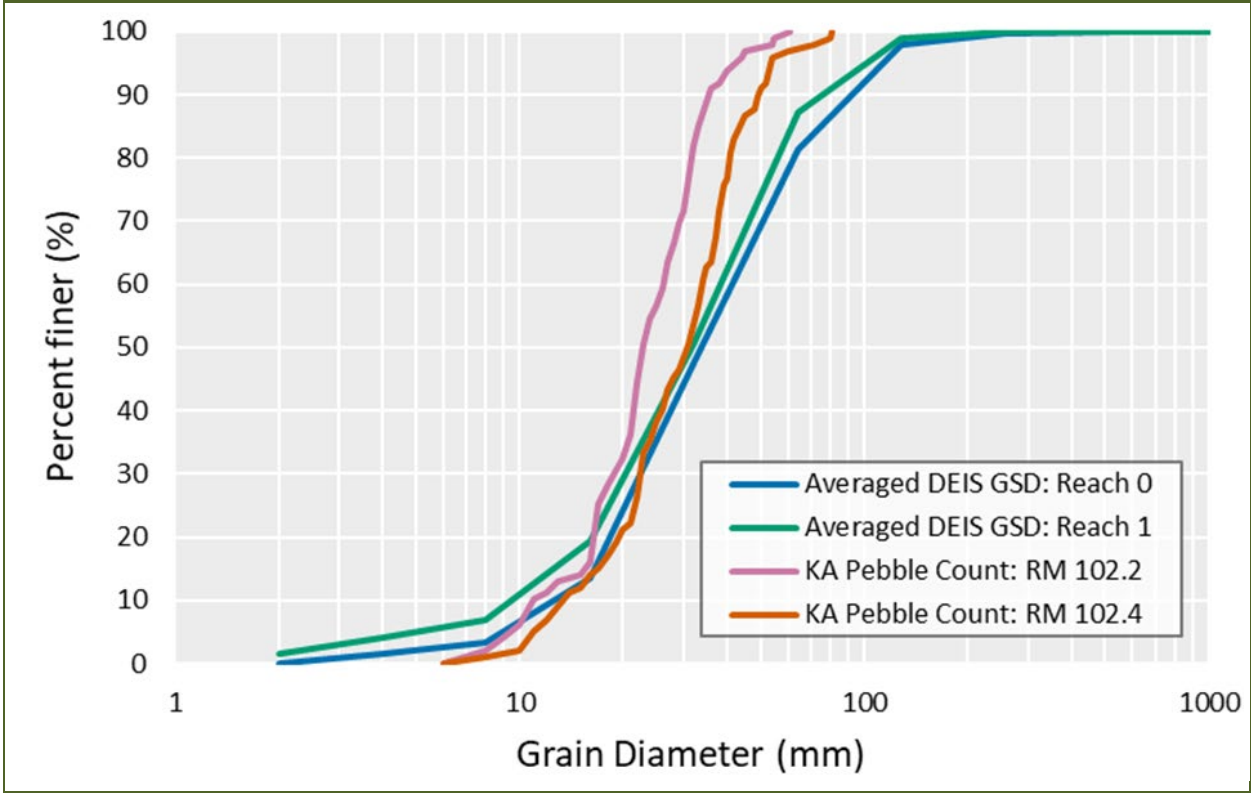

Importantly, there are no data available to calibrate coarse sediment transport rate estimates, which can vary by an order of magnitude depending on the sediment transport equation used. The DEISs' impact assessments were subject to the same limitation. Accordingly, the analyses performed for this assessment were based on evaluating relative differences in potential transport capacity and may not be representative of actual transport rates, which may be limited by local availability for transport and other factors. Hence, predictions of riverbed elevation and grain size distribution changes should be considered as relative indicators of potential for change, not accurate estimates of absolute magnitudes.

Evaluation of Incipient Motion Conditions

It is instructive to evaluate the mobility of sediments of different sizes that may be deposited during less frequent FRE operations, in comparison to smaller, more frequent flood events when the FRE is not in operation. It is the latter type of events that are typically associated with geomorphically effective flows that cumulatively transport more sediment on an annual basis than the larger, less frequent extreme flood events (cf. Wolman and Miller 1960). In that context, Shields' dimensionless shear stress equation was used to evaluate the grain size distribution that can be mobilized at each HEC-RAS cross-section during the 2-, 10-, and 100-year flood peaks:

$$\tau_{cr}{}^{*} = \left(\frac{\tau}{(\rho_s - \rho)gD_{50cr}}\right)$$

Where τ = average shear stress acting on the riverbed, $\tau_{cr}{}^{*}$ indicates critical dimensionless shear stress, ρ_s = sediment density, ρ = water density, and D_{50cr} = critical median particle size that is just stable for the specified shear stress and value of critical dimensionless shear stress. The dimensionless parameter represents a ratio between mobilizing (shear stress over the bed surface) and resistive (submerged stone weight) forces. The value of predicted shear stress was generated in HEC-RAS for the width of bed between the left and right bank stations as depicted in Figure 9. The value of $\tau_{cr}{}^{*}$ varies in natural rivers generally between 0.03 and 0.08 (Buffington and Montgomery 1997). A value around 0.030-0.035 is traditionally used for describing the first particles to move (e.g., Wilcock et al. 1996), whereas a value around 0.045-0.050 is often used to describe the general condition for bedload transport, as for example in the Meyer-Peter Muller equation (e.g., Wong and Parker 2006). For this analysis, $\tau_{cr}{}^{*}$=0.045 was used as a general purpose, midrange value for assessing streamwise variation in bed stability for larger flood events with the FRE in operation and smaller events otherwise.

Evaluation of Sediment Transport Capacity

Analogous to the evaluation of incipient motion, sediment transport capacity was calculated at the 2-, 10-, and 100-year floods to evaluate broadly whether smaller magnitude, more frequent floods would be able to transport spawning-sized gravels deposited during FRE operation at a sufficient rate downstream of the FRE location such that gravel availability to spawning habitat downstream would not be affected substantially. Shear stresses predicted by the HEC-RAS model for the active riverbed were input to Parker's (1990) surface-based equation for bedload transport, which is not currently available in HEC-RAS. This equation predicts transport rate per unit width of riverbed of grain sizes larger than 2 mm, which generally control riverbed morphology in gravel bed rivers like the Chehalis. Finer grain size classes mostly fill up the interstitial spaces of the coarser gravel framework and/or are transported downstream as suspended and wash loads. Total transport rate was calculated as kilograms per day across each HEC-RAS cross-section.

The predicted transport rates were found to be extremely large in magnitude upstream of approximately RM 107 (i.e., in the canyon reach above Pe Ell and upstream), which reflected notably high shear stresses predicted by the HEC-RAS model. The predicted magnitudes appeared to be substantially higher than would be expected, and were higher than the range on which Parker's (1990) equation was based. As a check, transport rates were also calculated based on equations developed by Hanes and Bowen (1985) and Recking (2010) for high intensity bedload transport conditions, and the predictions compared with the results based on Parker's (1990) equation. The two methods were found to bracket the Parker equation results, corroborating their use in the analysis.

To independently evaluate the cause of the high predicted transport rates, Pitlick et al.'s (2009) Bedload Assessment for Gravel-bed Streams (BAGS) software was used to calculate transport rates based on

both the surface-based bedload equation of Parker (1990) and the surface-based relation of Wilcock and Crowe (2003). The program implements bedload transport equations developed specifically for gravel-bed rivers. Transport capacities are calculated on the basis of channel geometry, energy slope, and bed material grain size. The BAGS software was run for three unique cross-sections and the results were used for comparing the magnitudes of transport rates predicted by the Wilcock and Crowe (2003) bedload equation used in the HEC-RAS sediment transport model with transport rates predicted by the Parker (1990) equation. The Wilcock and Crowe (2003) transport rates were approximately 25-50 percent of the transport rates calculated using the Parker (1990) equation, with a median ratio of approximately one-third across all flow scenarios. Overall, it was concluded that while the absolute magnitudes of predicted transport rates were higher than usually encountered in gravel bed rivers, inferences based on relative differences subject to analogous/similar prediction errors would still be suitable for purposes of this assessment.

The calculated 2-year and 10-year flood transport rates predicted using Parker's (1990) equation were then multiplied by 50 days and 10 days, respectively, and compared with the 1-day 100-year flood results to evaluate effective transport capacity in the sense of Wolman and Miller (1960). The objective was to determine the extent to which the 2-year sum exceeds the 100-year sum and 10-year sum and thus preclude long-term transport imbalances in a gravel-poor system like the upper Chehalis River.

Evaluation and Expansion of DEISs' Model Simulation Approach

The results of the two preceding analyses of sediment mobility provide indirect indications that the likelihood of FRE operations trapping gravel upstream of the FRE facility and reducing gravel transport downstream over the long term is generally low. To evaluate potential effects of the FRE more directly, a (morphodynamic) model of riverbed evolution is needed that simulates gravel transport and deposition patterns along the river by integrating transport rates over a range of flows, over time. The HEC-RAS model developed for the DEISs is but one representation of a morphodynamic model. Ideally, such a model would track sediment transport, erosion, and deposition of bed and banks, and predict the evolving channel form and profile over time. However, quantitatively accurate morphodynamic models do not exist because of inherent errors and limitations in model formulation, sediment transport equations, and errors in determining requisite input data and parameters. Instead, predictions of models like HEC-RAS are best used to qualitatively evaluate sensitivity of systems to perturbations, and/or reaffirm that general physical processes built into the model may be operating as expected in a given situation.

The 1D HEC-RAS model developed for the DEISs simulated morphodynamic changes in mean riverbed elevation over time and space. However, the model has various features in its architecture that affect what it predicts. Aside from predictive variability in sediment transport equations available to the user, there are two features of the ways in which the sediment transport and mass balance simulation algorithms are set up in the model that have a particularly strong influence on the outcome:

The option exists to specify a certain level of sediment loading at inflow points. However, when implemented, the model tends to distribute the sediments across the model domain and may predict aggradation where none would actually occur. In addition, there is a high level of uncertainty about estimated levels of loading, which can translate into high uncertainty regarding significance of predicted changes in riverbed elevation.

The sediment transport module includes specifying a parameter that defines the limits to degradation depth. Without detailed geophysical data, it is generally not possible to specify accurately the depth to bedrock or other residual lag layer that does not erode. But more importantly, the model will calculate gradual degradation at various locations until the limit is reached, at which time the predicted bed elevation remains static. The model will also predict degradation at locations in alluvial reaches where degradation has not occurred in the past, irrespective of whether or not the site is prone to degradation.

Predictions of aggradation and degradation trends in the DEISs reflect how these two options were treated and the assumptions made regarding their parameterization. Model sensitivity to each was accordingly evaluated as described below. In both cases, the 30-year flow time series described in Section 2.1 was run through the modified HEC-RAS model and predictions for different scenarios were compared.

In addition, the DEISs' HEC-RAS model output was evaluated in greater depth by looking at predicted aggradation and degradation volumes of specific sediment size classes at different locations in response to FRE operations. The DEISs' model simulation results focused on total sediment load, but not all size classes are important for Chinook salmon, which spawn in substrates composed of small cobble to small gravel (Kondolf and Wolman 1993). The objective was to evaluate where spawning-sized materials were predicted by the model to settle out most extensively in conjunction with FRE operations. Such information may be useful for designing FRE operations that minimize potential effects on transport and deposition of spawning-sized substrates in spawning areas.

Model Sensitivity to Variations in Sediment Loading from Upstream

Because of the propensity for the HEC-RAS model to redistribute externally 'supplied' sediments within the model reach, the model was first run with no sediment inflows to eliminate that source of variation. The sediment load was then increased incrementally up to the values used in the DEISs' model simulations, and signs looked for where the result may be an artifact of the model rather than being indicative of likely effect of the FRE. For example, an approximately linear relation of aggradation volume versus sediment load could indicate that the changes in bed elevation predicted by the model are an artifact of the way the model is set up. Sediment loading was simulated in four scenarios: (i) no input sediment load, (ii) one-third of the DIESs' model sediment load, (iii) two-thirds of the DEISs' model sediment load, and (iv) the full sediment load as specified in the DEISs' model simulations. The input sediment loads were introduced to the simulation as a function of flow at individual cross-sections in the HEC-RAS model. An example sediment load rating curve in the DEISs' model is shown in Table 2. Rating

curves for other sources are presented in Appendix F of Ecology (2020), including Thrash Creek, Roger Creek, Big Creek, Crim Creek, Rock Creek, and unidentified small sources locally upstream of the USGS Doty gage.

Table 2
Sediment Load Rating Curve Example for the Upstream Boundary Condition of the Mainstem Chehalis River.

	CHEHALIS RIVER – UPSTREAM BOUNDARY					
	RIVER MILE 118.1741					
Flow [cfs]	186	620	2,542	6,200	12,400	18,600
SEDIMENT LOADING SCENARIO	**TOTAL LOAD (TONS/DAY)**					
None	0	0	0	0	0	0
1/3 DEIS	1.1	39.6	2,420	14,520	60,500	108,900
2/3 DEIS	2.2	79.2	4,840	29,040	121,000	217,800
DEIS	3.3	118.8	7,260	43,560	181,500	326,700

Model Sensitivity to Scour Depth Limits

The model used in the DEISs' simulations specified maximum scour depth limits ranging from 0 feet to 5 feet of depth depending on location. A maximum scour depth limit of 0 feet was found to have been used for cross-sections with predominantly bedrock bottoms, while 5 feet was used in lower gradient alluvial sections. However, when running the model, it was noticed that certain locations such as alluvial hydraulic controls were predicted to degrade and flatten out, even though field observations suggested a low likelihood of such an occurrence. This outcome reflects a case where the local grain size distribution at a cross-section is fine relative to the simulated transport capacity such that the model proceeds with adjusting the riverbed elevation until an equilibrium regime channel grade is reached, or the scour depth limit is triggered. To evaluate this, the modified model was also run for the case where the maximum scour depth limits were all set to zero, and the results compared with the DEISs' model assumption.

Transport and Deposition of Different Grain Size Classes

Bedload transport volumes were calculated using the Wilcock and Crowe (2003) sediment transport equation built into HEC-RAS, which simulates both sand and gravel transport and calculates transport rates for each of a range of predefined grain size fractions. The output accordingly facilitated an evaluation of spatial erosion and deposition patterns predicted for both (i) the entire grain size distribution, and (ii) specific sediment size classes. For the latter, results were compared for four major size classes: sand (<2 mm), small (2-<32 mm) and large gravel (32-<64 mm) suitable for spawning, and cobble and small boulders (64-<512 mm). To eliminate the confounding effect of sediment loading on model predictions as described above and isolate the effect of transport capacity on differential deposition of different grain size classes, the model was run with no sediment loading input from upstream. For consistency with the DEISs, scour depth limits were not set to zero.

Long Term Sediment Trapping Efficiency Analysis

As an alternative approach, a long-term, within-reach sediment transport budget was developed. The HEC-RAS model was run to predict shear stresses at different sediment transporting flows. The shear stress predictions were used to predict sediment transport rates using Parker's (1990) bedload transport equation and integrated over a flow duration curve to calculate an approximate total load passing by each HEC-RAS model cross-section over a 50-year period following the approach outlined in DeVries and Aldrich (2015). The difference in net transport volumes in a segment between successive cross-sections is an indicator of the trapping efficiency within the segment, and can be converted to an average net change in bed elevation that is indicative of aggradation (=positive net change), degradation (=negative net change), or roughly equilibrium (=negligible net change) conditions. There was no attempt to route sediments quantitatively through the system given the absence of sufficient sediment transport rate calibration data and uncertainty in sediment loading amounts, both which preclude accurate prediction of absolute bed elevation changes. Trapping efficiency provides a relative index of bed elevation change potential instead.

Sediment trapping efficiency was computed for each flow in Table 2 and segment by estimating sediment transport rates at the bounding upstream and downstream cross-sections, and applying a mass balance equation for bed elevation change between cross-sections as a function of estimated input and output bedload mass transport rates per unit width (q_B), active width (W), distance between cross-sections (L), sediment density (ρ_s), and porosity (P):

$$Y_T = \int_{t1}^{t2} \frac{\partial Y}{\partial t} dt \cong -\sum_{t1}^{t2} \left[\frac{(q_B W)_{out} - (q_B W)_{in}}{0.5L(W_{in} + W_{out})\rho_s (1-P)} \right] \Delta t$$

where the incremental change in bed elevation ($\partial Y/\partial t$) was evaluated for each simulation flow and then multiplied by the histogram time increment (Δt) over which the modeled flow occurred during the 50-year period. This was repeated for other flows, and the results summed to estimate a net mean change in bed elevation Y_T between successive cross-sections. The active width was approximated as the distance between left and right bank toe stations in the HEC-RAS model (cf. Figure 9). A strongly positive value of the $\partial Y/\partial t$ sum was inferred as an indication of a strong tendency towards aggradation, and a strongly negative value as an indication of a stronger tendency towards degradation.

Seven aggradation/degradation potential classes were created subsequently and used to characterize deposition trends. The magnitudes of transport rates distinguishing each class was based on the sign and relative magnitude of the predicted bed elevation change along the river using professional judgment. Each analysis segment was classified accordingly and the results depicted graphically in ARC-GIS.

Results

The results for the four approaches are presented below. Their implications are discussed collectively in Section 4. All references to RM are based on the DEISs' HEC-RAS model assignments, which differ from USGS' RM assignments.

Evaluation of Incipient Motion Conditions

The HEC-RAS model shear stress predictions indicate that the Chehalis River has the capacity to fully mobilize spawning-sized substrates upstream of the proposed FRE facility location during frequent floods when the FRE is not in operation (Figure 12). Spawning substrates are also predicted to be mobilized in the primary spawning reaches downstream in the vicinity of Pe Ell. The calculated Shields stress parameter is substantially higher than the critical value (τ_{cr}^{*}=0.045) upstream of Fisk Falls (around RM 114 in the HEC-RAS model), and at some locations, it approaches or exceeds the level ($\tau^{*} \approx 0.5$) above which the riverbed starts to move as a 'traction carpet' that is thicker than the surface layer (cf. DeVries 2002). The same is true in the vicinity of the FRE and in the short, steeper canyon reach downstream. Between the FRE and Fisk Falls, the bed is also predicted to be highly mobile during the 2-year flood. While less mobile compared to in the canyon reach and upstream, native gravel and cobble bedload deposits are predicted to also be fully mobile at the 2-year flood peak downstream to the South Fork. Deposits are predicted to be more stable in the Pe Ell valley spawning reach (approximately RM 101-107) than in the spawning reach between the proposed FRE location and the bottom of Fisk Falls at approximately RM 114 in the HEC-RAS model (Figure 12).

Evaluation of Sediment Transport Capacity

The sediment transport rate predictions for the 2-, 10-, and 100-year flood peaks show upstream-downstream patterns that are similar to the incipient motion results (Figure 13). The magnitudes of predicted transport rates are notably higher than typically predicted for a gravel bed river upstream of RM 107, which appears to reflect predicted shear stresses that are higher than the range used to develop Parker's (1990) bedload transport equation. However, as indicated in Section 2.3, other bedload relations for high intensity transport and the Wilcock and Crowe (2003) equation also predict large transport rates and the same large-scale upstream-downstream patterns depicted in Figure 13. A key feature of the analysis results is that transport rates are predicted to be extremely high upstream of Fisk Falls and in the vicinity of the FRE facility and downstream canyon, and higher between Fisk Falls and the FRE facility than in the Pe Ell valley reach downstream of the canyon, even at the 2-year flood level. This suggests that the river has the transport capacity to subsequently move sediments that may temporarily deposit in the impoundment that forms during FRE operation to spawning habitat downstream. As corroboration, when summed over a 100-year period, the 2-year flood peak transports cumulatively more sediment than the 100- and 10-year flood peaks combined (Figure 14).

Figure 12
Predicted Mobility of Gravel-Cobble Bedload Deposits Along the Upper Chehalis River, Evaluated at the 2-Year Peak Flood. Top: Comparison of Calculated Shields Dimensionless Shear Stresses vs. Values Corresponding to Critical Level for Incipient Bedload Transport and Onset of Granular Flow. Bottom: Comparison of Predicted Stable D_{50} vs. Reach-Average D_{50} of Gravel-Cobble Bedload Deposits Depicted in Figure 2-11 and Upper Limit Used by Chinook Salmon As Reported by Kondolf and Wolman (1993).

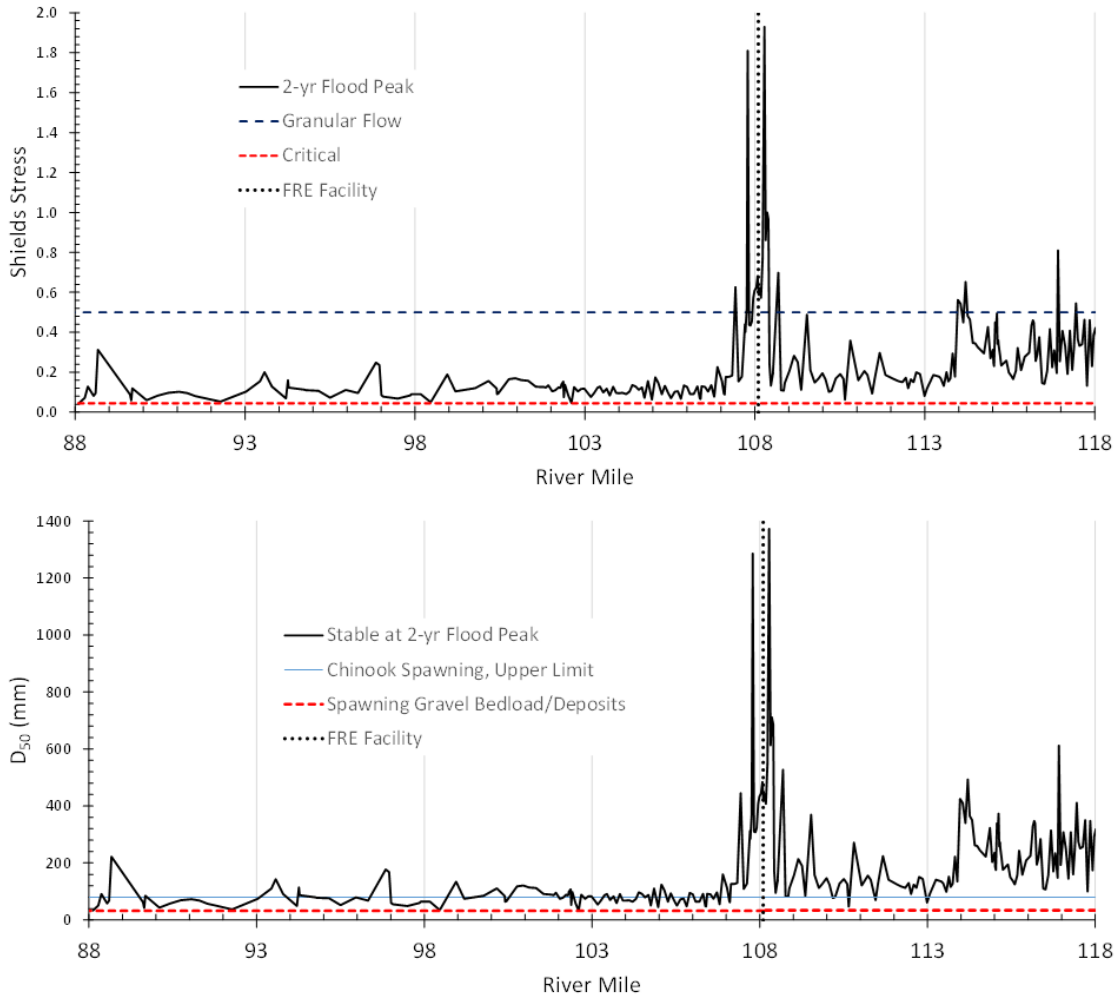

Figure 13
Instantaneous Gravel and Cobble Bedload Transport Rates Predicted for Each HEC-RAS Model Cross-section Along the Upper Chehalis River Using Parker's (1990) Equation for the 2-, 10-, and 100-year Flood Peaks.

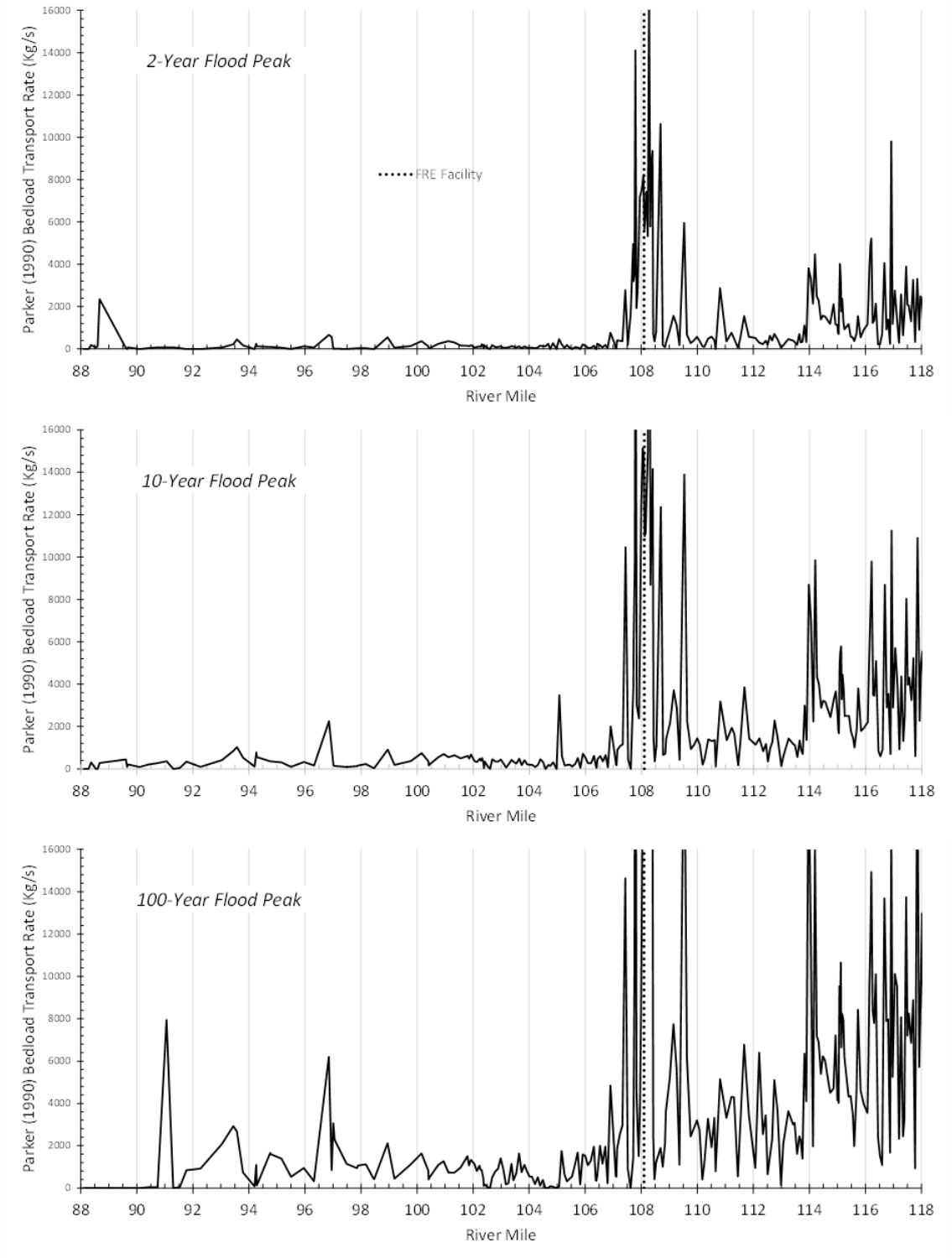

Figure 14
Comparison of Predicted Total Weight of Grain Sizes 2 mm and Larger Transported Over a 100-year Period at the 2-, 10-, and 100-year Flood Peaks Along the Upper Chehalis River.

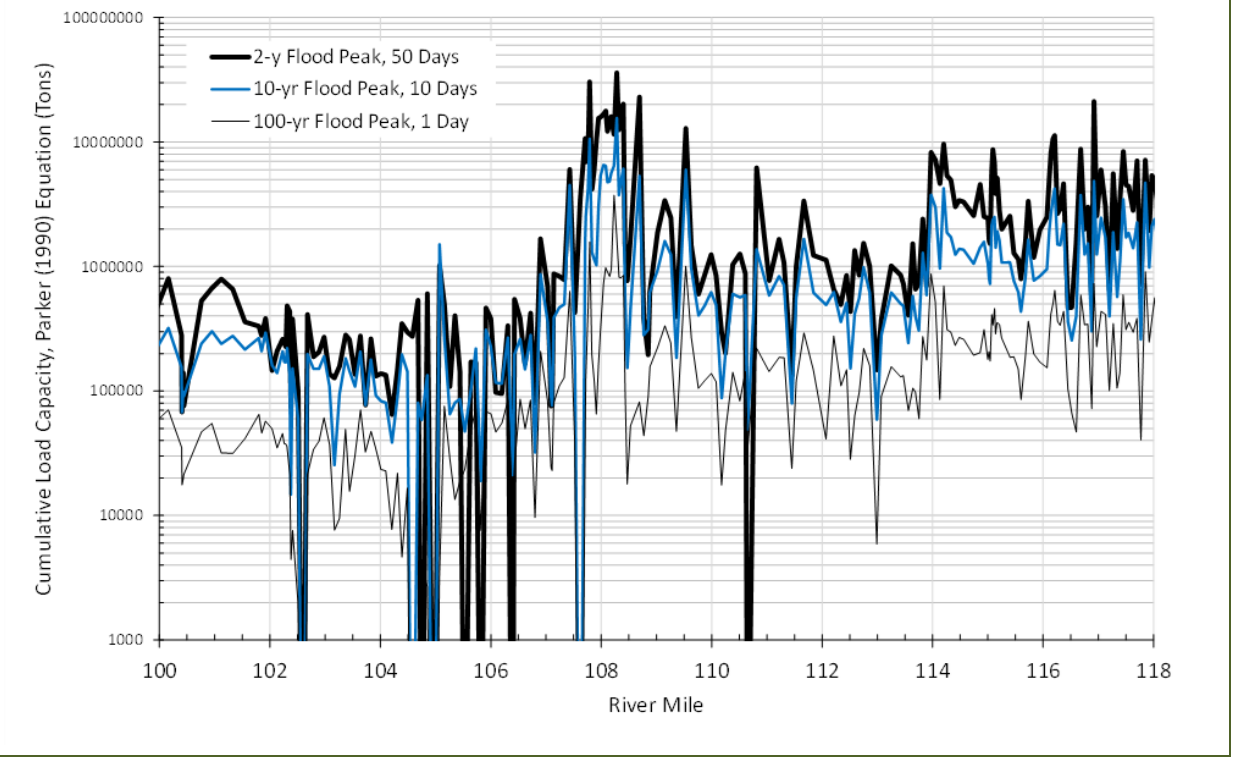

Evaluation and Expansion of DEISs' Model Simulation Approach

Influence of Sediment Loading on Model Predictions

As expected, the modified HEC-RAS model predicted a net increase in aggradation volume of sediment with increasing sediment loading irrespective of FRE operations over a 30-year time frame, for the entire modeled reach upstream of the South Fork to approximately RM 118 (Figure 15). Notably, the model predicted aggradation even with no sediment input. What was not expected, however, was that the model predicted net aggradation overall to be comparable or slightly lower for the with-FRE scenarios compared against the without-FRE scenarios. When looking at sub-reaches, results were more variable. While the DEISs' simulated loading resulted in greater net aggradation than the zero-loading scenario, the trend was not always consistent for the intervening sediment loading scenarios (Figure 15)[2]. In some

[2] These and following bar charts do not include or depict degradation quantities computed at various cross-sections that are confounded by the extensive presence of exposed and underlying bedrock.

cases, the with-FRE scenarios were associated with less aggradation than without-FRE, in other cases the reverse. It is difficult to tease out the reasons for the differences, which depend in part on how the model computes volumes and treats mass balancing accordingly.

In general, the modified HEC-RAS sediment transport model predicted aggradation to be greatest above Fisk Falls, within the lower three miles of the FRE operation inundation zone, and downstream of the FRE facility in the bedrock canyon with- and without-FRE operations (Figure 16). This result is counter-intuitive given that these are also the reaches with the highest sediment transport rates (Figure 13). Of particular relevance towards discerning impacts, is that the model predicted smaller, less variable aggradation within the first two and a half miles below Fisk Falls, and in the Pe Ell valley reach below RM 107 where higher densities of Chinook salmon spawning occurs (WG and Anchor 2017; WDFW redd survey data).

Figure 15
Net Average Aggradation Rates Predicted for with-FRE and without-FRE Scenarios in Different Reaches of the Chehalis River Based on the 30-year Flow Time Series, and for Different Annual Rates of Sediment Loading Ranging from Zero Input to the DEISs' Simulation Loadings.

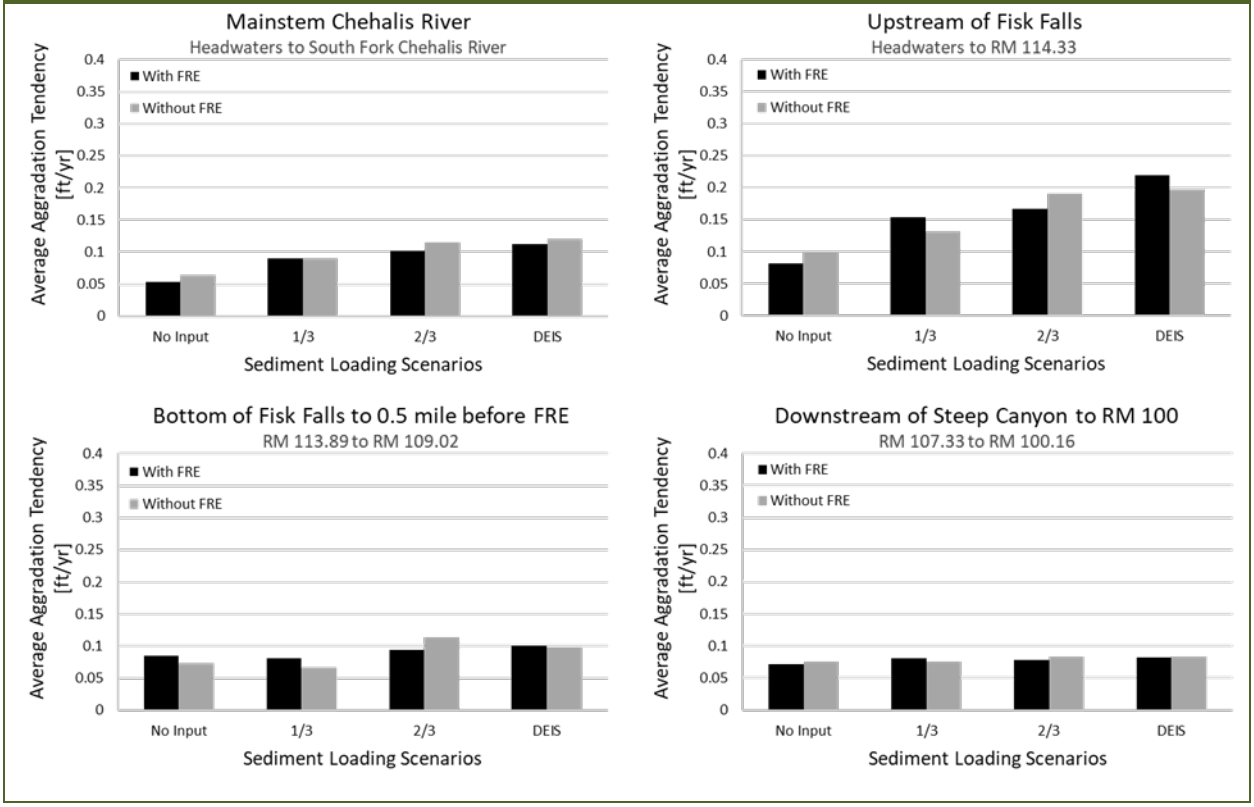

Figure 16
Net Average Aggradation Rates Predicted for with-FRE and without-FRE Scenarios in Different Reaches of the Chehalis River Based on the 30-year Flow Time Series, and for Different Annual Rates of Sediment Loading Ranging from Zero Input to the DEISs' Simulation Loadings.

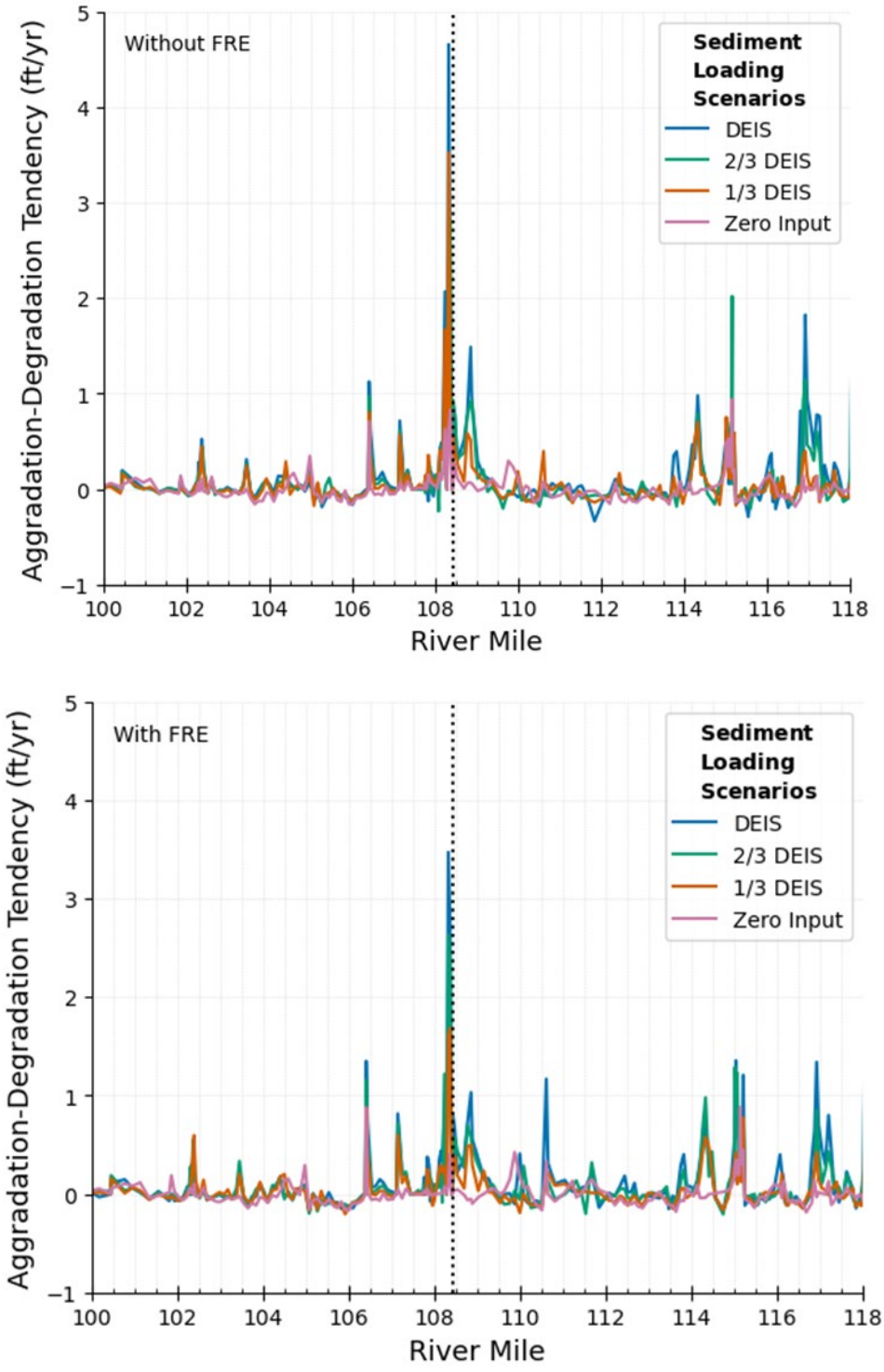

Influence of Scour Depth Limit on Model Predictions

Predictions of long-term aggradation over the 30-year simulation were seen to be sensitive to different settings of the scour depth limit parameter (Figure 17). Some locations with large amounts of aggradation predicted under the DEISs' scenario had little to no aggradation predicted under the scenario where scour was not allowed. In general, when the scour depth limit is set to greater than zero, the model effectively exhumes material defining the riverbed profile in the initial condition and redistributes it within the model reach. The resulting predictions can be unrealistic. Examples from the simulations included:

- The model will simulate erosion and consequent bed degradation down to the specified limit at locations where significant scour would not be expected. For example, the modified HEC-RAS model predicted the riverbed to scour significantly at cross-section RM 111.84, which is located across a large gravel bar deposit formed along the inside of a bend, in a reach where gravel deposition is noted primarily in association with major bends in the channel (Figure 17; Light and Herger 1994). Review of aerial photograph history in Google Earth indicates the feature is generally persistent over time. Similarly, the DEISs' model settings resulted in predicting significant lowering of the riverbed at hydraulic control locations farther downstream at HEC-RAS model cross-sections RM 88.60 and 89.68 that in actuality appear to have persisted over time in aerial photographs.
- "Murphy's Hole" is a large, deep pool located approximately 2.2 miles upstream of the proposed FRE facility location at HEC-RAS model cross-section RM 110.65. It appears to have been a generally persistent feature over time. In the with-FRE simulation, the DEISs' model scour depth limit settings resulted in simulating a headcut into the nearest upstream cross-sections followed by eventual aggradation until the profile was more in line with the upstream and downstream grade. When the scour limit was set to zero, there was effectively no aggradation predicted (Figure 17, lower graph).

Figure 17
Illustration of Effect of Setting Maximum Scour Depth Limits on Aggradation/Degradation Tendency Predicted by the HEC-RAS Sediment Transport Model for the Chehalis River for the Cases without- (top) and with- (bottom) FRE Operations, with the DEISs' Sediment Loading Settings, Based on the 30-year Flow Time Series.

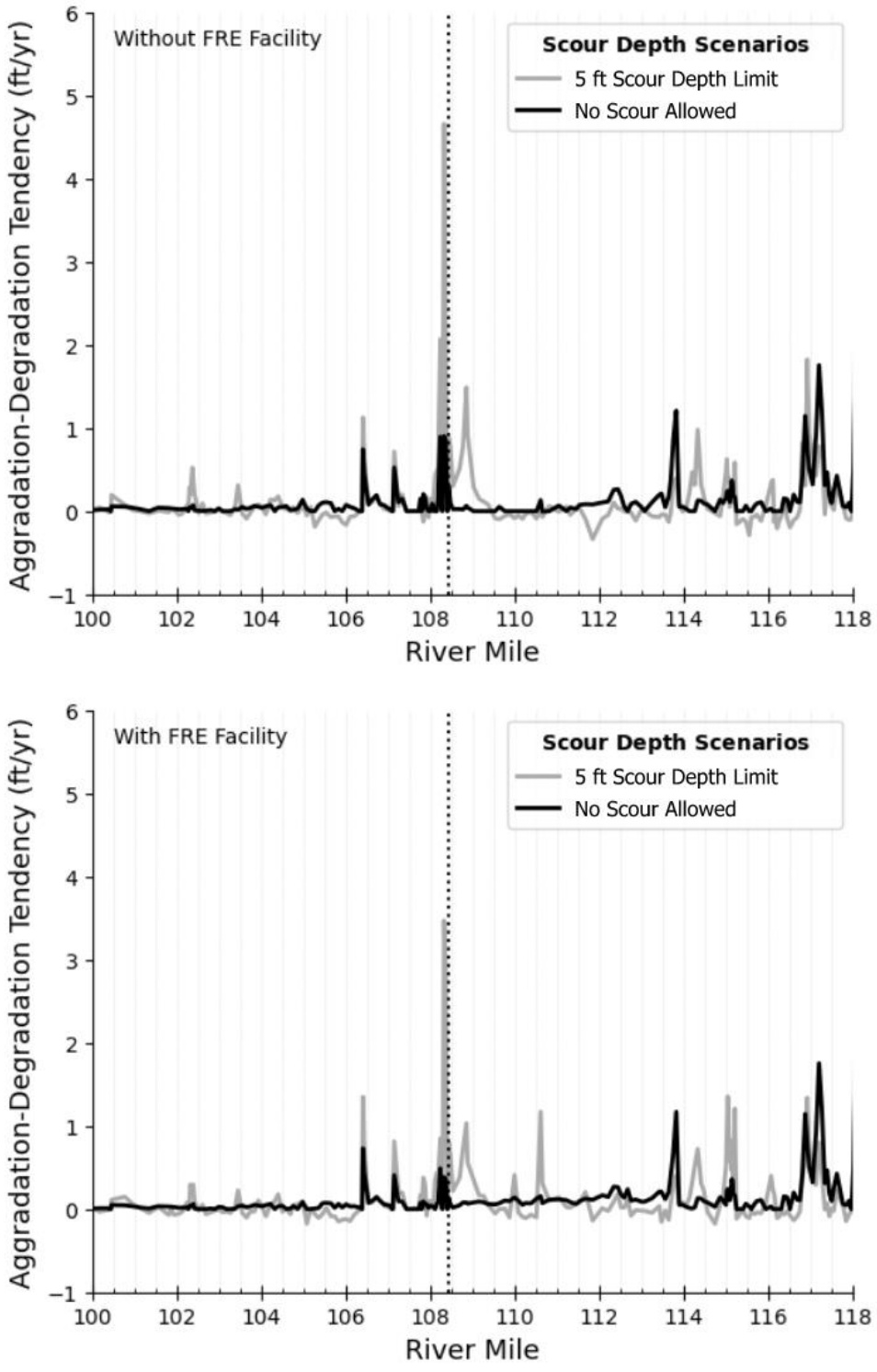

Transport and Deposition of Different Grain Size Classes

Predicted aggradation/degradation rates were calculated for different sediment size class volumes (as reported in the model output) for both the zero and DEISs' model sediment loading scenarios. FRE operations effects were represented as a difference in rates for each respective sediment loading scenario, calculated as the rate predicted for the with-FRE operation scenario minus the rate for the without-FRE scenario (Figure 18). A positive value denotes net gain with FRE operations, a negative value denotes a net loss. The modeling predicted minor to no difference in aggradation/degradation rates of sand-sized particles along the length of the river above Elk Creek. Results for small and large gravels were highly variable moving from one cross-section to the next, although there were some trends also evident in the predictions based on the 30-year flow time series (Figure 18):

- Gravels were predicted to generally accumulate between RM 110 and RM 112, and were scoured within the high transport rate reach in the vicinity of and below the FRE facility location;
- Gravels and cobbles were not predicted to accumulate or scour substantially within the higher density Chinook salmon spawning reaches.

Figure 19 and Figure 20 depict the results used to compute the differences depicted in Figure 18 for the zero and DEISs' model loading scenarios, respectively.

Evaluating Future Influence of Climate Change

The DEISs touched on potential effects of changes in hydrology associated with climate change on sediment transport predictions. The same flow files used in the DEISs' analyses were run through the model, for the "mid-century" period spanning from 2030 to 2060 and the "late-century" period spanning from 2060 to 2080. The DEISs' sediment loading settings were used. The model predicts that aggradation would increase slightly over time in the upper Chehalis River overall given the specified changes in hydrology, and that the with-FRE scenario would be associated with less aggradation than the without-FRE scenario (Figure 21). As was the case for varying levels of sediment loading, the hydrologic changes result in varying differences between the two scenarios. It is not immediately clear from examining the model output as to why.

Figure 18
Difference Between the "with-FRE" and "without-FRE" Predictions of Bed Elevation Change Rates Along the Chehalis River, Computed for Different Sediment Size Classes and the Zero and DEISs' Model Sediment Loading Scenarios. The "without-FRE" Results Are Subtracted from the "with-FRE" Results, Each Based on the 30-year Flow Time Series. The Red Boxes Encompass the Primary Chinook Salmon Spawning Reaches in the Upper Chehalis Basin.

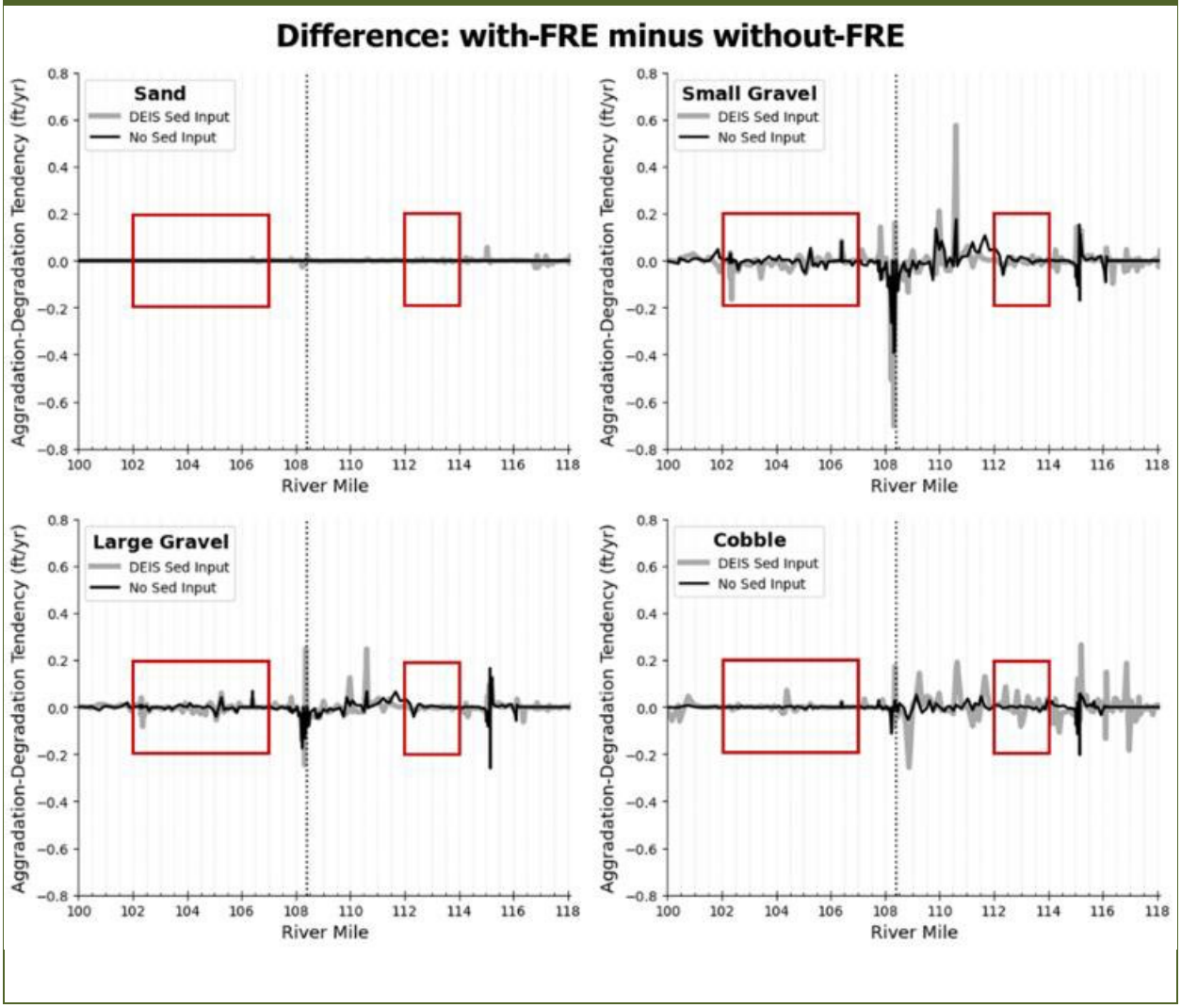

Figure 19
Predictions of Bed Elevation Change Rates Along the Chehalis River Computed for Different Sediment Size Classes, for the with-FRE and without-FRE Scenarios, and Assuming Zero Sediment Loading. Based on the 30-year Flow Time Series.

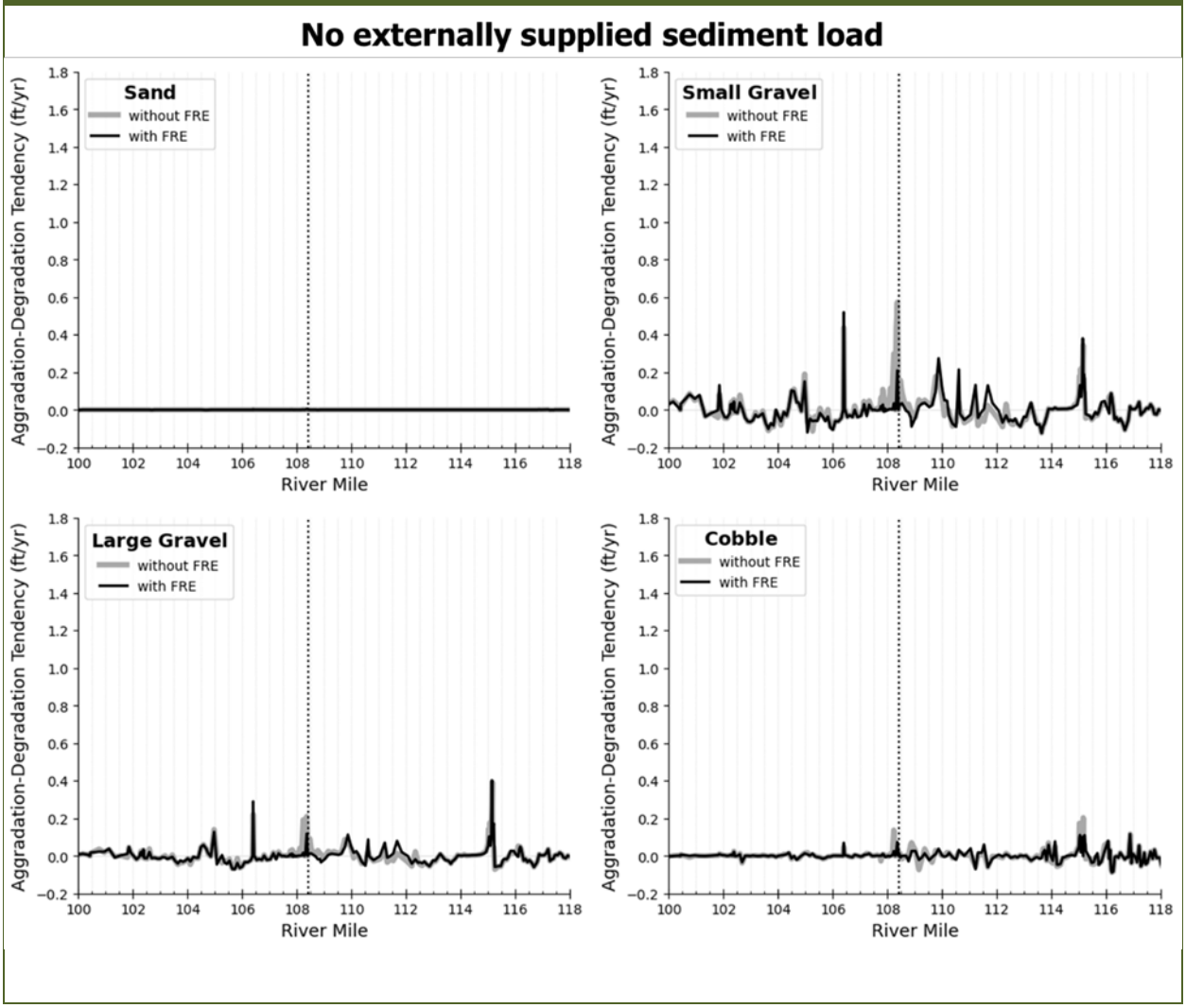

Figure 20
Predictions of Bed Elevation Change Rates Along the Chehalis River Computed for Different Sediment Size Classes, for the with-FRE and without-FRE Scenarios, and Using the DEISs' Sediment Loading Setting. Based on the 30-year Flow Time Series.

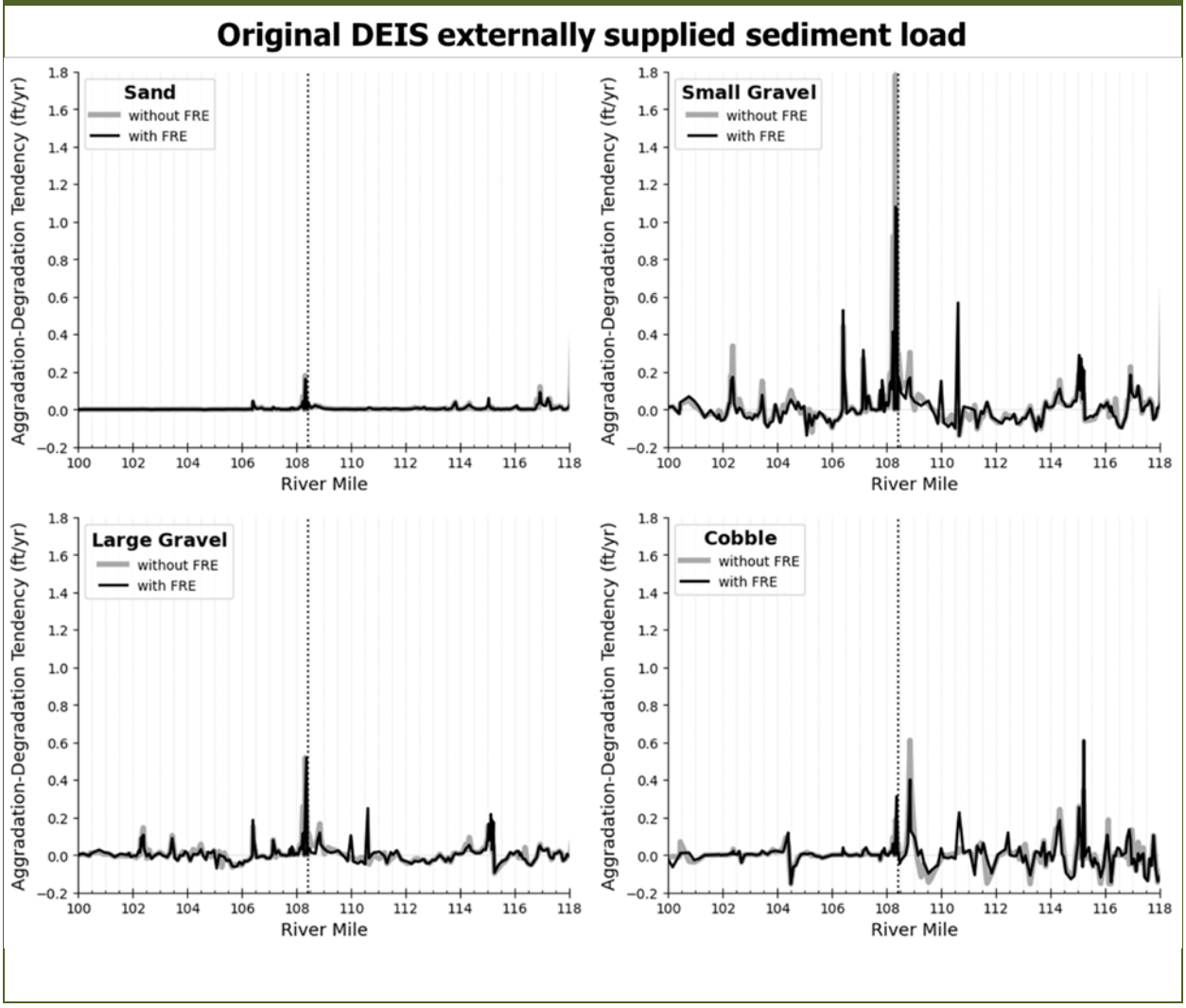

Figure 21
Sensitivity of Model Predictions of Aggradation Rates for the with-FRE and without-FRE Scenarios in Different Reaches of the Chehalis River, Using the 30-year Flow Time Series Representing the DEISs' Historic and Projected Climate Change Hydrology Scenarios.

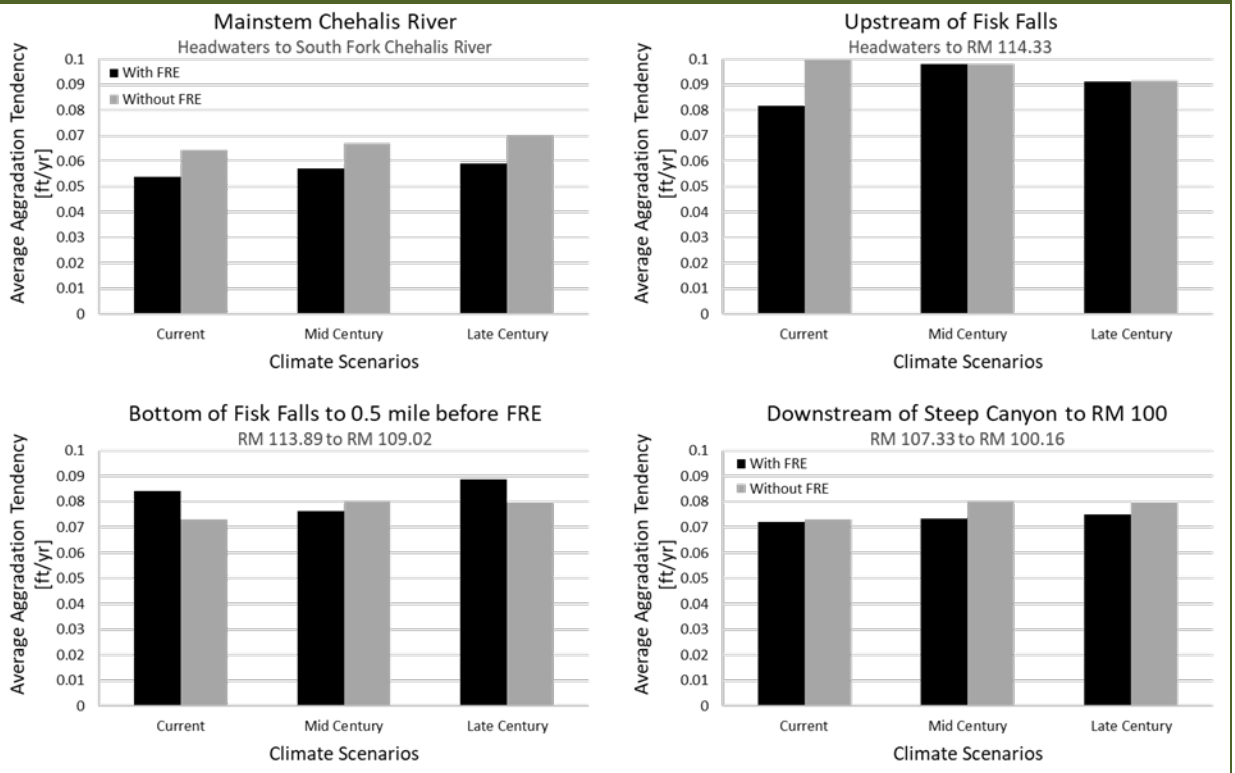

Long Term Sediment Trapping Efficiency

The aggradation-degradation analysis results indicate that there is greater upstream-downstream variability in sediment trapping efficiency in the steeper reaches upstream of the Pe Ell valley (Figure 22). In the Pe Ell valley and downstream to the confluence with the South Fork Chehalis River, the calculated sediment transport rate imbalances were more muted and less variable.

Greatest variability was predicted in the steeper reach upstream of Fisk Falls, in the vicinity of the proposed FRE facility and in the steep canyon reach downstream. These three reaches are also where substrate instability and sediment transport rates were predicted to be greatest based on the shear stress and Parker (1990) bedload equation estimates (Figure 12 and Figure 13), and where the DEISs' modeling approach predicted greatest aggradation (Figure 16). The simulations predicted relatively large alternating rates of erosion upstream and deposition downstream in these reaches, where the channel bed was predominantly bedrock and the morphology alternated between narrow, bedrock dominated features followed by wider sections.

Aggradation and degradation trends computed below Fisk Falls appear consistent with qualitative field observations. Significant aggradation was predicted in the vicinity of High Bridge below Rogers Creek, and in the first two riffle areas downstream of the bridge. The tendency for aggradation/degradation was mild to neutral in the next one and a half miles downstream, consistent with the predominant use of this reach by spawning Chinook salmon.

Consistent with its persistence, the simulation predicted a significant degradation tendency at Murphy's Hole around RM 110.65, and a significant aggradation tendency upstream where gravel deposits are evident in aerial photographs. This result stands in contrast to the DEISs' model simulations, which predicted headcutting upstream and filling of the pool.

The simulation indicated that sediment transport imbalances were generally small and in equilibrium over most of the river downstream of approximately RM 107. There were selected locations predicted to have relatively higher rates of aggradation and degradation that were generally associated with bedrock controls and locally pronounced widening of the channel. Most of the river was predicted to process gravels downstream steadily.

Figure 22
Spatial Variation in Modeled Erosional and Depositional Trends Within the Chehalis River's Active Channel, As Suggested by Sediment Transport Modeling Using Parker's (1990) Bedload Transport Equation; Classifications Were Defined Using Professional Judgment. Lateral Extent of Polygons Depicted Reflects the Bounds of HEC-RAS Model Cross-Section Placement, Not Erosion or Deposition Risk Across the Floodplain.

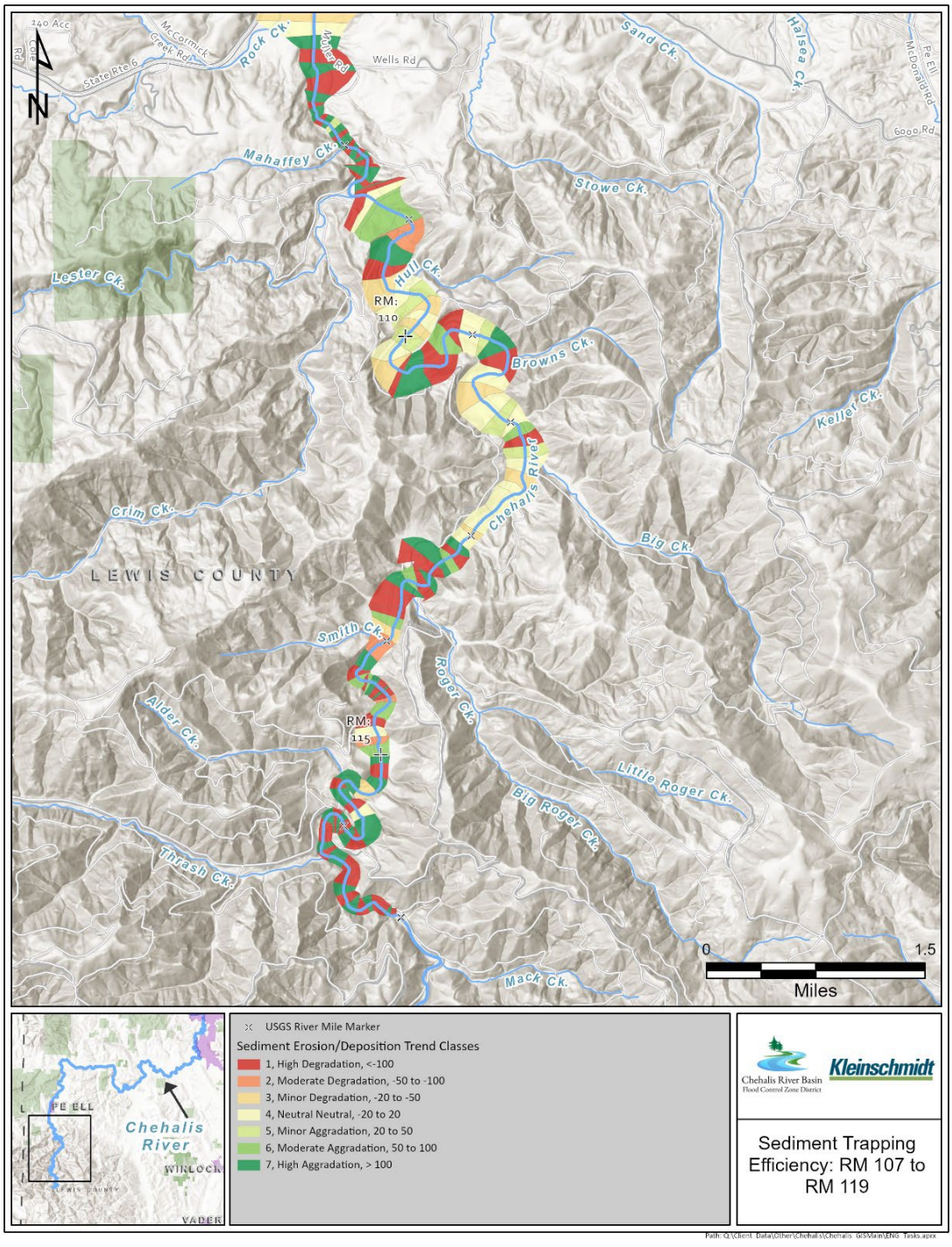

Figure 22
Continued (RM 97 to RM 107).

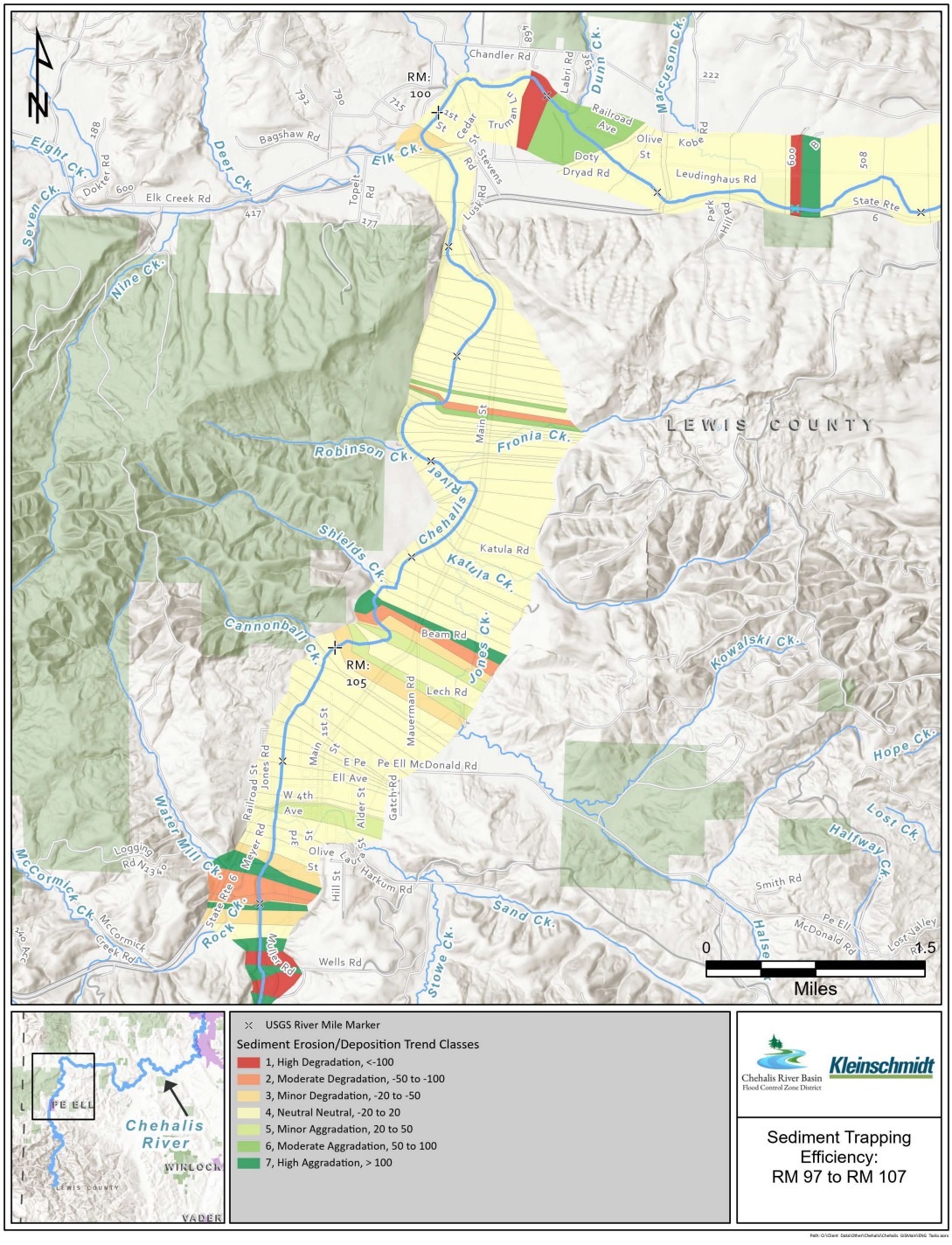

Figure 22
Continued (RM 84 to RM 97).

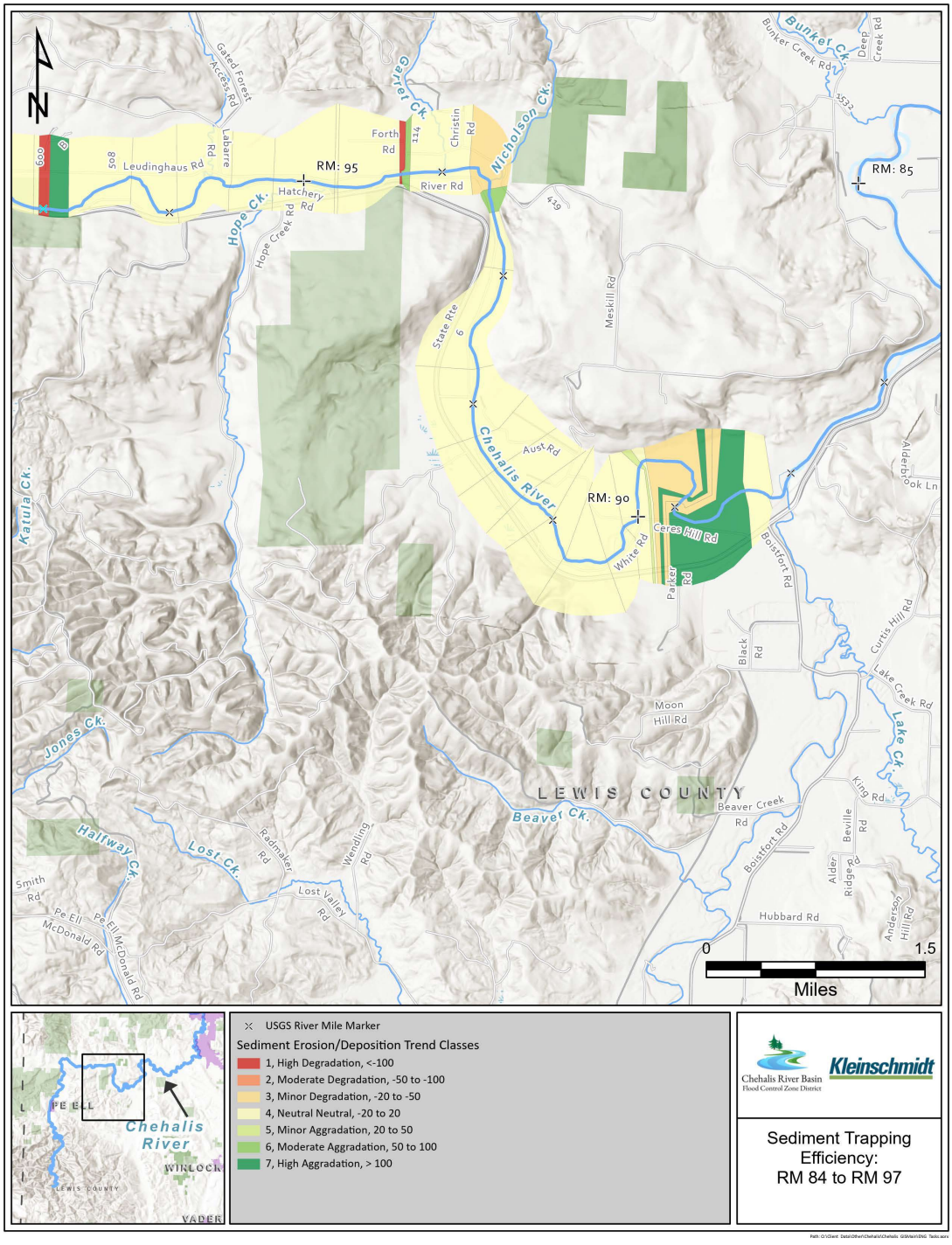

Discussion

The analyses presented here provide additional insights regarding potential species and reach-specific effects of the proposed FRE on the transport and deposition of Chinook salmon spawning substrates in the mainstem Chehalis River. Insights gained include a more specific understanding of the predictive limitations of the HEC-RAS sediment transport model relied on in the DEISs' impacts analysis, implications of results of other alternative analyses on the potential for impacts to occur, and the influence of basin-scale processes controlling the distribution and susceptibility of spawning habitat in the context of FRE operation effects. These three topics are discussed below. The collective information is expected to inform the design of mitigation operations that could potentially reduce or avoid significant effects to mainstem spawning habitat for Chinook salmon both within the operational footprint and downstream.

Predictive Limitations of HEC-RAS Model

Overall, the results are illustrative of ways in which sediment transport and deposition predictions, and thus their implications regarding impacts of FRE operations, depend on how a model is set up. Models are never true representations, so their usefulness reflects uncertainty in, and relevance of, the input data, assumptions, parameterizations, and equations built into them (Box 1979). Different inputs and model formulations will determine whether a predicted effect will have physical significance, what the corresponding biologic outcome will be, and thus what impacts would need to be mitigated for.

As summarized in Section 3, the HEC-RAS sediment transport model relied on by the DEISs for inferring impacts involved certain specific settings, assumptions, and internal coding algorithms that strongly influenced the outcome and subsequent interpretations, where changes in each could result in materially different outcomes and conclusions. Among the more influential aspects of the DEISs' model that warrant special caution include the following considerations:

- The DEISs' model calculated total sediment load (i.e., bedload and suspended combined) using the Ackers-White equation instead of one tailored to specifically bedload. The Ackers-White equation was developed based on flume data for sand and fine gravel transport. Besides the feature common to all sediment transport equations where the prediction error of the Ackers-White equation is characteristically within +/- two orders of magnitude (or more) in gravel bed streams (e.g., Barry et al. 2004), setting the model to simulate total sediment load for the DEISs precludes discerning impacts specific to Chinook salmon spawning habitat. This is because the erosion and deposition changes ascribed to FRE operations reflect in large part simulation of the transport of wash load (i.e., ultrafines) and sand, whereas effects should be linked more directly to transport and deposition of a certain size range of gravel and cobble stones characteristic of Chinook salmon spawning gravels (cf. Kondolf and Wolman 1993). These concerns were accounted for more directly in this assessment by using the Wilcock and Crowe (2003) bedload transport equation for sand and gravel/cobble built into HEC-RAS and Parker's (1990) bedload transport equation for gravel/cobble. Both equations predict fractional bedload transport rates

of different grain sizes and are thus better suited for evaluating potential effects to salmon spawning habitat.

- The DEISs' HEC-RAS model formulation was based on assuming bedload-sized material comprised 10% of the total estimated loading from upstream. Ward and Russell (1994) estimated 60% fine and 40% coarse sediments were delivered to channels by landslides in the basin, and that input was estimated to exceed the amounts of material delivered from surface erosion by a factor of 10 (Sullivan and Clark 1994). The effect of simulating different proportions of bedload to suspended load was not evaluated. Nonetheless, this feature of the DEISs simulation is pointed out because it will have affected the interpretation of the results in the impacts analysis.
- The HEC-RAS model is coded in a way that appears to result in distributing externally input sediment mass within the simulated drainage network, and thus tends to lead to predictions of aggradation overall. The results showed this to be the case even with no externally supplied sediment. It was noted that in addition to smoothing out the longitudinal profile, the DEISs' model will 'fill' portions of the channel outside the specified active bed limits including in the overbank. It is not clear in the DEISs whether the depths of aggradation reported include or exclude the volume of sediment simulated to deposit at other locations. The resulting change in bed elevation will directly influence subsequent prediction of deposition and erosion. Given that, caution is warranted because estimates of annual sediment loads vary for the upper Chehalis River basin; for example:
  - Ward and Russell (1994) estimated average delivery to streams on Weyerhaeuser lands upstream of RM 107 to be on the order of 3 tons/acre/year, which translates to approximately 134,000 tons per year at RM 107 above Rock Creek and Pe Ell (drainage area ≈ 70 square miles according to StreamStats).
  - Nelson and Dubé (2016) estimated a typical basin sediment yield of approximately 3,370 tons per square mile per year above Pe Ell, or approximately 236,000 tons per year at RM 107.
  - Using the flows in Table 2 and drainage area ratios to approximate comparable flows at the various boundary condition locations where a sediment discharge rating curve was specified in the DEISs' model (cf. Ecology 2020), the total average annual sediment loading from upstream was estimated to be approximately 120,000 tons per year at RM 107.
- The HEC-RAS model has a feature that allows specification of a scour depth limit to simulate degradation relative to the starting bed elevation. At cross-sections where the bottom was composed of primarily bedrock, the scour depth parameter was set in the DEISs' model to zero feet; elsewhere, it was set up to a maximum value of 5 feet. Implementing this limiting parameter in the model can confound predictions of aggradation at other locations, and can also be associated with predictions of deep scouring down to the limit at locations where little to no scour would be expected. To get a better sense of the sensitivity of the model to this

parameterization, simulations using the DEISs' model parameterization of scour depth were compared with the case where the bed elevation is prevented from degrading in the simulation.

In addition, as noted in Section 3, channel roughness coefficients and ineffective flow parameters in the DEISs' model resulted in atypical predictions of hydraulic properties in the main channel in some reaches. Specifically, Manning's n values were modified in the reach upstream of the FRE location to emulate more typical sub-critical flow conditions, and ineffective flow geometry was modified at various locations to reflect slower velocity floodplain areas. In updating the model, the changes that were made to the respective parameterizations would inherently result in differences in aggradation predictions compared with what was presented in the DEISs.

The results of runs using the updated model indicated the predictions were sensitive to the sediment transport equation, specified sediment loading rate, and scour depth limit applied. Depending on the combination, long-term aggradation was either predicted or was not predicted at a given location. Patterns also varied depending on grain size. These factors all require further examination as to their influence on model predictions. At present, the modified model runs indicate that conclusions in the DEISs regarding impacts of FRE operation on Chinook salmon spawning habitat require more detailed and specific inspection.

Overall, the modified HEC-RAS model results indicate that the areas with highest densities of Chinook salmon spawning activity, namely the 2 to 3 miles immediately downstream of Fisk Falls and the approximately 4- to 5-mile reach in the Pe Ell valley, appear to be least affected by effects of FRE operations on coarse sediment transport and deposition. There were negligible differences predicted in sand aggradation rates along the entire length of the river between the with- and without-FRE scenarios. The greatest likelihood of aggradation was predicted to occur for gravels in the reach approximately 0.5 to 2.5 miles upstream of the proposed FRE facility location. However, it is unclear if the predicted aggradation rates are sufficiently large enough to result in impacts over the long term, whereas increased rates may even contribute to increased area available for spawning.

Insights From the More Detailed Analyses

Additional insights were gained regarding the river's ability to process coarse sediments downstream by evaluating (i) the capacity of the channel to transport sediment at a given cross-section in terms of grain size mobility and predicted coarse sediment transport rates, and (ii) the difference in transport capacity between successive cross-sections to characterize whether the intervening segment of channel bed would be expected to exhibit an aggradational or degradational tendency (also termed 'trapping efficiency').

The incipient motion calculations indicated that frequent, small magnitude floods are capable of mobilizing gravels of the size that are used by Chinook salmon for spawning upstream of Elk Creek. Recking et al.'s (2016) equation for minimum dimensionless shear stress for full mobility as a function of

slope indicates critical values of τ^*=0.05 between the FRE facility and Fisk Falls, and τ^*=0.04 in the Pe Ell valley and downstream to the South Fork. These values are exceeded at all major spawning habitat locations upstream of Elk Creek (RM 100.2) at the 2-year flood (Figure 12). Kondolf and Wolman (1993) reported a general range of median grain size (D_{50}) values used by Chinook salmon between 11 mm and 80 mm. The 2-year flood was predicted to mobilize native gravel and cobble substrates with D_{50} values smaller than 80 mm at effectively all locations upstream of the FRE facility (Figure 12). Thus, gravels and cobbles used by Chinook salmon for spawning would be expected to be available for transport downstream to the major spawning areas above Elk Creek.

Calculated bedload transport rates using both the Parker (1990) and Wilcock and Crowe (2003) equations were extremely high in magnitude. This result appeared to be a consequence of the high shear stresses predicted by the HEC-RAS model. The same is true of the Ackers-White equation applied in the DEISs' HEC-RAS model. The Parker equation generally predicted transport rates that were approximately two to three times higher than predicted by the Wilcock and Crowe equation. Thus, volumetric changes in the Chehalis River predicted by bedload transport equations should not be considered accurate representations of expected magnitudes of bed elevation changes over time. However, relative differences in transport rates between cross-sections, and resulting calculations of net directional change in volume in terms of aggradational or degradational tendency, can still be useful for identifying segments of the river more susceptible to deposition during FRE operations in terms of transport capacity differences. That knowledge in turn can be used to help identify Chinook salmon spawning habitats that are more sensitive to deposition, and design operations accordingly that avoid or minimize potential for related impacts to occur. The analysis performed here suggests that the two reaches with the most extensive historic mainstem spawning activity, namely the first 2.5 miles below Fisk Falls and in the PE Ell Valley, have strongest aggradational tendencies at their upstream ends proximal to the reach scale decreases in gradient, and tend to be closer to conditions of equilibrium transport of gravels downstream.

The bedload transport capacity predictions based on the Parker (1990) equation indicate that the 2-year flood is capable of fully mobilizing the surface armor layer of spawning substrates everywhere in the river upstream of Elk Creek. The predicted D_{50} and D_{90} values of the bedload predicted by the equation effectively mirror the grain size distributions in Figure 11. In terms of a general model of bedload transport of coarse substrates, the state of equal mobility of all grain size fractions in the surface armor layer (cf. Parker and Toro-Escobar 2002) is achieved at relatively low flood flows. The results imply that gravels trapped upstream temporarily during FRE operations would be transported downstream subsequently at relatively low flood flows such that a significant, long-term decline in spawning substrate availability in the Pe Ell valley reach is unlikely. Coarse bedload transport rates are predicted to be highest upstream of Fisk Falls, in the vicinity of the FRE facility location, and in the canyon reach downstream.

The additional analysis results imply that the major spawning areas below Fisk Falls and in the Pe Ell valley reach will continue to receive spawning-size substrates from upstream, and that coarse sediment transport processes in those reaches may not be susceptible to significant effects of FRE operations.

Influence of Basin-Scale Processes on Interpretations of Effect

The longitudinal elevation profile of the Chehalis River in the HEC-RAS model indicates there are two reaches where most long-term gravel and cobble deposition would be expected, both with- and without-FRE operation (Figure 23):

- Below the slope break at Fisk Falls, and
- Below the slope break where the river enters the Pe Ell valley.

As noted above, these areas correspond with major historic Chinook salmon spawning areas both before (Phinney et al. 1975) and after Fisk Falls was modified in 1970 and 1980 to allow upstream passage (Light and Herger 1994; WG and Anchor 2017; WDFW redd count data). However, Light and Herger (1994) noted that substrates in the spring Chinook salmon dominant-use-zone between Fisk Falls and the Pe Ell valley were mostly boulder and bedrock with patches of gravel occurring most commonly at bends. Chinook salmon redds were considered especially vulnerable to scour in the mainstem. Spawning gravels showed little evidence of fine sediment intrusion, where observed surface and sub-surface fines were not abundant. Fines appeared to be transported efficiently through the system. These observations are consistent with the incipient motion and bedload transport capacity calculations indicating a high transport capacity in the river overall.

The reach slope and transport capacity are particularly high upstream of Fisk Falls, and accordingly, there appear to be few spawning gravel deposits presently based on screening level assessments of spawning gravel retention project opportunities (Kleinschmidt 2020; Kleinschmidt 2023). Although the maximum extent of inundation is within a mile upstream of Fisk Falls, the incipient motion and Parker (1990) equation bedload transport rate results indicate that gravel and cobble settling out within or above Fisk Falls would be expected to be re-entrained and deposit below Fisk Falls in successive high flow events.

Figure 23
Longitudinal Elevation Profile of the Chehalis River Thalweg in the DEIS's HEC-RAS Model and Simulated 2-year Flood Level Upstream of the Newaukum River Confluence. Five Distinct Large Scale Slope Breaks Are Evident in Addition to the Highly Localized Geologic Control at Rainbow Falls, at the Locations Indicated by the Vertical Dashed Lines, with Corresponding Regressed Reach Slopes Derived from the Water Surface Profile. Inset: Predicted Peak Temporary Reservoir Levels Associated with Specific Flood Recurrence Intervals and the 2007 Flood Event.

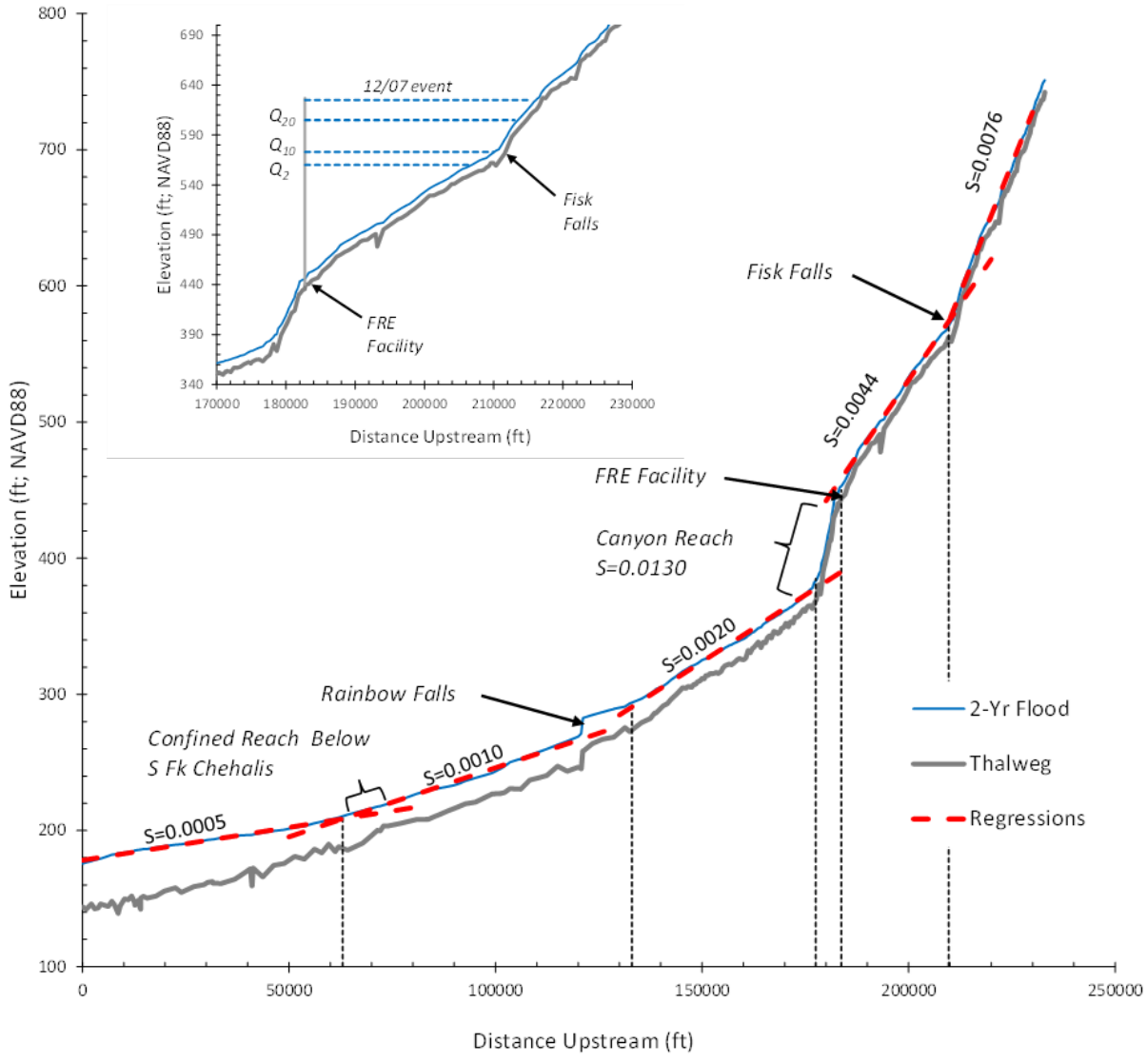

Given the high transport capacity in the vicinity of Pe Ell and upstream, it is plausible that the availability of key Chinook salmon spawning habitat in the river depends primarily on the frequency and spatial extent of episodic mass wasting inputs over large areas, similar to various other streams in western

Washington and Oregon (e.g., Everest and Meehan 1981; Benda and Dunne 1997; Miller et al. 2008). Such events are relatively infrequent, with records indicating their having occurred three times in the upper Chehalis basin over the past 50+ years, in 1972, 1990, and 2007. The 2007 event was associated with substantially more landslide inputs than the other two years (Sullivan and Carlson 1994; Smith and Wenger 2001; Nelson and Dubé 2016). Sediment sampling and corresponding gravel characterizations performed for the DEISs consequently may not have been representative of conditions in most years, and may have reflected the unusually large landslide volume delivered to the channel during the 2007 event (Nelson and Dubé 2016).

Consistent with the processes described by Miller et al. (2008), a hypothesis can be formulated that mainstem spawning habitat quantities within the inundation zone and downstream fluctuate over time. Smith and Wenger (2001) reported landslides to be the primary source of sediments to the upper Chehalis River. Montgomery et al. (1998) found the upper Chehalis watershed to have among the greatest number of landslides per unit drainage area in western Washington and Oregon. Quantities likely increased substantially after episodic, major events like 1972, 1990, and 2007, but given the high transport capacity and low threshold for motion indicated in this assessment, spawning gravel quantities would be expected to decrease over time as the material is moved downstream until the next major event (e.g., WG and Anchor 2017). Moreover, with implementation of more protective forest management practices compared with historic times, it is assumed that landslide input volumes and rates should be less extensive in the future and that this may lead to reduced future availability of spawning habitat overall. Noting that the spawning habitat characterizations in Phinney et al. (1975) and in Weyerhaeuser's watershed analysis completed in 1994 were completed not long after the major January 1972 and January 1990 events, respectively, it is possible that spring Chinook salmon spawning habitat availability in the upper Chehalis River mainstem may be lower in years or decades prior to the next major disturbance event.

The grain size specific results suggest that spawning habitat availability may increase particularly between HEC-RAS model RM 110 and RM 112 in years following large scale episodic sediment inputs from landslides. However, that reach may also be prone to excessive scour in more years than in the higher density spawning areas given the higher transport capacity, consistent with the observations of Light and Herger (1994). In years between significant landslide events, redd scour may become increasingly prevalent in that reach irrespective of FRE operations until the next event because of local sediment transport rate imbalances developing as more material is transported downstream than is supplied from upstream (cf. DeVries 2008).

References

Barry, J.J., J.M. Buffington, and J.G. King, 2004. A general power equation for predicting bed load transport rates in gravel bed rivers. Water Resources Research, 40, W10401, doi:10.1029/2004WR003190.

Benda, L.E., and T. Dunne, 1997. Stochastic forcing of sediment routing and storage in channel networks. Water Resources Research 33(12): 2865-2880.

Box, G.E., 1979. Some problems of statistics and everyday life. Journal of the American Statistical Association 74(365): 1-4.

Buffington, J.M., and D.R. Montgomery, 1997. A systematic analysis of eight decades of incipient motion studies, with special reference to gravel-bedded rivers. Water Resources Research, 33(8): 1993-2029.

Comiti, F., L. Mao, A. Wilcox, E.E. Wohl, and M.A. Lenzi. 2007. Field-derived relationships for flow velocity and resistance in high-gradient streams. Journal of Hydrology, 340(1-2): 48-62.

Corps (United States Army Corps of Engineers), 2020. Chehalis River Basin Flood Damage Reduction Project: NEPA Environmental Impact Statement. Seattle District.

DeVries, P., 2002. Bedload layer thickness and disturbance depth in gravel bed streams. J. Hydraulic Engineering 128: 983-991.

DeVries, P., 2008. Bed disturbance processes and the physical mechanisms of scour in salmonid spawning habitat. Pages 121-147 in Sear, D.A., and P. DeVries, editors. Salmonid spawning habitat in rivers: Physical controls, biological responses, and approaches to remediation. American Fisheries Society, Symposium 65, Bethesda, Maryland.

DeVries, P., and R. Aldrich, 2015. Assessment Approach for Identifying Compatibility of Restoration Projects with Geomorphic and Flooding Processes in Gravel Bed Rivers. Environmental Management, 10.1007/s00267-015-0518-9, 549-568.

Ecology (Washington Department of Ecology), 2020. State Environmental Policy Act Draft Environmental Impact Statement: Proposed Chehalis River Basin Flood Damage Reduction Project. Publication No.: 20-06-002.

Elliot, B., and L. Karpack, 2014. Chehalis Basin Strategy: Reducing Flood Damage and Enhancing Aquatic Species – Development and Calibration of Hydraulic Model. Watershed Science & Engineering memorandum to R. Montgomery, Anchor QEA. July 22.

Everest, F.H., and W.R. Meehan, 1981. Forest management and anadromous fish habitat productivity. Transactions 46th N. Am. Wildlife and Nat. Resources Conf., p. 521-530.

Ferguson, J., N. Kendall, and R. Vadas, Jr., 2017. Literature review of the potential changes in aquatic and terrestrial systems associated with a seasonal flood retention only reservoir in the Upper Chehalis Basin. Memorandum to WDFW, March.

Hanes, D.M., and A.J. Bowen, 1985. A granular-fluid model for steady intense bed-load transport. Journal of Geophysical Research: Oceans, 90(C5): 9149-9158.

Hill, A. (Anchor QEA) and L. Karpack (Watershed Science & Engineering), 2019. Memorandum to: Andrea McNamara Doyle and Chrissy Bailey, Office of Chehalis Basin. Regarding: Chehalis River Basin Climate Change Flows and Flooding Results. May 6, 2019.

Kleinschmidt (Kleinschmidt Associates), 2020. Chehalis Basin Strategy: Draft Mitigation Opportunities Assessment, Reducing Flood Damage and Restoring Aquatic Species Habitat. Report prepared for Chehalis River Basin Flood Control Zone District. June.

Kleinschmidt (Kleinschmidt Associates), 2023. Chehalis River FRE Facility Mitigation: Chinook Salmon Spawning Gravel Mitigation Opportunities Assessment. Draft Technical Memorandum to Chehalis River Basin Flood Control Zone District. January.

Kondolf, G.M., and M.G. Wolman, 1993. The sizes of salmonid spawning gravels. Water Resources Research 29(7): 2275-2285.

Light, J., and L. Herger, 1994. Appendix F: Chehalis headwaters watershed analysis fish habitat assessment. Weyerhaeuser Company. Available: https://fortress.wa.gov/dnr/protectionsa/ApprovedWatershedAnalyses.

Miller, D.J., K. Burnett, and L. Benda, 2008. Factors controlling availability of spawning habitat for salmonids at the basin scale. Pages 103-120 in Sear, D.A., and P. DeVries, editors. Salmonid spawning habitat in rivers: Physical controls, biological responses, and approaches to remediation. American Fisheries Society, Symposium 65, Bethesda, Maryland.

Montgomery, D.R., K. Sullivan, and H.M. Greenberg, 1998. Regional test of a model for shallow landsliding. Hydrological Processes, 12(6): 943-955.

Nelson, A., and K. Dubé, 2016. Channel response to an extreme flood and sediment pulse in a mixed bedrock and gravel-bed river. Earth Surface Processes and Landforms 41(2): 178-195.

Parker, G., 1990. Surface-based bedload transport relation for gravel rivers. Journal of Hydraulic Research 28(4): 417-436.

Parker, G., and C.M. Toro-Escobar, 2002. Equal mobility of gravel in streams: The remains of the day. Water Resources Research 38(11), 1264, doi:10.1029/2001WR000669.

Phinney, L. A., P. Bucknell, and R.W. Williams, 1975. A catalog of Washington streams and salmon utilization, Volume 2: Coastal regions. Washington Department of Fisheries.

Pitlick, J., Y. Cui, and P. Wilcock, 2009. Manual for computing bedload transport using BAGS (Bedload Assessment for Gravel-bed Streams) Software. Gen. Tech. Rep. RMRS-GTR-223. Fort Collins, CO: U.S. Department of Agriculture, Forest Service, Rocky Mountain Research Station. 45 p.

Recking, A., 2010. A comparison between flume and field bed load transport data and consequences for surface-based bed load transport prediction. Water Resources Research 46, W03518, doi:10.1029/2009WR008007.

Recking, A., G. Piton, D. Vazquez-Tarrio, and G. Parker. 2016. Quantifying the morphological print of bedload transport. Earth Surface Processes and Landforms 41(6): 809-822.

Richards, K., 1982. Rivers: Form and process in alluvial channels. Methuen, London. 361 p.

Ronne L., N. VanBuskirk, and M. Litz, 2020. Spawner Abundance and Distribution of Salmon and Steelhead in the Upper Chehalis River, 2019 and Synthesis of 2013-2019, FPT 20-06 Washington Department of Fish and Wildlife, Olympia, Washington

Schmidt, L.J., and J.P. Potyondy, 2004. Quantifying channel maintenance instream flows: an approach for gravel-bed streams in the Western United States. Gen. Tech. Rep. RMRS-GTR-128. Fort Collins, CO: U.S. Department of Agriculture, Forest Service, Rocky Mountain Research Station. 33 p.

Smith, C.J., and M. Wenger, 2001. Salmon and steelhead habitat limiting factors: Chehalis basin and nearby drainages Water Resource Inventory Areas 22 and 23. Final report, Washington State Conservation Commission. May.

Sullivan, K., and J. Clark, 1994. Appendix B: Chehalis headwaters watershed analysis surface erosion assessment. Weyerhaeuser Company. Available: https://fortress.wa.gov/dnr/protectionsa/ApprovedWatershedAnalyses.

Sullivan, K., and K. Carlson, 1994. Appendix C: Chehalis headwaters watershed analysis hydrologic assessment. Weyerhaeuser Company. Available: https://fortress.wa.gov/dnr/protectionsa/ApprovedWatershedAnalyses.

Ward, J., and P. Russell, 1994. Chehalis headwaters watershed analysis: Appendix A, mass wasting assessment. Weyerhaeuser Company. Available: https://fortress.wa.gov/dnr/protectionsa/ApprovedWatershedAnalyses.

WG and Anchor (Watershed GeoDynamics and Anchor QEA, LLC), 2017. Chehalis Basin Strategy: Geomorphology, Sediment Transport, and Large Woody Debris Report – Reducing Flood Damage and restoring Aquatic Species Habitat.

Wilcock, P.R., A.F. Barta, C.C. Shea, G.M. Kondolf, W.G. Matthews, and J. Pitlick, 1996. Observations of flow and sediment entrainment on a large gravel-bed river. Water Resources Research 32(9): 2897-2909.

Wilcock, P.R., and J.C. Crowe, 2003. Surface-Based Transport Model for Mixed-Size Sediment. Journal of Hydraulic Engineering 129(2): 120-128.

Wilcox, A.C., and E.E. Wohl, 2007. Field measurements of three-dimensional hydraulics in a step-pool channel. Geomorphology, 83(3-4): 215-231.

Wohl, E.E., D.M. Thompson, and A.J. Miller, 1999. Canyons with undulating walls. Geological Society of America Bulletin, 111(7): 949-959.

Wolman, M.G., and J.P. Miller, 1960. Magnitude and frequency of forces in geomorphic processes. The Journal of Geology 68(1): 54-74.

Wong, M., and G. Parker, 2006. Reanalysis and correction of bed-load relation of Meyer-Peter and Müller using their own database. Journal of Hydraulic Engineering 132(11): 1159-1168.

ATTACHMENT 1

SUMMARY OF DEISs' HEC-RAS MODEL REPARAMETERIZATION FOR THIS ANALYSIS: MANNING'S *N* ROUGHNESS COEFFICIENTS AND INEFFECTIVE FLOW GEOMETRY

Summary of Model Reparameterization																									
Unchanged or Modified?	River Station	Kleinschmidt								River Station	QEA DEIS														
		Manning's Roughness Coefficents									Manning's Roughness Coefficents														
modified	**118.1741**	0.08	0.06	0.08	0.025	0.08				**118.1741**	0.08	0.045	0.08												
modified	**118.1287**	0.08	0.06	0.08	0.025	0.08				**118.1287**		0.045	0.08												
modified	**118.0959**	0.08	0.06	0.08	0.025	0.08				**118.0959**	0.08	0.045	0.08												
modified	**118.0556**	0.08	0.06	0.08	0.025	0.08				**118.0556**	0.08	0.045	0.08												
modified	**118.024**	0.08	0.06	0.08	0.025	0.08				**118.024**	0.08	0.045	0.08												
modified	**117.9683**	0.08	0.06	0.08	0.025	0.08				**117.9683**	0.08	0.045	0.08												
modified	**117.9196**	0.08	0.06	0.08	0.025	0.08				**117.9196**	0.08	0.045	0.08												
modified	**117.8451**	0.08	0.06	0.08	0.025	0.08				**117.8451**	0.08	0.045	0.08												
modified	**117.7661**	0.08	0.06	0.08	0.025	0.08				**117.7661**	0.08	0.045	0.08												
modified	**117.7**	0.08	0.06	0.08	0.025	0.08				**117.7**	0.08	0.045	0.08												
modified	**117.6256**	0.08	0.06	0.08	0.025	0.08				**117.6256**	0.08	0.045	0.08												
modified	**117.551**	0.08	0.06	0.08	0.025	0.08				**117.551**	0.08	0.045	0.08												
modified	**117.5018**	0.08	0.06	0.08	0.025	0.08				**117.5018**	0.08	0.045	0.08												
modified	**117.4486**	0.08	0.06	0.08	0.025	0.08				**117.4486**	0.08	0.045	0.08												
modified	**117.392**	0.08	0.06	0.08	0.025	0.08				**117.392**	0.08	0.045	0.08												
modified	**117.3395**	0.08	0.06	0.08	0.025	0.08				**117.3395**	0.08	0.045	0.08												
modified	**117.2704**	0.08	0.06	0.08	0.025	0.08				**117.2704**	0.08	0.045	0.08												
modified	**117.2025**	0.08	0.06	0.08	0.025	0.08				**117.2025**	0.08	0.045	0.08												
modified	**117.1311**	0.08	0.06	0.08	0.025	0.08	0.025	0.08		**117.1311**	0.08	0.045	0.08												
modified	**117.0519**	0.08	0.06	0.08	0.025	0.08	0.025	0.08		**117.0519**	0.08	0.045	0.08												
modified	**116.9695**	0.08	0.06	0.08	0.025	0.08	0.025	0.08		**116.9695**	0.08	0.045	0.08												
modified	**116.924**	0.08	0.06	0.08	0.025	0.08				**116.924**	0.08	0.045	0.08												
modified	**116.8766**	0.08	0.06	0.08	0.025	0.08				**116.8766**	0.08	0.045	0.08												
modified	**116.8068**	0.08	0.025	0.08	0.06	0.08				**116.8068**	0.08	0.045	0.08												
modified	**116.75**	0.08	0.025	0.08	0.06	0.08				**116.75**	0.08	0.045	0.08												
modified	**116.6825**	0.08	0.025	0.08	0.06	0.08				**116.6825**	0.08	0.045	0.08												
modified	**116.6043**	0.08	0.025	0.08	0.06	0.08				**116.6043**	0.08	0.045	0.08												
modified	**116.5157**	0.08	0.025	0.08	0.06	0.08				**116.5157**	0.08	0.045	0.08												
modified	**116.4459**	0.08	0.025	0.08	0.025	0.08	0.06	0.08		**116.4459**	0.08	0.045	0.08												
modified	**116.3723**	0.08	0.025	0.08	0.06	0.08				**116.3723**	0.08	0.045	0.08												
modified	**116.31**	0.08	0.025	0.08	0.06	0.08				**116.31**	0.025	0.08	0.045	0.08											
modified	**116.26***	0.08	0.06	0.08	0.08					**N/A**	Interpolated cross section														
modified	**116.21**	0.08	0.025	0.08	0.06	0.08				**116.21**	0.03	0.08	0.025	0.045	0.08										
modified	**116.18***	0.08	0.06	0.08	0.08					**N/A**	Interpolated cross section														
modified	**116.14***	0.08	0.06	0.08	0.08					**N/A**	Interpolated cross section														
modified	**116.11***	0.08	0.06	0.08	0.08					**N/A**	Interpolated cross section														
modified	**116.07**	0.08	0.025	0.08	0.06	0.08				**116.07**	0.08	0.045	0.08												
modified	**115.94**	0.08	0.025	0.08	0.06	0.08				**115.94**	0.08	0.025	0.08	0.03	0.045	0.08									
modified	**115.83**	0.08	0.025	0.08	0.06	0.08				**115.83**	0.08	0.025	0.08	0.045	0.08										
modified	**115.73**	0.08	0.025	0.08	0.06	0.08				**115.73**	0.08	0.025	0.08	0.03	0.045	0.03	0.08								
modified	**115.68**	0.08	0.025	0.08	0.06	0.08				**115.68**	0.08	0.025	0.08	0.045	0.08										
modified	**115.6**	0.08	0.025	0.08	0.06	0.08				**115.6**	0.08	0.025	0.08	0.045	0.08										
modified	**115.55**	0.08	0.025	0.08	0.06	0.08				**115.55**	0.08	0.025	0.08	0.045	0.08										
modified	**115.47**	0.08	0.025	0.08	0.06	0.08				**115.47**	0.025	0.08	0.025	0.08	0.03	0.045	0.03	0.08							

Summary of Model Reparameterization																								
Unchanged or Modified?	River Station	Kleinschmidt								River Station	QEA DEIS													
		Manning's Roughness Coefficents									Manning's Roughness Coefficents													
modified	**115.4**	0.08	0.025	0.08	0.06	0.08				**115.4**	0.08	0.025	0.08	0.045	0.08									
modified	**115.25**	0.08	0.025	0.08	0.06	0.08				**115.25**	0.08	0.045	0.08											
modified	**115.21***	0.08	0.06	0.08	0.08					**N/A**	Interpolated cross section													
modified	**115.17**	0.08	0.025	0.08	0.06	0.08				**115.17**	0.08	0.025	0.08	0.045	0.08									
modified	**115.16***	0.08	0.077	0.06	0.08	0.08				**N/A**	Interpolated cross section													
modified	**115.14**	0.08	0.025	0.08	0.06	0.08				**115.14**	0.08	0.025	0.08	0.03	0.045	0.045	0.08							
modified	**115.12***	0.08	0.079	0.06	0.08	0.08				**N/A**	Interpolated cross section													
modified	**115.09**	0.08	0.025	0.08	0.06	0.08				**115.09**	0.08	0.025	0.08	0.045	0.08									
modified	**115.07***	0.08	0.077	0.06	0.08	0.08				**N/A**	Interpolated cross section													
modified	**115.04**	0.08	0.025	0.08	0.06	0.08				**115.04**	0.08	0.025	0.08	0.045	0.045	0.035	0.08							
modified	**115.02***	0.08	0.073	0.06	0.08	0.08				**N/A**	Interpolated cross section													
modified	**115**	0.08	0.025	0.08	0.06	0.08				**115**	0.08	0.025	0.08	0.045	0.08									
modified	**114.93**	0.08	0.025	0.08	0.06	0.08				**114.93**	0.08	0.025	0.08	0.045	0.045	0.045	0.08							
modified	**114.86**	0.08	0.025	0.08	0.06	0.08				**114.86**	0.025	0.08	0.045	0.08										
modified	**114.74**	0.08	0.025	0.08	0.06	0.08				**114.74**	0.08	0.025	0.08	0.045	0.08									
modified	**114.56**	0.08	0.025	0.08	0.06	0.08				**114.56**	0.08	0.045	0.08											
modified	**114.48***	0.08	0.071	0.06	0.08	0.08				**N/A**	Interpolated cross section													
modified	**114.41***	0.08	0.075	0.06	0.08	0.08				**N/A**	Interpolated cross section													
modified	**114.33**	0.08	0.025	0.08	0.06	0.08				**114.33**	0.08	0.025	0.08	0.045	0.08									
modified	**114.26***	0.08	0.078	0.06	0.08	0.08	0.08			**N/A**	Interpolated cross section													
modified	**114.20***	0.08	0.076	0.06	0.08	0.08	0.08			**N/A**	Interpolated cross section													
modified	**114.13**	0.08	0.025	0.08	0.06	0.08	0.08			**114.13**	0.08	0.025	0.08	0.045	0.08	0.025	0.08							
modified	**114.05***	0.08	0.076	0.06	0.08	0.08	0.08			**N/A**	Interpolated cross section													
modified	**113.97***	0.08	0.073	0.06	0.08	0.08	0.08			**N/A**	Interpolated cross section													
modified	**113.89**	0.08	0.06	0.08						**113.89**	0.08	0.035	0.08											
modified	**113.82**	0.08	0.06	0.08	0.025	0.08				**113.82**	0.08	0.025	0.08	0.025	0.08	0.035	0.08	0.025	0.08					
modified	**113.75**	0.08	0.06	0.08	0.025	0.08				**113.75**	0.025	0.08	0.035	0.035	0.035	0.08	0.025	0.08						
modified	**113.69**	0.025	0.08	0.06	0.08	0.025	0.08			**113.69**	0.025	0.08	0.035	0.08	0.025	0.08								
modified	**113.64**	0.08	0.06	0.08	0.025	0.08				**113.64**	0.08	0.035	0.035	0.035	0.025	0.08								
modified	**113.56**	0.08	0.06	0.08	0.025	0.08				**113.56**	0.08	0.025	0.08	0.035	0.08	0.025	0.08							
modified	**113.47**	0.08	0.06	0.08	0.025	0.08				**113.47**	0.08	0.035	0.035	0.035	0.08									
modified	**113.42**	0.08	0.06	0.08	0.025	0.08				**113.42**	0.08	0.035	0.08	0.025	0.08									
modified	**113.25**	0.08	0.06	0.08	0.025	0.08				**113.25**	0.08	0.035	0.08	0.025	0.08									
modified	**113.07**	0.08	0.06	0.08	0.025	0.08				**113.07**	0.08	0.035	0.08											
modified	**112.99**	0.08	0.06	0.08	0.025	0.08				**112.99**	0.08	0.035	0.035	0.08	0.025	0.08								
modified	**112.86**	0.08	0.06	0.08	0.025	0.08				**112.86**	0.08	0.035	0.08	0.025	0.08									
modified	**112.75**	0.08	0.06	0.08	0.025	0.08				**112.75**	0.08	0.035	0.035	0.035	0.08	0.025	0.08							
modified	**112.67**	0.08	0.06	0.08	0.025	0.08				**112.67**	0.08	0.035	0.08	0.025	0.08									
modified	**112.59**	0.08	0.06	0.08	0.025	0.08				**112.59**	0.08	0.04	0.035	0.04	0.08									
modified	**112.51**	0.08	0.06	0.08	0.025	0.08				**112.51**	0.08	0.035	0.035	0.08										
modified	**112.44**	0.08	0.06	0.08	0.025	0.08	0.08			**112.44**	0.08	0.035	0.08	0.025	0.08									
modified	**112.34**	0.08	0.06	0.08	0.025	0.08				**112.34**	0.08	0.035	0.035	0.035	0.08									
modified	**112.21**	0.08	0.06	0.08	0.025	0.08				**112.21**	0.08	0.035	0.035	0.04	0.025	0.08								
modified	**112.07**	0.08	0.06	0.08	0.025	0.08				**112.07**	0.08	0.035	0.08											

Summary of Model Reparameterization																								
Unchanged or Modified?	River Station	Kleinschmidt								River Station	QEA DEIS													
		Manning's Roughness Coefficents									Manning's Roughness Coefficents													
modified	**111.84**	0.08	0.06	0.08	0.025	0.08				**111.84**	0.08	0.035	0.025	0.08										
modified	**111.67**	0.08	0.06	0.08	0.025	0.08				**111.67**	0.08	0.035	0.025	0.08										
modified	**111.53**	0.08	0.06	0.08	0.025	0.08				**111.53**	0.08	0.035	0.08											
modified	**111.45**	0.08	0.06	0.08	0.025	0.08	0.08			**111.45**	0.08	0.035	0.035	0.025	0.08	0.025	0.08							
modified	**111.31**	0.08	0.06	0.08	0.025	0.08	0.025			**111.31**	0.08	0.035	0.025	0.08	0.025									
modified	**111.22**	0.08	0.06	0.08	0.025	0.08				**111.22**	0.08	0.035	0.025	0.08										
modified	**111.04**	0.08	0.06	0.08	0.025	0.08				**111.04**	0.08	0.035	0.08	0.025	0.08									
modified	**110.81**	0.08	0.06	0.08	0.025	0.08				**110.81**	0.08	0.035	0.08											
modified	**110.65**	0.08	0.06	0.08	0.08	0.025	0.08			**110.65**	0.025	0.08	0.035	0.03	0.08	0.03	0.08	0.025	0.08					
modified	**110.61**	0.08	0.06	0.08	0.03	0.025	0.08			**110.61**	0.08	0.035	0.08	0.03	0.025	0.03	0.08							
modified	**110.51**	0.08	0.025	0.08	0.06	0.08	0.03	0.025	0.08	**110.51**	0.08	0.025	0.08	0.04	0.035	0.04	0.08	0.03	0.025	0.03	0.08			
modified	**110.38**	0.08	0.025	0.08	0.06	0.08	0.025	0.08		**110.38**	0.08	0.025	0.08	0.035	0.08	0.025	0.08							
modified	**110.25**	0.08	0.025	0.08	0.06	0.08				**110.25**	0.08	0.035	0.08											
modified	**110.18**	0.08	0.025	0.08	0.06	0.08				**110.18**	0.08	0.025	0.05	0.08	0.035	0.025	0.08							
modified	**110.08**	0.08	0.025	0.08	0.04	0.06	0.08	0.08		**110.08**	0.08	0.025	0.05	0.08	0.04	0.035	0.045	0.08	0.025	0.08				
modified	**109.99**	0.08	0.025	0.08	0.08	0.06	0.08			**109.99**	0.08	0.025	0.08	0.03	0.08	0.03	0.08	0.045	0.08					
modified	**109.87**	0.08	0.025	0.08	0.045	0.06	0.08			**109.87**	0.08	0.025	0.08	0.03	0.08	0.045	0.045	0.04	0.08					
modified	**109.76**	0.08	0.025	0.08	0.06	0.08				**109.76**	0.08	0.025	0.08	0.045	0.08									
modified	**109.63**	0.08	0.025	0.08	0.06	0.08				**109.63**	0.08	0.025	0.08	0.025	0.045	0.045	0.04	0.08						
modified	**109.53**	0.08	0.025	0.08	0.06	0.08				**109.53**	0.08	0.035	0.045	0.035	0.08									
modified	**109.36**	0.08	0.025	0.08	0.06	0.08	0.06	0.08		**109.36**	0.08	0.025	0.045	0.08										
modified	**109.26**	0.08	0.025	0.08	0.04	0.06	0.08			**109.26**	0.08	0.025	0.08	0.04	0.045	0.04	0.08							
modified	**109.15**	0.08	0.025	0.08	0.06	0.08	0.03			**109.15**	0.08	0.025	0.08	0.045	0.08	0.03								
modified	**109.02**	0.08	0.025	0.08	0.06	0.08				**109.02**	0.08	0.025	0.08	0.045	0.08									
modified	**108.88**	0.08	0.06	0.08	0.025	0.08				**108.88**	0.08	0.045	0.08											
modified	**108.85**	0.08	0.06	0.08	0.025	0.08				**108.85**	0.08	0.045	0.045	0.08	0.025	0.08								
modified	**108.77**	0.08	0.06	0.08	0.025	0.08				**108.77**	0.08	0.025	0.08	0.045	0.08	0.025	0.08							
modified	**108.69**	0.08	0.045	0.06	0.08	0.025	0.08			**108.69**	0.08	0.05	0.08	0.025	0.08	0.025	0.08	0.045	0.045	0.045	0.08	0.025	0.08	
modified	**108.53**	0.08	0.06	0.08						**108.53**	0.08	0.045	0.08											
modified	**108.47**	0.08	0.06	0.08	0.06	0.08				**108.47**	0.08	0.045	0.08											
modified	**108.425**	0.08	0.06	0.08						**108.425**	0.08	0.045	0.08											
modified	**108.4**	0.08	0.07	0.08						**108.4**	0.08	0.045	0.08											
modified	**108.36***	0.08	0.07	0.08						**N/A**	Interpolated cross section													
modified	**108.32***	0.08	0.07	0.08						**N/A**	Interpolated cross section													
modified	**108.28**	0.08								**108.28**	0.08	0.045	0.08											
modified	**108.23***	0.08	0.07	0.08						**N/A**	Interpolated cross section													
modified	**108.18**	0.08	0.07	0.08						**108.18**	0.08	0.045	0.08											
modified	**108.15***	0.08	0.07	0.08						**N/A**	Interpolated cross section													
modified	**108.11***	0.08	0.07	0.08						**N/A**	Interpolated cross section													
modified	**108.08**	0.08	0.07	0.08						**108.08**	0.08	0.045	0.08											
modified	**108.04***	0.08	0.07	0.08						**N/A**	Interpolated cross section													
modified	**107.995***	0.08	0.07	0.08						**107.995***	0.08	0.045	0.08											
modified	**107.95**	0.08	0.07	0.08						**N/A**	Surveyed Transect													
modified	**107.91**	0.08	0.07	0.08						**107.91**	0.08	0.045	0.08											

Summary of Model Reparameterization																						
Unchanged or Modified?	**River Station**	**Kleinschmidt**								**River Station**	**QEA DEIS**											
		Manning's Roughness Coefficents									**Manning's Roughness Coefficents**											
modified	**107.87***	0.08	0.07	0.08						**N/A**	Interpolated cross section											
modified	**107.83***	0.08	0.07	0.08						**N/A**	Interpolated cross section											
modified	**107.79**	0.08	0.07	0.08						**107.79**	0.08	0.045	0.08									
modified	**107.76***	0.08	0.07	0.08						**N/A**	Interpolated cross section											
modified	**107.72**	0.08	0.07	0.08						**107.72**	0.08	0.045	0.08									
modified	**107.71**	0.08	0.06	0.08						**107.71**	0.08	0.045	0.08									
modified	**107.62**	0.08	0.06	0.08	0.06	0.08				**107.62**	0.08	0.045	0.08									
modified	**107.52**	0.08	0.05	0.08						**107.52**	0.08	0.045	0.08									
modified	**107.43**	0.08	0.05	0.08						**107.43**	0.08	0.045	0.08									
modified	**107.33**	0.08	0.045	0.08						**107.33**	0.08	0.05	0.08									
modified	**107.24**	0.08	0.045	0.08						**107.24**	0.08	0.05	0.08									
modified	**107.14**	0.08	0.045	0.08						**107.14**	0.08	0.05	0.08									
modified	**107.11**	0.08	0.045	0.08						**107.11**	0.08	0.05	0.08									
unchanged	**107.1**	Bridge								**107.1**	Bridge											
modified	**107.09**	0.08	0.045	0.08						**107.09**	0.08	0.05	0.08									
modified	**107.03**	0.08	0.045	0.08						**107.03**	0.08	0.05	0.08									
modified	**106.9**	0.08	0.045	0.08						**106.9**	0.08	0.05	0.08									
modified	**106.8**	0.08	0.045	0.08						**106.8**	0.08	0.05	0.08									
modified	**106.72**	0.08	0.045	0.08						**106.72**	0.08	0.05	0.08									
modified	**106.62**	0.08	0.045	0.08						**106.62**	0.08	0.05	0.08									
modified	**106.53**	0.08	0.045	0.08						**106.53**	0.08	0.05	0.08									
modified	**106.43**	0.08	0.045	0.08						**106.43**	0.08	0.05	0.08									
modified	**106.4**	0.08	0.045	0.08						**106.4**	0.08	0.05	0.08									
unchanged	**106.39**	Bridge								**106.39**	Bridge											
modified	**106.38**	0.08	0.045	0.08						**106.38**	0.08	0.05	0.08									
modified	**106.31**	0.08	0.045	0.08						**106.31**	0.08	0.05	0.08									
modified	**106.2**	0.08	0.045	0.08						**106.2**	0.08	0.05	0.08									
modified	**106.09**	0.08	0.045	0.08						**106.09**	0.08	0.05	0.08									
modified	**106**	0.08	0.045	0.08						**106**	0.08	0.05	0.08									
modified	**105.91**	0.08	0.045	0.08						**105.91**	0.08	0.05	0.08									
modified	**105.82**	0.08	0.045	0.08	0.06	0.08				**105.82**	0.08	0.05	0.08									
modified	**105.73**	0.08	0.045	0.08	0.06	0.08				**105.73**	0.08	0.05	0.08									
modified	**105.64**	0.08	0.045	0.08						**105.64**	0.08	0.05	0.08									
modified	**105.53**	0.08	0.045	0.08						**105.53**	0.08	0.05	0.08									
modified	**105.44**	0.08	0.045	0.08	0.06	0.08				**105.44**	0.08	0.05	0.08									
modified	**105.35**	0.08	0.045	0.08	0.06	0.08				**105.35**	0.08	0.05	0.08									
modified	**105.26**	0.08	0.045	0.08	0.06	0.08				**105.26**	0.08	0.05	0.08									
modified	**105.16**	0.08	0.045	0.08	0.06	0.08				**105.16**	0.08	0.05	0.08									
modified	**105.07**	0.08	0.045	0.08	0.06	0.08				**105.07**	0.08	0.05	0.08									
modified	**104.97**	0.08	0.045	0.08	0.045	0.08				**104.97**	0.08	0.05	0.08									
modified	**104.85**	0.08	0.045	0.08						**104.85**	0.08	0.05	0.08									
modified	**104.75**	0.08	0.045	0.08						**104.75**	0.08	0.05	0.08									
modified	**104.68**	0.08	0.045	0.08						**104.68**	0.08	0.05	0.08									
modified	**104.58**	0.08	0.06	0.045	0.08					**104.58**	0.08	0.05	0.08									

Summary of Model Reparameterization																						
Unchanged or Modified?	River Station	Kleinschmidt								River Station	QEA DEIS											
		Manning's Roughness Coefficents									Manning's Roughness Coefficents											
modified	**104.49**	0.08	0.045	0.08						**104.49**	0.08	0.05	0.08									
modified	**104.39**	0.08	0.045	0.08						**104.39**	0.08	0.05	0.08									
modified	**104.31**	0.08	0.045	0.08						**104.31**	0.08	0.05	0.08									
modified	**104.21**	0.08	0.045	0.08						**104.21**	0.08	0.05	0.08									
modified	**104.1**	0.08	0.045	0.08						**104.1**	0.08	0.05	0.08									
modified	**104.01**	0.08	0.045	0.08						**104.01**	0.08	0.05	0.08									
modified	**103.92**	0.08	0.045	0.08						**103.92**	0.08	0.05	0.08									
modified	**103.83**	0.08	0.045	0.08						**103.83**	0.08	0.05	0.08									
modified	**103.73**	0.08	0.045	0.08						**103.73**	0.08	0.05	0.08									
modified	**103.64**	0.08	0.045	0.08						**103.64**	0.08	0.05	0.08									
modified	**103.54**	0.08	0.045	0.08						**103.54**	0.08	0.05	0.08									
modified	**103.44**	0.08	0.06	0.045	0.08					**103.44**	0.08	0.05	0.08									
modified	**103.37**	0.08	0.045	0.08						**103.37**	0.08	0.05	0.08									
modified	**103.26**	0.08	0.045	0.08						**103.26**	0.08	0.05	0.08									
modified	**103.17**	0.08	0.045	0.08						**103.17**	0.08	0.05	0.08									
modified	**103.08**	0.08	0.045	0.08						**103.08**	0.08	0.05	0.08									
modified	**102.98**	0.08	0.045	0.08						**102.98**	0.08	0.05	0.08									
modified	**102.89**	0.08	0.045	0.06	0.08					**102.89**	0.08	0.05	0.08									
modified	**102.79**	0.08	0.045	0.06	0.08					**102.79**	0.08	0.05	0.08									
modified	**102.68**	0.08	0.045	0.06	0.08					**102.68**	0.08	0.05	0.08									
modified	**102.6**	0.08	0.045	0.06	0.08					**102.6**	0.08	0.05	0.08									
modified	**102.51**	0.08	0.045	0.06	0.08					**102.51**	0.08	0.05	0.08									
modified	**102.41**	0.08	0.045	0.06	0.08					**102.41**	0.08	0.05	0.08									
modified	**102.38**	0.08	0.06	0.045	0.06	0.08				**N/A**	New Kleinschmidt surveyed cross sections											
modified	**102.36**	0.08	0.06	0.045	0.08					**N/A**	New Kleinschmidt surveyed cross sections											
modified	**102.31**	0.08	0.06	0.045	0.08					**102.31**	0.08	0.05	0.08									
modified	**102.29**	0.08	0.06	0.045	0.08					**N/A**	New Kleinschmidt surveyed cross sections											
modified	**102.26**	0.08	0.06	0.045	0.08					**N/A**	New Kleinschmidt surveyed cross sections											
modified	**102.23**	0.08	0.06	0.045	0.08					**102.23**	0.08	0.05	0.08									
modified	**102.13**	0.08	0.045	0.08						**102.13**	0.08	0.05	0.08									
modified	**102.04**	0.08	0.045	0.08						**102.04**	0.08	0.05	0.08									
modified	**101.92**	0.08	0.045	0.08						**101.92**	0.08	0.05	0.08									
modified	**101.85**	0.08	0.045	0.08						**101.85**	0.08	0.05	0.08									
modified	**101.8**	0.08	0.045	0.08						**101.8**	0.08	0.05	0.08									
modified	**101.549**	0.08	0.06	0.045	0.08					**101.549**	0.08	0.05	0.08									
modified	**101.334**	0.11	0.045	0.11						**101.334**	0.11	0.05	0.11									
modified	**101.12**	0.11	0.045	0.08	0.06	0.08				**101.12**	0.11	0.05	0.08									
modified	**100.95**	0.11	0.045	0.09						**100.95**	0.11	0.05	0.09									
modified	**100.76**	0.09	0.045	0.08						**100.76**	0.09	0.05	0.08									
modified	**100.44**	0.08	0.045	0.08						**100.44**	0.08	0.05	0.08									
modified	**100.43**	0.08	0.045	0.08						**100.43**	0.08	0.05	0.08									
unchanged	**100.425**	Bridge								**100.425**	Bridge											
unchanged	**100.41**	0.08	0.045	0.08						**100.41**	0.08	0.045	0.08									
unchanged	**100.4**	0.08	0.045	0.08						**100.4**	0.08	0.045	0.08									

Summary of Model Reparameterization																						
Unchanged or Modified?	River Station	Kleinschmidt									River Station	QEA DEIS										
		Manning's Roughness Coefficents										Manning's Roughness Coefficents										
unchanged	**100.16**	0.08	0.045	0.06							**100.16**	0.08	0.045	0.06								
unchanged	**99.77**	0.08	0.045	0.06							**99.77**	0.08	0.045	0.06								
unchanged	**99.19**	0.08	0.045	0.05							**99.19**	0.08	0.045	0.05								
unchanged	**98.95**	0.08	0.045	0.05							**98.95**	0.08	0.045	0.05								
unchanged	**98.47**	0.08	0.045	0.06							**98.47**	0.08	0.045	0.06								
unchanged	**98.455**	Bridge									**98.455**	Bridge										
unchanged	**98.44**	0.08	0.045	0.06							**98.44**	0.08	0.045	0.06								
unchanged	**98.165***	0.08	0.045	0.06							**98.165***	0.08	0.045	0.06								
unchanged	**97.89**	0.08	0.045	0.06							**97.89**	0.08	0.045	0.06								
unchanged	**97.875**	Bridge									**97.875**	Bridge										
unchanged	**97.86**	0.09	0.045	0.09							**97.86**	0.09	0.045	0.09								
modified	**97.49**	0.06	0.11	0.045	0.11						**97.49**	0.11	0.045	0.11								
modified	**97.06**	0.11	0.06	0.11	0.045	0.11					**97.06**	0.11	0.045	0.11								
unchanged	**97.01**	0.11	0.045	0.11							**97.01**	0.11	0.045	0.11								
unchanged	**97**	Inline Structure									**97**	Inline Structure										
modified	**96.95**	0.06	0.11	0.045	0.11						**96.95**	0.08	0.045	0.11								
unchanged	**96.85**	0.06	0.045	0.08							**96.85**	0.06	0.045	0.08								
unchanged	**96.32**	0.06	0.045	0.06							**96.32**	0.06	0.045	0.06								
unchanged	**95.96**	0.08	0.045	0.08							**95.96**	0.08	0.045	0.08								
unchanged	**95.9**	Lateral Structure									**95.9**	Lateral Structure										
modified	**95.5**	0.11	0.06	0.045	0.06						**95.5**	0.11	0.045	0.06								
unchanged	**95.3**	Lateral Structure									**95.3**	Lateral Structure										
unchanged	**95.16**	0.06	0.045	0.06							**95.16**	0.06	0.045	0.06								
unchanged	**94.78**	0.06	0.045	0.08							**94.78**	0.06	0.045	0.08								
unchanged	**94.77**	Bridge									**94.77**	Bridge										
unchanged	**94.76**	0.06	0.045	0.08							**94.76**	0.06	0.045	0.08								
unchanged	**94.28**	0.06	0.045	0.08							**94.28**	0.06	0.045	0.08								
unchanged	**94.26**	0.08	0.045	0.08							**94.26**	0.08	0.045	0.08								
unchanged	**94.2**	0.06	0.045	0.08							**94.2**	0.06	0.045	0.08								
unchanged	**93.79**	0.08	0.045	0.11							**93.79**	0.08	0.045	0.11								
unchanged	**93.57**	0.11	0.045	0.11							**93.57**	0.11	0.045	0.11								
unchanged	**93.44**	0.11	0.045	0.11							**93.44**	0.11	0.045	0.11								
unchanged	**93.03**	0.11	0.045	0.11							**93.03**	0.11	0.045	0.11								
unchanged	**92.27**	0.11	0.045	0.06							**92.27**	0.11	0.045	0.06								
unchanged	**91.77**	0.08	0.045	0.11							**91.77**	0.08	0.045	0.11								
modified	**91.533***	0.073	0.045	0.11							**N/A**	Interpolated cross section										
modified	**91.297***	0.067	0.045	0.11							**N/A**	Interpolated cross section										
unchanged	**91.06**	0.06	0.045	0.11							**91.06**	0.06	0.045	0.11								
modified	**90.740***	0.06	0.11	0.045	0.093						**N/A**	Interpolated cross section										
modified	**90.420***	0.06	0.11	0.045	0.077						**N/A**	Interpolated cross section										
unchanged	**90.1**	0.06	0.045	0.06							**90.1**	0.06	0.045	0.06								
modified	**89.68**	0.11	0.08	0.045	0.08	0.06					**N/A**	New Kleinschmidt surveyed cross sections										
modified	**89.65**	0.11	0.08	0.045	0.08	0.06					**N/A**	New Kleinschmidt surveyed cross sections										
modified	**89.61**	0.11	0.045	0.08	0.06						**89.61**	0.08	0.045	0.08								

Summary of Model Reparameterization																							
Unchanged or Modified?	**River Station**	**Kleinschmidt**								**River Station**	**QEA DEIS**												
		Manning's Roughness Coefficents									**Manning's Roughness Coefficents**												
modified	**N/A**	Removed b/c RM 88.9 intersected the new surveyed XS								**88.9**	0.08	0.045	0.08										
modified	**88.67**	0.06	0.11	0.045	0.11	0.06				**N/A**	New Kleinschmidt surveyed cross sections												
modified	**88.6**	0.06	0.11	0.045	0.11	0.06				**N/A**	New Kleinschmidt surveyed cross sections												
modified	**88.54**	0.06	0.11	0.06	0.045	0.06	0.045	0.11	0.11	**N/A**	New Kleinschmidt surveyed cross sections												
modified	**88.37**	0.06	0.11	0.06	0.045	0.11				**N/A**	New Kleinschmidt surveyed cross sections												
unchanged	**88.28**	0.08	0.045	0.1						**88.28**	0.08	0.045	0.1										
unchanged	**88.2**	Lateral Structure								**88.2**	Lateral Structure												
unchanged	**88.128**	Lateral Structure								**88.128**	Lateral Structure												
unchanged	**88.12**	0.1	0.045	0.08						**88.12**	0.1	0.045	0.08										
modified	**N/A**	Removed because RM 88.118 was a redundant XS								**88.118**	0.1	0.045	0.08										

Summary of Model Reparameterization																													
Unchanged or Modified?	River Station	Kleinschmidt													River Station	QEA DEIS													
		Ineffective Flow Regions														Ineffective Flow Regions													
		Left (ft)	Right (ft)	Elev (ft)	Left (ft)	Right (ft)	Elev (ft)	Left (ft)	Right (ft)	Elev (ft)	Left (ft)	Right (ft)	Elev (ft)			Left (ft)	Right (ft)	Elev (ft)	Left (ft)	Right (ft)	Elev (ft)	Left (ft)	Right (ft)	Elev (ft)	Left (ft)	Right (ft)	Elev (ft)			
unchanged	**108.53**														**108.53**														
unchanged	**108.47**														**108.47**														
unchanged	**108.425**														**108.425**														
unchanged	**108.4**														**108.4**														
unchanged	**108.36***														**N/A**														
unchanged	**108.32***														**N/A**														
unchanged	**108.28**		389.49	450.1											**108.28**		389.49	450.1											
unchanged	**108.23***														**N/A**														
unchanged	**108.18**														**108.18**														
unchanged	**108.15***														**N/A**														
unchanged	**108.11***														**N/A**														
unchanged	**108.08**														**108.08**														
unchanged	**108.04***														**N/A**														
unchanged	**107.995***														**107.995***														
unchanged	**107.95**														**N/A**														
unchanged	**107.91**														**107.91**														
unchanged	**107.87***														**N/A**														
unchanged	**107.83***														**N/A**														
unchanged	**107.79**														**107.79**														
unchanged	**107.76***														**N/A**														
unchanged	**107.72**														**107.72**														
unchanged	**107.71**														**107.71**														
unchanged	**107.62**				598.91		408.35								**107.62**				598.91		408.35								
unchanged	**107.52**														**107.52**														
unchanged	**107.43**														**107.43**														
unchanged	**107.33**														**107.33**														
unchanged	**107.24**		1146.32	443.59	2256.27		432.51								**107.24**		1146.32	443.59	2256.27		432.51								
unchanged	**107.14**		1351.64	440.14	2355.8		430.72								**107.14**		1351.64	440.14	2355.8		430.72								
unchanged	**107.11**		1332.62	439.14	2039.42		430.58								**107.11**		1332.62	439.14	2039.42		430.58								
unchanged	**107.09**		1340.03	439.01	2032.1		433.27								**107.09**		1340.03	439.01	2032.1		433.27								
unchanged	**107.03**		1000.89	437.6	2327.43		428.74								**107.03**		1000.89	437.6	2327.43		428.74								
unchanged	**106.9**		1480.67	433.26	2980.22		427.38								**106.9**		1480.67	433.26	2980.22		427.38								
unchanged	**106.8**				2263.25		422.6								**106.8**				2263.25		422.6								
unchanged	**106.72**				2263.64		418.27								**106.72**				2263.64		418.27								
unchanged	**106.62**				2287.83		415.88								**106.62**				2287.83		415.88								
unchanged	**106.53**				2324.48		414.71								**106.53**				2324.48		414.71								
unchanged	**106.43**				3148.57		430								**106.43**				3148.57		430								
unchanged	**106.4**														**106.4**														
unchanged	**106.38**														**106.38**														
unchanged	**106.31**														**106.31**														
unchanged	**106.2**				1160.72		392.18								**106.2**				1160.72		392.18								
unchanged	**106.09**				1104.19		389.73								**106.09**				1104.19		389.73								
unchanged	**106**														**106**														
unchanged	**105.91**		392.27	388.83											**105.91**		392.27	388.83											
unchanged	**105.82**		175.89	430.05											**105.82**		175.89	430.05											
unchanged	**105.73**				1070.2		390.01								**105.73**				1070.2		390.01								
unchanged	**105.64**		212.81	390.88											**105.64**		212.81	390.88											
unchanged	**105.53**				1985.22		388.4								**105.53**				1985.22		388.4								
unchanged	**105.44**				2340		384.83								**105.44**				2340		384.83								
modified	**105.35**				1871.9		375.84								**105.35**		587.71	333.1	1871.9		375.84								
unchanged	**105.26**		464.21	408.67	1597.14		373.57								**105.26**		464.21	408.67	1597.14		373.57								
unchanged	**105.16**				1469.66		362.47								**105.16**				1469.66		362.47								
unchanged	**105.07**				1132.18		354.12								**105.07**				1132.18		354.12								
unchanged	**104.97**		672.24	358.77	1289.51		348.76								**104.97**		672.24	358.77	1289.51		348.76								
unchanged	**104.85**		935.54	354.8	1532.29		347.79								**104.85**		935.54	354.8	1532.29		347.79								
unchanged	**104.75**		861.89	351.67	1353.06		379.09								**104.75**		861.89	351.67	1353.06		379.09								
unchanged	**104.68**		752.92	349.96	1385.02		354.3								**104.68**		752.92	349.96	1385.02		354.3								
unchanged	**104.58**		377.14	348.13	1662.09		352.9								**104.58**		377.14	348.13	1662.09		352.9								
unchanged	**104.49**		201.39	370.45	429.45		350.39								**104.49**		201.39	370.45	429.45		350.39								
unchanged	**104.39**		128.17	407.23	623.08		348.88								**104.39**		128.17	407.23	623.08		348.88								
unchanged	**104.31**		167.55	419.86	797.91		374.66								**104.31**		167.55	419.86	797.91		374.66								
unchanged	**104.21**														**104.21**														
unchanged	**104.1**														**104.1**														
unchanged	**104.01**														**104.01**														
unchanged	**103.92**														**103.92**														
unchanged	**103.83**				870.65		364.11								**103.83**				870.65		364.11								
unchanged	**103.73**														**103.73**														

Summary of Model Reparameterization

Unchanged or Modified?	River Station	Kleinschmidt												River Station	QEA DEIS										
		Ineffective Flow Regions													Ineffective Flow Regions										
		Left (ft)	Right (ft)	Elev (ft)	Left (ft)	Right (ft)	Elev (ft)	Left (ft)	Right (ft)	Elev (ft)	Left (ft)	Right (ft)	Elev (ft)		Left (ft)	Right (ft)	Elev (ft)	Left (ft)	Right (ft)	Elev (ft)	Left (ft)	Right (ft)	Elev (ft)	Left (ft)	Right (ft)	Elev (ft)
unchanged	**103.64**													**103.64**											
unchanged	**103.54**				1358.87		362.23							**103.54**				1358.87		362.23						
unchanged	**103.44**				1610.42		361.81							**103.44**				1610.42		361.81						
unchanged	**103.37**				2021.3		360.85							**103.37**				2021.3		360.85						
unchanged	**103.26**				1407.14		351.76							**103.26**				1407.14		351.76						
unchanged	**103.17**				1479.05		357.25							**103.17**				1479.05		357.25						
unchanged	**103.08**				1133.03		355.25							**103.08**				1133.03		355.25						
unchanged	**102.98**													**102.98**											
unchanged	**102.89**													**102.89**											
unchanged	**102.79**				1042.89		345.03							**102.79**				1042.89		345.03						
unchanged	**102.68**													**102.68**											
unchanged	**102.6**													**102.6**											
unchanged	**102.51**													**102.51**											
unchanged	**102.41**													**102.41**											
unchanged	**102.38**													**N/A**											
unchanged	**102.36**													**N/A**											
unchanged	**102.31**													**102.31**											
unchanged	**102.29**													**N/A**											
unchanged	**102.26**													**N/A**											
unchanged	**102.23**				1519.84		344.49							**102.23**				1519.84		344.49						
unchanged	**102.13**				1833.06		345.77							**102.13**				1833.06		345.77						
unchanged	**102.04**													**102.04**											
unchanged	**101.92**				1855.55		338.94							**101.92**				1855.55		338.94						
unchanged	**101.85**				2624.1		347.12							**101.85**				2624.1		347.12						
unchanged	**101.8**		1713.91	337.56	2661.89		346.07							**101.8**		1713.91	337.56	2661.89		346.07						
unchanged	**101.549**				2395.91		343.76							**101.549**				2395.91		343.76						
unchanged	**101.334**													**101.334**											
unchanged	**101.12**				751.7		330.29							**101.12**				751.7		330.29						
unchanged	**100.95**				373.45		331.5							**100.95**				373.45		331.5						
unchanged	**100.76**		438.03	327.4	917.95		328.04							**100.76**		438.03	327.4	917.95		328.04						
unchanged	**100.44**		1400	324.76										**100.44**		1400	324.76									
unchanged	**100.43**		1949.09	325.29										**100.43**		1949.09	325.29									
unchanged	**100.41**		1472.46	325.03										**100.41**		1472.46	325.03									
unchanged	**100.4**		1440	321.53										**100.4**		1440	321.53									
unchanged	**100.16**		287.46	319.92	1146.67		323.72							**100.16**		287.46	319.92	1146.67		323.72						
unchanged	**99.77**				856.92		315.75							**99.77**				856.92		315.75						
unchanged	**99.19**													**99.19**											
unchanged	**98.95**				803.46		311.79							**98.95**				803.46		311.79						
unchanged	**98.47**	0	1159.517	310.75	1159.517	1680.711	309.1	1932.818	2259.918	309.1	2259.918	3308.219	309.02	**98.47**	0	1159.517	310.75	1159.517	1680.711	309.1	1932.818	2259.918	309.1	2259.918	3308.219	309.02
unchanged	**98.44**	0	837.303	310.75	837.303	1680.711	309.1	1932.818	2042.353	309.1	2042.353	3606.613	307.57	**98.44**	0	837.303	310.75	837.303	1680.711	309.1	1932.818	2042.353	309.1	2042.353	3606.613	307.57
unchanged	**98.165***		1848.28	305.215	2374.205		309.735							**98.165***		1848.28	305.215	2374.205		309.735						
unchanged	**97.89**		2352.89	304.84	2634.39		311.86							**97.89**		2352.89	304.84	2634.39		311.86						
unchanged	**97.86**		2379.46	305	2645		311.98							**97.86**		2379.46	305	2645		311.98						
unchanged	**97.49**		2055.09	294.86	2306.61		294.07							**97.49**		2055.09	294.86	2306.61		294.07						
unchanged	**97.06**		332.91	295.75										**97.06**		332.91	295.75									
unchanged	**97.01**		305.83	295										**97.01**		305.83	295									
unchanged	**96.95**		365.87	293.84	2868.96		287.3							**96.95**		365.87	293.84	2868.96		287.3						
unchanged	**96.85**		237.07	291.22	2743.16		286.95							**96.85**		237.07	291.22	2743.16		286.95						
unchanged	**96.32**		1294.44	285.26	1654.44		281.39							**96.32**		1294.44	285.26	1654.44		281.39						
unchanged	**95.96**		2737.48	277.45	3199.07		278.85							**95.96**		2737.48	277.45	3199.07		278.85						
unchanged	**95.5**		1681.96	277.62	2080.21		275.96							**95.5**		1681.96	277.62	2080.21		275.96						
unchanged	**95.16**		1354.97	271.99	1597.83		272.5							**95.16**		1354.97	271.99	1597.83		272.5						
unchanged	**94.78**		2853.64	268.71	3105.71		268.78							**94.78**		2853.64	268.71	3105.71		268.78						
unchanged	**94.76**		2853.64	268.71	3105.71		268.78							**94.76**		2853.64	268.71	3105.71		268.78						
unchanged	**94.28**	1674.7	1768.1	262.17										**94.28**	1674.7	1768.1	262.17									
unchanged	**94.26**													**94.26**											
unchanged	**94.2**													**94.2**											
unchanged	**93.79**		1922.89	262.05	2654.81		261.46							**93.79**		1922.89	262.05	2654.81		261.46						
unchanged	**93.57**		410.41	274.15	999.05		271.63							**93.57**		410.41	274.15	999.05		271.63						
unchanged	**93.44**													**93.44**											
unchanged	**93.03**		224.6	258.51	919.08		259							**93.03**		224.6	258.51	919.08		259						
unchanged	**92.27**				1966.55		246.36							**92.27**				1966.55		246.36						
unchanged	**91.77**	330.37	837.07	243.967	840	1736.28	243.207	3000.07	3997.79	244.631				**91.77**	330.37	837.07	243.967	840	1736.28	243.207	3000.07	3997.79	244.631			
modified	**91.533***	350.03	892.97	239.37	896.86	1867.61	239.3375	3248.29	4312.38	242.62				**N/A**												
modified	**91.297***	205.35	2725.58	238.54	3789.67	4405.73	238.87							**N/A**												
unchanged	**91.06**		2911.35	238.41	4063.83		237.77							**91.06**		2911.35	238.41	4063.83		237.77						
modified	**90.740***		2716.88	236.66	3782		236.8133							**N/A**												

Summary of Model Reparameterization																									
Unchanged or Modified?	River Station	Kleinschmidt												River Station	QEA DEIS										
		Ineffective Flow Regions													Ineffective Flow Regions										
		Left (ft)	Right (ft)	Elev (ft)	Left (ft)	Right (ft)	Elev (ft)	Left (ft)	Right (ft)	Elev (ft)	Left (ft)	Right (ft)	Elev (ft)		Left (ft)	Right (ft)	Elev (ft)	Left (ft)	Right (ft)	Elev (ft)	Left (ft)	Right (ft)	Elev (ft)	Left (ft)	Right (ft)	Elev (ft)
modified	**90.420***		2522.41	234.91	3500.17		235.8567							**N/A**												
unchanged	**90.1**		2327.94	233.16	3218.34		234.9							**90.1**		2327.94	233.16	3218.34		234.9						
modified	**89.68**	100	411.8	230.46	3509.27	5000	233							**N/A**												
modified	**89.65**	300	445.77	225.76	3351.89	4800	233							**N/A**												
modified	**89.61**		377.34	235.21	3290.52		233							**89.61**		377.34	235.21	3290.52		232.86						
modified	**N/A**													**88.9**				5678.35		233.48						
modified	**88.67**	500	2704.75	225	5781.89	7200	232.68							**N/A**												
modified	**88.6**	500	2999.92	223.64	5604.21	7000	233.13							**N/A**												
modified	**88.54**	300	3411.91	225.12	4855.99	5372.22	250	5372.22	7200	232.47				**N/A**												
modified	**88.37**	300	4108.02	225.2	4453.09	5114.03	250	5114.03	7000	232.05				**N/A**												
unchanged	**88.28**		518.15	227.48	3611.3		230.31							**88.28**		518.15	227.48	3611.3		230.31						
unchanged	**88.12**		293.88	232.63	2638.63		225.84							**88.12**		293.88	232.63	2638.63		225.84						
modified	**N/A**													**88.118**		293.88	232.63	2638.63		225.84						

A2 Fine Sediment Transport Technical Memorandum

TECHNICAL MEMORANDUM

Date: July 9, 2024
To: Matt Dillin, Chehalis River Basin Flood Control Zone District
From: Paul DeVries, PhD, PE, CFP and Robert Schomp, MS, EIT, Kleinschmidt Associates
Cc: MaryLouise Keefe, PhD and Jason Kent, PE, PMP, Kleinschmidt Associates
Re: Evaluation of Potential Fine Sediment Transport Impacts of FRE Operations on Chinook Salmon Spawning Habitat

Preface

Following the release of Draft Environmental Impact Statements (DEISs) by the Washington Department of Ecology and the United States Army Corp of Engineers for the proposed Flood Reduction Expandable Facility, the project's proponent, the Chehalis Basin Flood Control Zone District (District) has undertaken more detailed technical studies to better understand the nature of potential project impacts to environmental resources. These studies have been undertaken to provide the basis for development of avoidance, minimization and mitigation measures for the project. The transport of sediments within the Chehalis River was identified among potentially affected resources in the DEISs that could affect aquatic habitat. This technical memorandum describes a more detailed analysis of fine sediment transport processes performed for the District than was available in the DEISs. It is a companion to separate technical memoranda that address coarse bedload transport processes, salmonid spawning habitat availability, and salmonid spawning habitat scour risk. These technical memoranda are necessary for developing an understanding of the mechanisms affecting sediment transport and aquatic habitat sufficient for the District to formulate appropriate avoidance, minimization and mitigation measures for the proposed project. These measures will be fully described in the District's forthcoming mitigation plan, which will incorporate the memoranda as technical appendices.

Executive Summary

This technical memorandum describes analyses performed to improve understanding of fine sediment deposition and erosion processes operating within the mainstem reach of the Upper Chehalis River that would be impounded temporarily during operation of the proposed Flood Reduction Expandable (FRE) facility. This information is necessary to understand the feasibility of species and life stage specific mitigation actions that would compensate for any impacts associated with effects of the FRE facility operation on fine sediment transport processes, with emphasis on impacts to Chinook salmon spawning and incubation which occur predominantly in the mainstem.

Previous modeling completed as part of the NEPA and SEPA Draft Environmental Impact Statements' (DEISs') analyses relied on a one-dimensional (1D) Hydrologic Engineering Center's River Analysis System (HEC-RAS) sediment transport model of long-term changes in the longitudinal riverbed profile. Impacts in the DEISs were qualified based on model output in terms of broad level effects of predicted aggradation of sediments associated with FRE operations. Sediments were evaluated as a total load, without distinguishing between coarse and fine sediments, bedload and suspended load, or short-term vs. long-term effects. Thus, the DEISs' assessment of the effects of project operations on sediments was insufficiently specific to be able to evaluate the mechanisms of deposition and subsequent re-entrainment and transport of fine sediments that could affect the quality of mainstem Chinook salmon spawning habitat. To address this gap, the District undertook extensive analyses identifying effects of FRE operations more specifically with respect to fine sediments. The results of the analyses can then be used to determine appropriate avoidance, minimization, and mitigation requirements with respect to potential impacts of fine sediments to Chinook salmon spawning habitat quality.

Accordingly, the same HEC-RAS model and hydrology used in preparing the DEISs was applied to evaluate the quantity of fine sediments deposited in the temporary reservoir during FRE operation, and the length of time before the deposited sediments are flushed downstream and the coarse riverbed framework underneath is re-exposed to the water column. The model was used to predict hydraulic conditions during the February 1996 and January 2009 flood events approximately representing the 20- and 10-year recurrence interval peak flow events at the United States Geological Survey (USGS) gage near Doty, respectively. FRE operations were assumed to follow the conceptual scheme identified and modeled for the DEISs. The predicted hydraulics were then used to calculate potential fine sediment transport rates along the length of the mainstem Chehalis River inundation zone. The resulting rate estimates were then tracked under a mass balance framework to approximate the amount of fine sediments that could be deposited along the length of affected riverbed as the reservoir rose, and the time to move the deposits progressively downstream again as the reservoir receded. The results were compared with other case studies involving the flushing of fine sediments, and with biological criteria related to incubation survival as affected by water depth, permissible dissolved oxygen concentrations, and intragravel velocity.

The results of the new modeling analyses and literature reported in this document indicated the following for the FRE operation evaluated in the DEISs:

1. Both events were associated with temporary inundation up to the base of Fisk Falls. Deposition of fine sediments was accordingly predicted along the entire length of the approximately 6-mile reach between the proposed FRE facility location and Fisk Falls.
2. The predicted length of time of inundation upstream of the modeled FRE facility location, and thereby existence of lake instead of riverine conditions, was shortest below Fisk Falls (around 6-8 days) and increased in the downstream direction to a maximum of approximately 30 days. More Chinook salmon spawn within the first 2 miles below Fisk Falls than downstream.
3. The predicted time to re-entrain and evacuate fine sediments deposited during filling operations within a specific segment of river was relatively short compared to the time the same location is inundated under lake conditions.
4. The predicted total amount of sediment depositing in a segment increased progressively in the downstream direction because of successive entrainment upstream and re-deposition downstream that followed the receding lake level. This resulted in the total time to evacuate deposited fine sediments increasing rapidly in the downstream direction.
5. In the case of the 20-year recurrence interval peak flow event, the predicted time to evacuate sediments ranged from a few days a short distance below Fisk Falls to approximately two months at two miles downstream of Fisk Falls, and longer downstream in the case where the river transports and deposits fine sediments to the extent it can. In the case of the 10-year flood, predicted time to evacuate deposited fine sediments was longer because predicted sediment transport rates were lower after drawdown operations. This was likely due to a lower predicted sediment transport capacity overall.
6. Intragravel flow will be an important determinant of survival of developing embryos and alevins at locations where lake conditions and sediment deposition would occur.
7. Potential effects of fine sediments on survival to emergence within the inundation zone with the project may be offset by scour mortality during extreme flood events without the project.

Background

The Chehalis Basin Flood Control Zone District (District) is proposing to construct a Flood Reduction Expandable (FRE) facility to reduce the risk of flood damage along the mainstem Chehalis River. The proposed FRE facility is located approximately 1.7 miles upstream from the city of Pe Ell, Washington in the upper Chehalis River watershed (Figure 1). The primary purpose of the FRE facility is to reduce flooding coming from the Willapa Hills by storing floodwaters in a temporary reservoir during major or larger floods. In 2020, the two draft Environmental Impact Statements (DEISs) released for this project (the Washington State Department of Ecology's [Ecology] under the State's Environmental Policy Act and the United States Army Corps of Engineers' [Corps] under the National Environmental Policy Act [NEPA]) expected that by temporarily storing peak flows during major or catastrophic flood events, the FRE facility operations would alter sediment transport and deposition processes and thereby impact channel forming processes and spawning habitat quantity and quality. This, in turn, was hypothesized to impact reproductive success of fish species relying on spawning habitat within the potential reservoir footprint and downstream (Ecology 2020; USACE 2020). Impacts were generally represented as occurring upstream of Elk Creek (around river mile [RM] 100).

While fall Chinook salmon (*Oncorhynchus tshawytscha*), coho salmon (*O. kisutch*), and steelhead (*O. mykiss*) are all found in the basin and have segments of their populations that are mainstem spawners (Ronne et al. 2020), the DEISs expect spring Chinook salmon populations to suffer the greatest potential impact on spawning habitat. This is largely due to their restricted distribution as compared to other salmonid species in the basin. In the Upper Chehalis Basin, both spring and fall Chinook salmon spawn predominantly in the mainstem, with greatest concentrations of redds recorded in the first two and one-half miles below Fisk Falls and within the upper four to five miles of the Pe Ell valley reach below where the river exits the Willapa Hills (Washington Department of Fish and Wildlife [WDFW] electronic data for 2015-2021 received from Ecology; Phinney et al. 1975; WG and Anchor 2017; Ferguson et al. 2017; Ronne et al. 2020) (Figure 2). There are few tributaries large enough in the basin with sufficient gravel deposits to provide spawning habitat for Chinook salmon and they are primarily located downstream of the proposed location of the FRE. Steelhead and coho salmon spawn more extensively than Chinook salmon in tributary habitats, most of which would not be influenced by FRE operations (Ronne et al. 2020). In addition, there would likely be more locations and opportunities to mitigate for impacts to those two species by providing access to disconnected spawning habitat than there would be for Chinook salmon. Thus, the focus for mitigation of sediment impacts to mainstem spawning habitat will primarily be most important for Chinook salmon.

Figure 1
Map of Chehalis River Study Reach, Including Location of Important Landmarks Indicated.

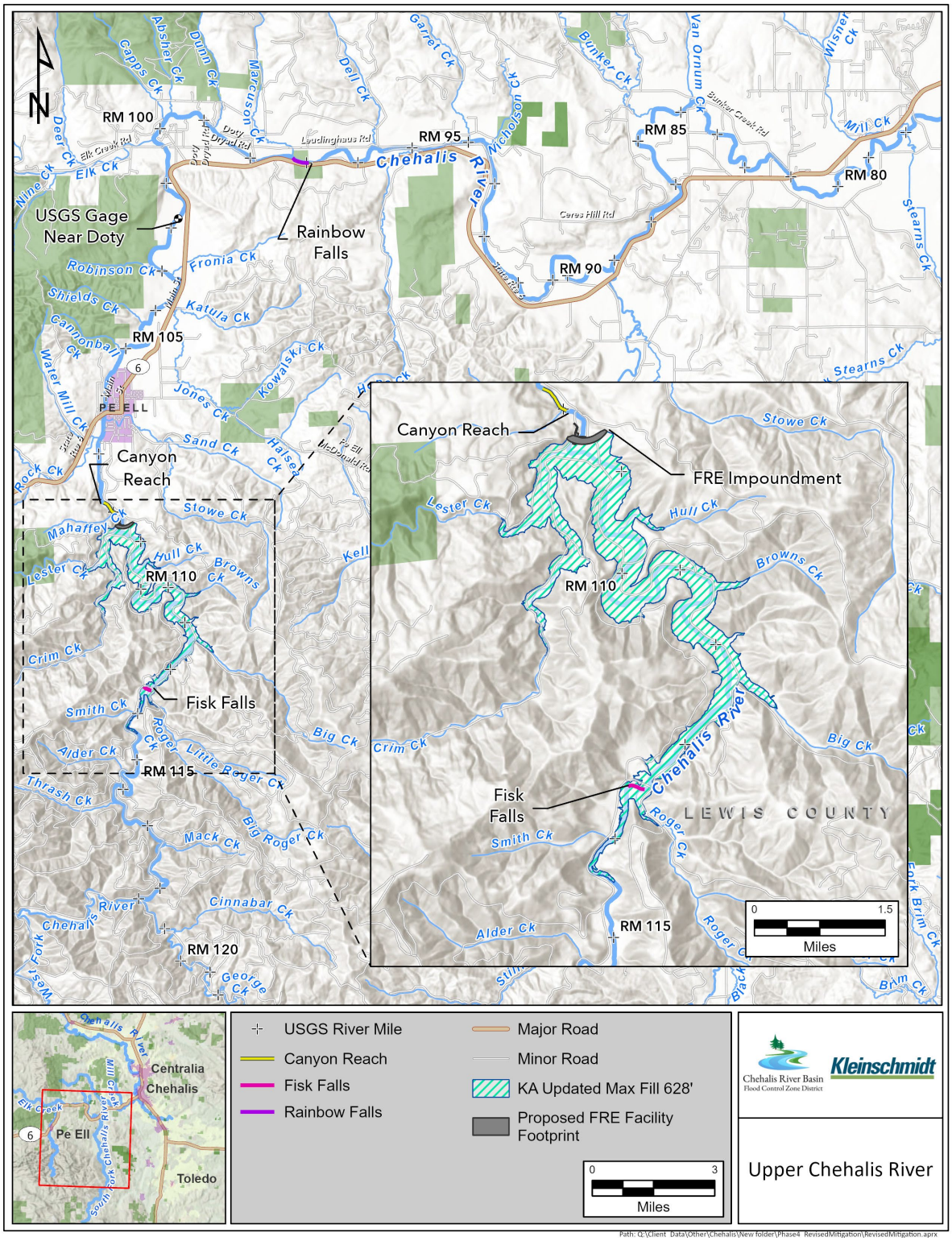

Figure 2
Redd Numbers Counted in Four Reaches of the Mainstem Chehalis River Between the Newaukum River and the West Fork-East Fork Confluence Each Year from 2017-2020. Data Were Not Collected Downstream of RM 103 in 2019 and 2020 ("ND").

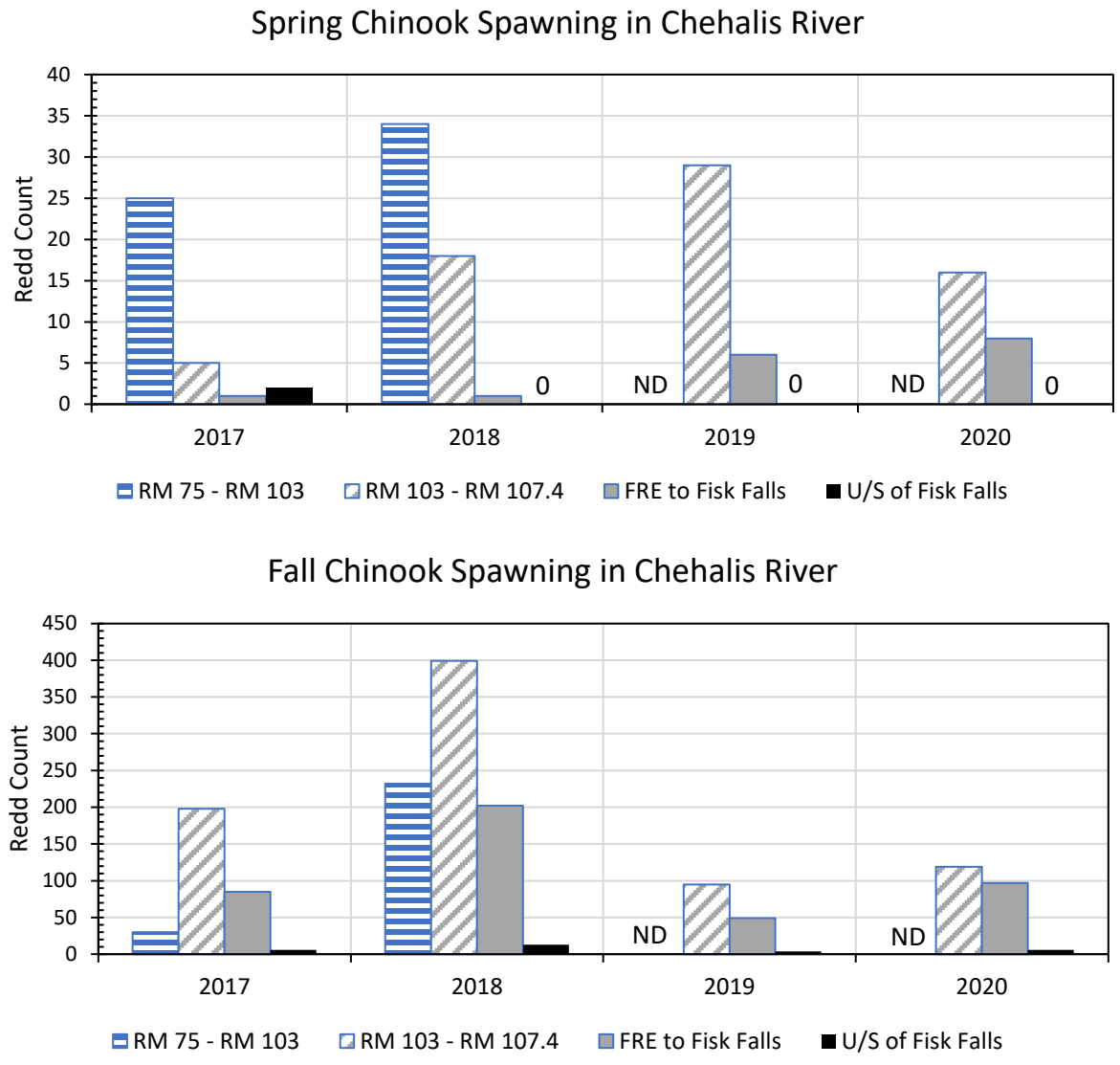

The DEISs implied that changes to sediment transport rates and grain size within and downstream of the facility could have a direct impact on Chinook salmon spawning habitat, but with limited descriptions of relevant mechanisms and context. The DEISs' simplified simulation results were interpreted as predicting a net increase in total coarse and fine sediment stored upstream of the facility and a net decrease downstream, with potential impacts identified primarily upstream of Elk Creek. The amount of sediment accumulated within the inundation zone was projected to increase in the downstream

direction after major flood events. These modeled changes in sediment storage were then taken to represent significant adverse impacts.

Specificity was missing, however, in terms of aquatic habitat changes associated with coarse vs. fine sediment deposition and transport, and how each size fraction may affect reproductive success. The most specific description of a sediment transport-associated impact on fish and aquatic habitat associated with project operations was hypothesized in the DEISs to occur through increases in fine sediment deposition in the riverbed within the affected reach of the reservoir, but the relevant mechanisms and levels required to cause impact(s), or what the impact(s) would be, were not identified. Rather, the temporary conversion of the affected reach from riverine to lake habitat was projected in the DEISs to result in suffocating salmonid embryos and alevins developing in redds constructed within the temporary inundation footprint. This process would be expected to act in concert with fine sediment deposition.

Given the corresponding uncertainty in the DEIS's evaluation of impacts on sediment transport processes and corresponding impacts to Chinook salmon spawning success in the mainstem Chehalis River, it is generally not possible to identify species- and reach-specific appropriate and commensurate mitigation measures to offset what those potential impacts on habitat may be. To do so, the District conducted a separate assessment to refine our understanding of FRE operations of sediment transport. An initial analysis of long-term coarse sediment transport and deposition processes (Kleinschmidt 2024) indicated that fine sediments are transported rapidly and would not be expected to build up over the long term (i.e., over several years). However, the results of that analysis did not address short-term processes within a monthly time frame, which brackets the duration of intragravel residence of developing embryos and alevins.

This technical memorandum describes analyses performed for, and synthesizes the results of, an independent assessment of short-term fine sediment transport dynamics in the mainstem. The analyses focused on quantifying the amount and residence time for fine sediments deposited in the inundation zone during FRE operations, as well as the length of time that river flow is effectively stagnant under lake conditions. The information resulting from this analysis is critical for assessing potential impacts to spawning habitat areas in terms of how long it would take to evacuate deposited fine sediments and re-expose gravel-cobble substrates, and how long intragravel flows may be reduced or precluded while the impoundment is filling and draining. At locations where groundwater inflow rates and/or dissolved oxygen levels are negligible, either mechanism can impact the development and survival of salmonid embryos and alevins in terms of reduced (i) dissolved oxygen needed for growth and (ii) flushing of carbon dioxide and other metabolic waste products to prevent localized buildup of adverse water quality conditions (Danner 2008; Malcolm et al. 2008).

Methods

The analysis involved simulating the hydraulics of specific flood events with different recurrence intervals using a version of the same one-dimensional (1D) Hydrologic Engineering Center's River Analysis System (HEC-RAS) hydraulic model relied on by the DEISs and used in the District's modeling of coarse sediment transport (Kleinschmidt 2024). In contrast with the DEISs, however, sediment transport rates were computed externally using the model's hydraulic predictions to evaluate transport capacity directly. This was done because the model's intrinsic sediment transport programming and parameterization were conditioned to report results in a certain way that precluded direct estimation of transport capacity of sand-sized material at each model cross-section. A direct estimate was needed of volume of material that could potentially deposit between successive cross-sections as the edge of the impoundment shifts upstream during impoundment filling, and the capacity of the river to transport sand-sized material potentially deposited between cross-sections as the edge recedes downstream again during draining. The approach is summarized below, with example calculations presented in Attachment 1.

Hydrology

Sediment deposition and erosion volumes were approximated for two hydrograph events representing the 10- and 20-year peak flood events at the United States Geological Survey (USGS) gaging station (Station No. 12020000) on the Chehalis River near Doty, Washington. The station is located downstream of the proposed FRE facility at approximately RM 101.8, which is also near the downstream extent of the majority of mainstem spawning by Chinook salmon. Hydrology determined previously for the DEISs was used, (Hill and Karpack 2019), of which two specific flood events were simulated (Figure 3):

- The February 1996 flood event was extracted from the DEISs' model 30-year flow time series to represent the 20-year flood frequency event at the Doty gage. The event was classified as a major flood with peak flow rate exceeding 38,800 cubic feet per second (cfs) at the USGS Chehalis River Grand Mound gage (Station No. 12027500), where the DEISs' model simulated FRE operation according to the proposed plan. The February 1996 flood event was considered a 7-year flood event at the Grand Mound gage. It was followed by a second peak flow event that occurred approximately two and one-half months after the temporary reservoir was simulated to be completely drained, in late April. The FRE facility was not operated during that subsequent event.
- The January 2009 flood event was selected from the 30-year flow time series to represent the 10-year flood frequency event as measured at the Doty gage. The FRE facility was operated during this event.

Figure 3
Simulated Hydrographs at the USGS Doty Gage for the February 1996 (top) and January 2009 (bottom) Flood Events.

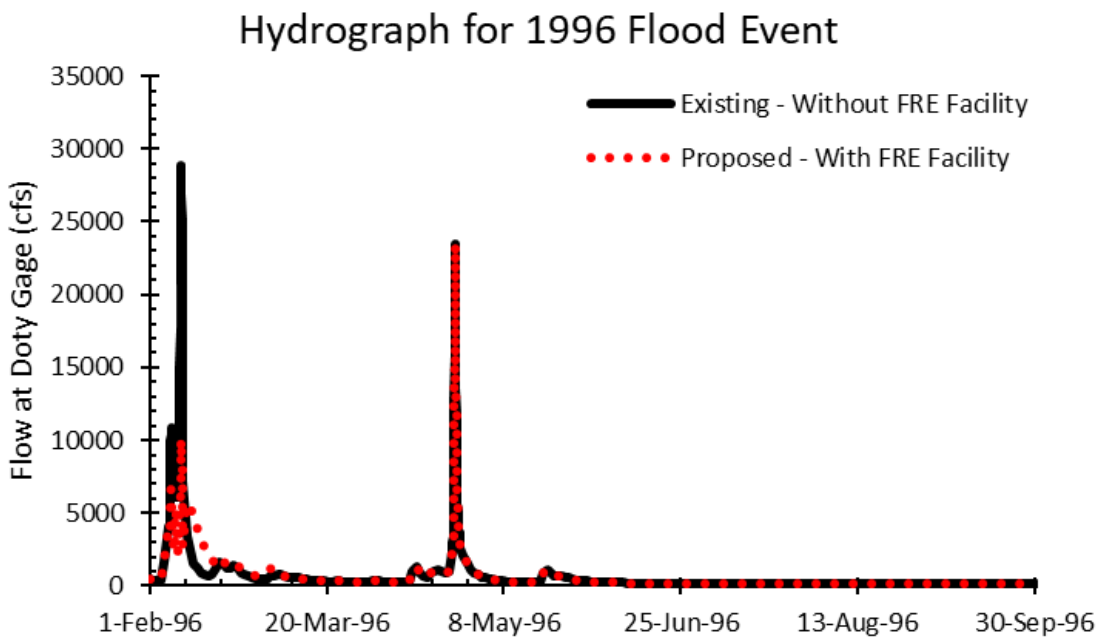

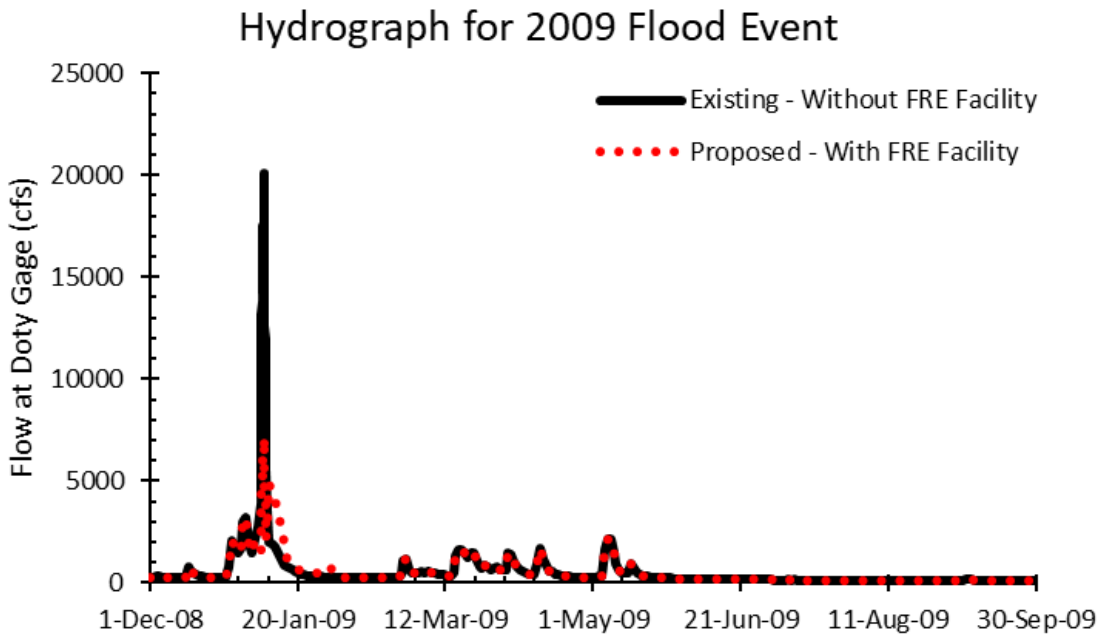

Hydraulic and Sediment Transport Modeling

A modified version of the DEISs' HEC-RAS hydraulic model was run. The modifications involved changing various parameter values to yield more realistic hydraulic predictions under certain flow conditions and are described in Kleinschmidt's technical memorandum evaluating coarse sediment transport and deposition effects (Kleinschmidt 2024). The model hydraulic predictions were then used to predict sand transport rates at various locations in the temporary impoundment footprint via the Engelund-Hansen sediment transport equation (Engelund and Hansen 1967). The model was run in the "Quasi-Unsteady" sediment transport mode with no sediment loading and scour, where each time step was simulated as a steady flow for predicting shear stress and mean velocity at each simulated cross-section.

Importantly, there are insufficient data available to calibrate total fine sediment transport rate estimates, which can vary by an order of magnitude depending on the sediment transport equation used. The DEISs' analyses were subject to the same limitation. Accordingly, the analyses performed for this assessment were based on evaluating relative differences in potential transport capacity and may not be representative of actual transport rates, which may be limited by local availability for transport and other factors. Hence, predictions of fine sediment deposition and erosion volumes should be considered as relative indicators of potential for change, not accurate estimates of absolute magnitudes.

Simulating FRE Facility Operations

FRE operations were simulated for the same location as specified in the DEISs' model, and following the same initial conceptual set of operational rules simulated in the DEISs' modeling and depicted in Figure 4. As part of that, the same hydrology representing gate control of flow releases downstream was incorporated. FRE operation accordingly was simulated with filling of the temporary reservoir approximately 48 hours before the flow rate at the USGS gage near Grand Mound (Station No. 12027500) reached 38,800 cubic feet per second (cfs). Flow through the FRE facility gate opening was reduced to 300 cfs until the peak flood level was reached. The drawdown process began once the flood risk had passed, with the reservoir taking up to approximately 32 days to completely empty when filled to maximum capacity. The simulated maximum outflow during drawdown was limited to 5,200 cfs, which corresponded to roughly the 0.4 percent exceedance flow and approximates the annual flood. It should be noted that gate operation rules may change as the design progresses.

Figure 4
Representative FRE Facility Operation Simulated in the DEISs (figure originally from Ecology 2020).

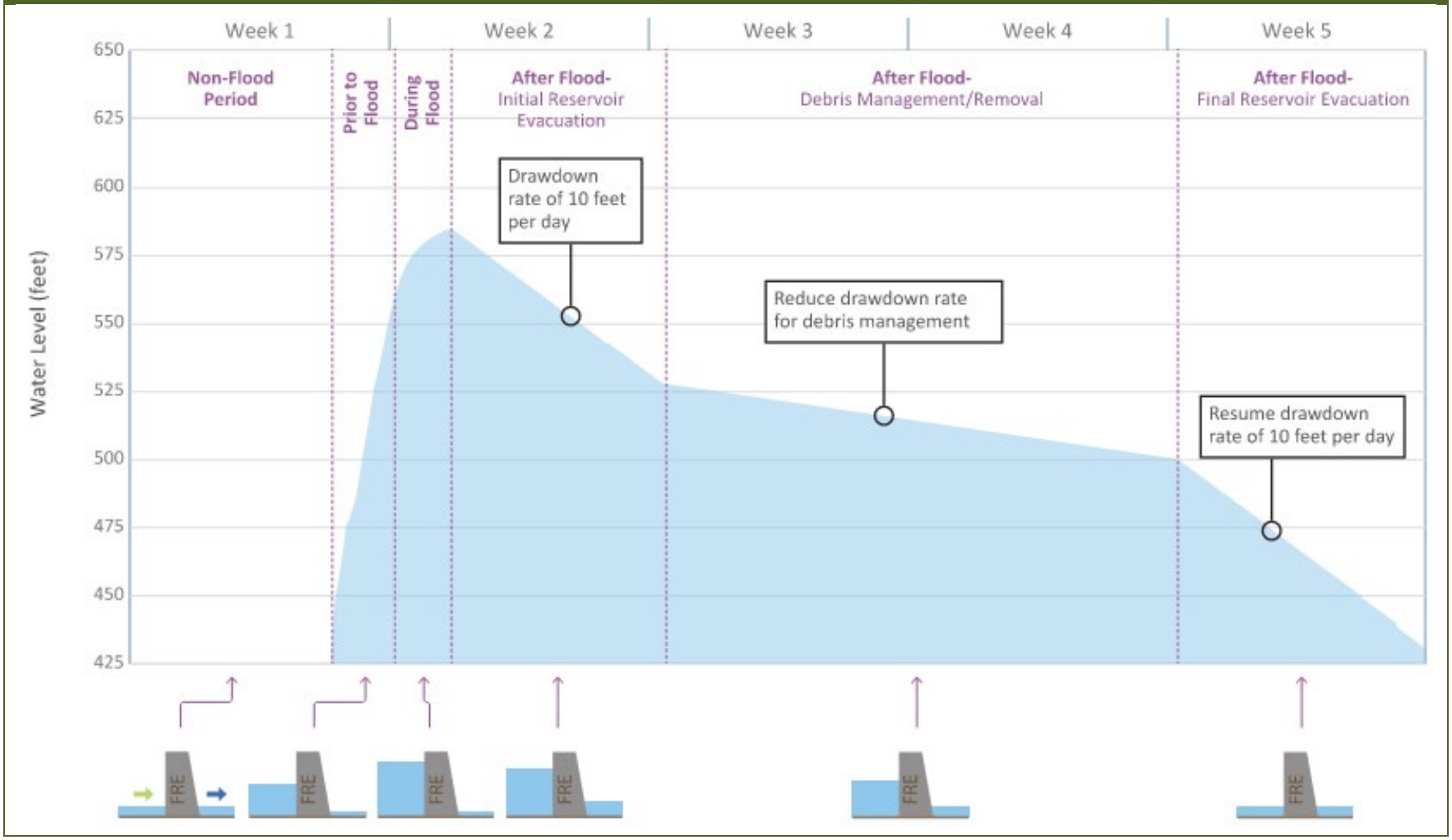

Calculation of Sediment Transport Rate

The Engelund-Hansen (1967) sediment transport equation was used to calculate the theoretical fine sediment mass transport rate for each timestep in the HEC-RAS simulation. The equation predicts total load and was developed from flume data using relatively uniform sand sizes between 0.19 millimeters (mm) and 0.93 mm. The formula is appropriate for riverbeds and deposits composed of fine sediments (USACE 2023). The equation is:

$$q_s = 0.05 \cdot \gamma_s \cdot V^2 \cdot \left(\frac{\tau_b}{(\gamma_s - \gamma_w) \cdot D_f}\right)^{\frac{3}{2}} \cdot \sqrt{\frac{D_f}{g \cdot \left(\frac{\gamma_s}{\gamma_w} - 1\right)}} \cdot B$$

Where:

q_s = sediment transport rate (pounds per second [lb/s])
g = acceleration due to gravity (feet per second squared[ft/s^2]) = 32.2
γ_w = unit weight of water (pounds per cubic foot [lb/ft^3]) = 62.4
γ_s = unit weight of sediment (lb/ft^3) = 2.65γ_w = 165
V = average channel velocity (feet per second [ft/s])
τ_b = bed shear stress (pounds per square foot [lb/ft^2])
D_f = particle fall diameter (ft)
B = width of channel bed (ft)

Fall diameter is defined as:

$$D_f = \begin{cases} -69.07 \cdot {D_{50}}^2 + 1.0755 \cdot D_{50} + 0.000007 & (if\ D_{50} \leq\ 0.00591\ ft) \\ 0.1086 \cdot D_{50}^{0.6462} & (otherwise) \end{cases}$$

Where D_{50} = median particle diameter. A D_{50} particle size of 0.85 millimeters (mm) (0.0028 feet) was chosen for this study to approximate the accumulation and evacuation of sands in the FRE temporary reservoir.

Determining Amount of Sediment Deposited at Different Locations in the Temporary Impoundment

Predicting the amount of sediment that is deposited at a given river location as the water level rises until velocities are slow enough that transport from upstream ceases is complicated because the transport and settling rates change non-uniformly over time and space, and vary with sediment size. A simplifying assumption was made that should be sufficient for an order or magnitude analysis, where the point in time was identified when the upstream edge of the filling impoundment water level was simulated to reach a specific model transect location. Calculated total fine sediment inflow volumes were then summed over subsequent time steps in the simulation until significant sediment transport to the

location from upstream was calculated to have ceased. This was approximated to occur when the channel bed shear stress predicted by the model decreased to 0.01 lb/ft^2 or less. After that time, transport to the location was assumed to be negligible, and thus further deposition was also assumed to be negligible. All suspended material, including clay and silt washload which might remain in suspension, was assumed to be deposited. It is recognized that some fines may still be in transport at this limiting shear stress (cf. Parker et al. 2003), and that reservoir trapping efficiency varies with particle size and reservoir area.

Calculating Time to Erode and Evacuate Deposited Fines

For simplicity, it was then assumed that fine sediment transport resumes at a location when the predicted edge of the temporarily impounded water moves downstream and the channel bed shear stress begins to exceed 0.01 lb/ft^2. The total volume of fine sediment calculated to be transported was then summed over successive time steps until the calculated cumulative volume of sediment transported matched or exceeded the amount calculated to have been deposited. The corresponding duration was taken as an approximate estimate of the time it would take for the river to evacuate and transport the accumulated sediment downstream, thereby re-exposing the gravel bed. This was calculated in two ways, in terms of (i) just the amount of sediment deposited as the temporary impoundment water level rises, and (ii) the cumulative amount of sediment transported downstream from one model segment to the next as sediment deposits near the receding water's edge and then is re-entrained. These two calculations approximate our expectation of lower and upper bounds of time needed to erode deposited sediments, respectively.

Calculating the Duration of Lake Conditions at a Location

The duration of time that water was predicted to be effectively stagnant at a location with negligible mean column velocity resembling conversion of riverine to lake conditions was calculated as the difference in time between the rising and falling water levels when shear stress was predicted by the model to be equal to or less than 0.01 lb/ft^2. This was assumed to correspond to the duration of time that intragravel velocities would be negligible at locations where groundwater inflows are also negligible. It does not indicate by itself that intragravel flow conditions would be stagnant, but provides an indicator as to where embryo and alevin survival and growth may be most impacted if there is no other form of intragravel hydraulic gradient present.

Results

Both the February 1996 and January 2009 flood events, with roughly 20-year and 10-year recurrence intervals, respectively, were associated with predicted peak reservoir inundation levels that reached Fisk Falls (Figure 5). Spawning habitat below Fisk Falls, which is located at around RM 114, was thus predicted to experience both temporary lake conditions and fine sediment deposition during FRE operation at those flood levels.

Figure 5
Simulated Maximum Reservoir Inundation Levels During the 20-year February 2009 (Q_{20}) and 10-year January 2009 (Q_{10}) Flood Events.

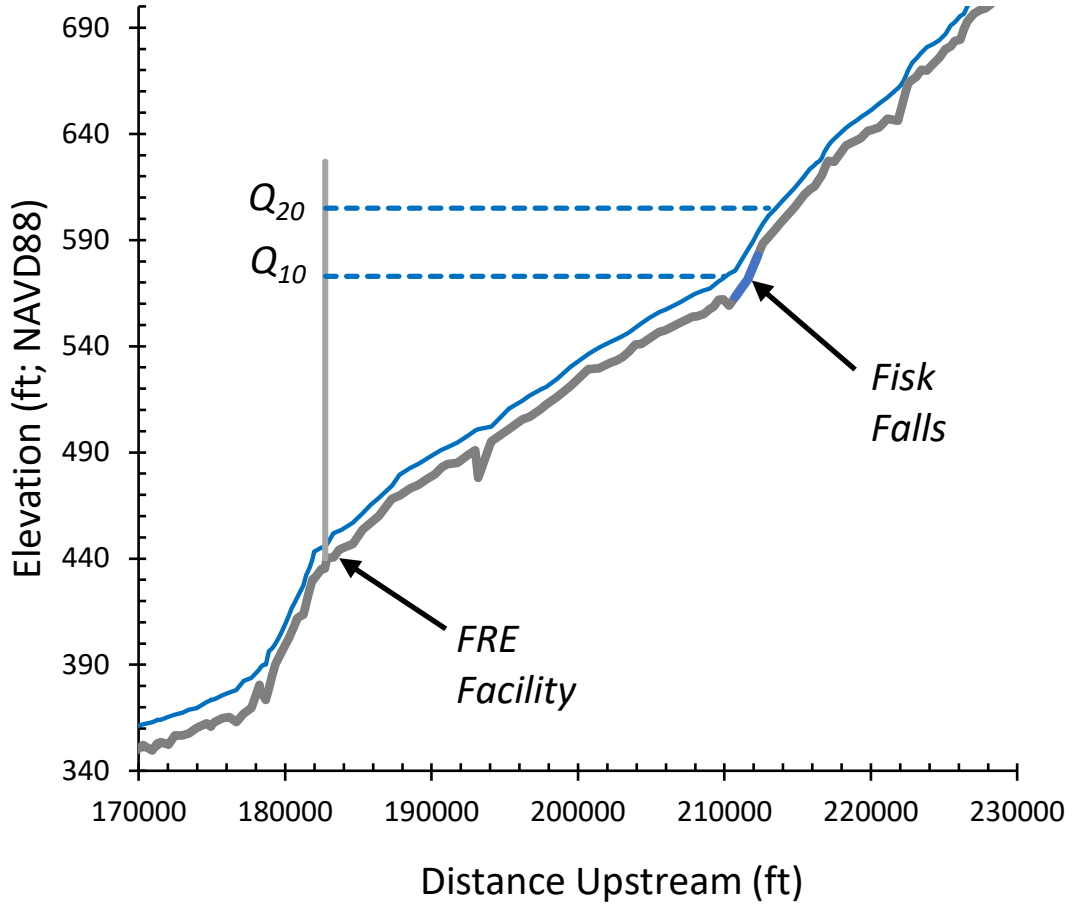

In the case of the February 1996 flood event with a recurrence interval of roughly 20 years at the USGS gage near Doty, the amount of fine sediment deposited was estimated to be greater in the first 1.5 miles at the upstream end below Fisk Falls compared with downstream (Figure 6, top; quantities are plotted relative to each other). The analysis indicated that it would take roughly four days or less at most locations to flush out just the amount of fine sediments deposited initially between the two bounding HEC-RAS transects (upper bars in middle graph of Figure 6). This is generally shorter than the duration of inundation, which was shortest upstream and longest downstream (lower bars in middle graph of Figure 6). However, the total time to evacuate all fine sediments potentially deposited in the temporary reservoir was estimated to take considerably longer than the duration of inundation, ranging from a few days at the upstream end below Fisk Falls (RM 114) to approximately two months at 1.5 miles downstream (Figure 6, bottom). The reason is that the river has to entrain not only the fine sediment

that deposited initially, but also the cumulative volume of material that is entrained upstream, transported and then redeposited successively downstream as the temporary impoundment is drained and the lake level drops.

Another pattern was predicted for the case of the January 2009 flood event with a recurrence interval of roughly 10 years at the gage near Doty. The amount of sediment deposited as the temporary impoundment fills was estimated to be greatest in the first two miles at the upstream end below Fisk Falls between approximately RM 112-114 and was also relatively high farther downstream (Figure 7, top). The hydraulic modeling predicted a similar downstream-increasing pattern, but with roughly 2-3 days fewer of reservoir inundation overall, prior to sediment flushing compared with the case of the February 1996 flood event (compare middle graphs in Figure 7 and Figure 6). The analysis indicated that it would take roughly six days or less at most locations in the first one and a half miles below Fisk Falls to flush out the initial local deposit of fine sediments, but there were more locations with longer times estimated compared with the February 1996 flood event (Figure 7, middle[1]). This appears to reflect a reduced transport capacity after the January 2009 flood event peak compared with after the smaller February 1996 flood event. Accordingly, the analysis predicted a substantially longer time to flush out all of the accumulated sediment (Figure 7, bottom).

[1] Sediment data are not plotted below RM 110.25 because the time steps in the DEIS simulation of the January 2009 event changed from hourly to daily for the last two days of the reservoir drawdown period, which resulted in different bases for calculating sediment volume. This had no effect on conclusions.

Figure 6
Estimated Quantity of Sediment Deposited Between HEC-RAS Model Transects While the Temporary Reservoir is Filling During FRE Operations Simulated for the February 1996 Flood Event (top), Corresponding Number of Days the Riverbed is Inundated by Impounded Water and Then Flush the Initial Deposit of Fine Sediment (middle), and Cumulative Number of Days the Riverbed Is Inundated by Fine Sediment As It Is Progressively Flushed Downstream (bottom).

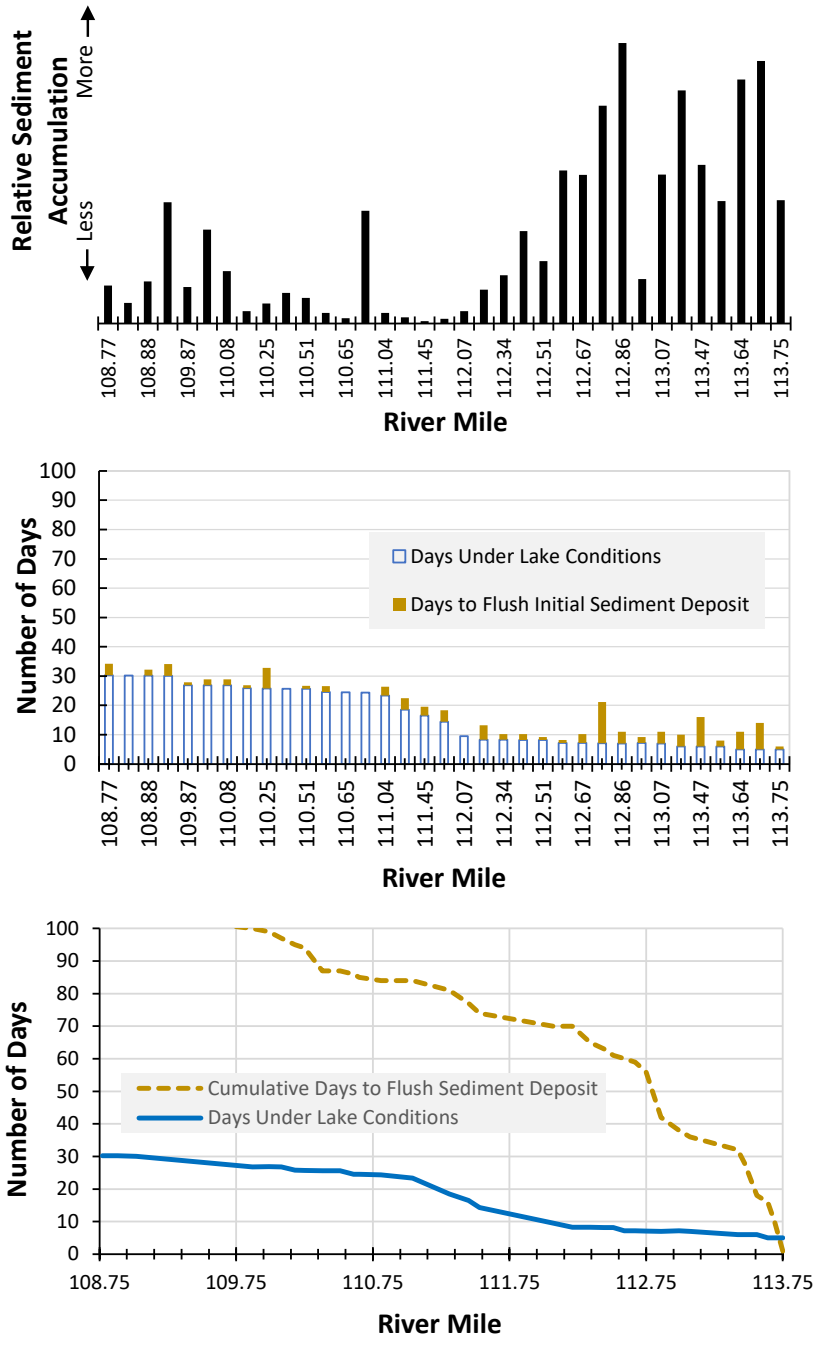

Figure 7
Estimated Quantity of Sediment Deposited Between HEC-RAS Model Transects While the Temporary Reservoir Is Filling During FRE Operations Simulated for the January 2009 Flood Event (top), Corresponding Number of Days the Riverbed Is Inundated by Impounded Water and to Then Flush the Initial Deposit of Fine Sediment (middle), and Cumulative Number of Days the Riverbed Is Inundated by Fine Sediment As It Is Progressively Flushed Downstream (bottom). See Text Footnote Regarding Data Omitted from Middle Graph.

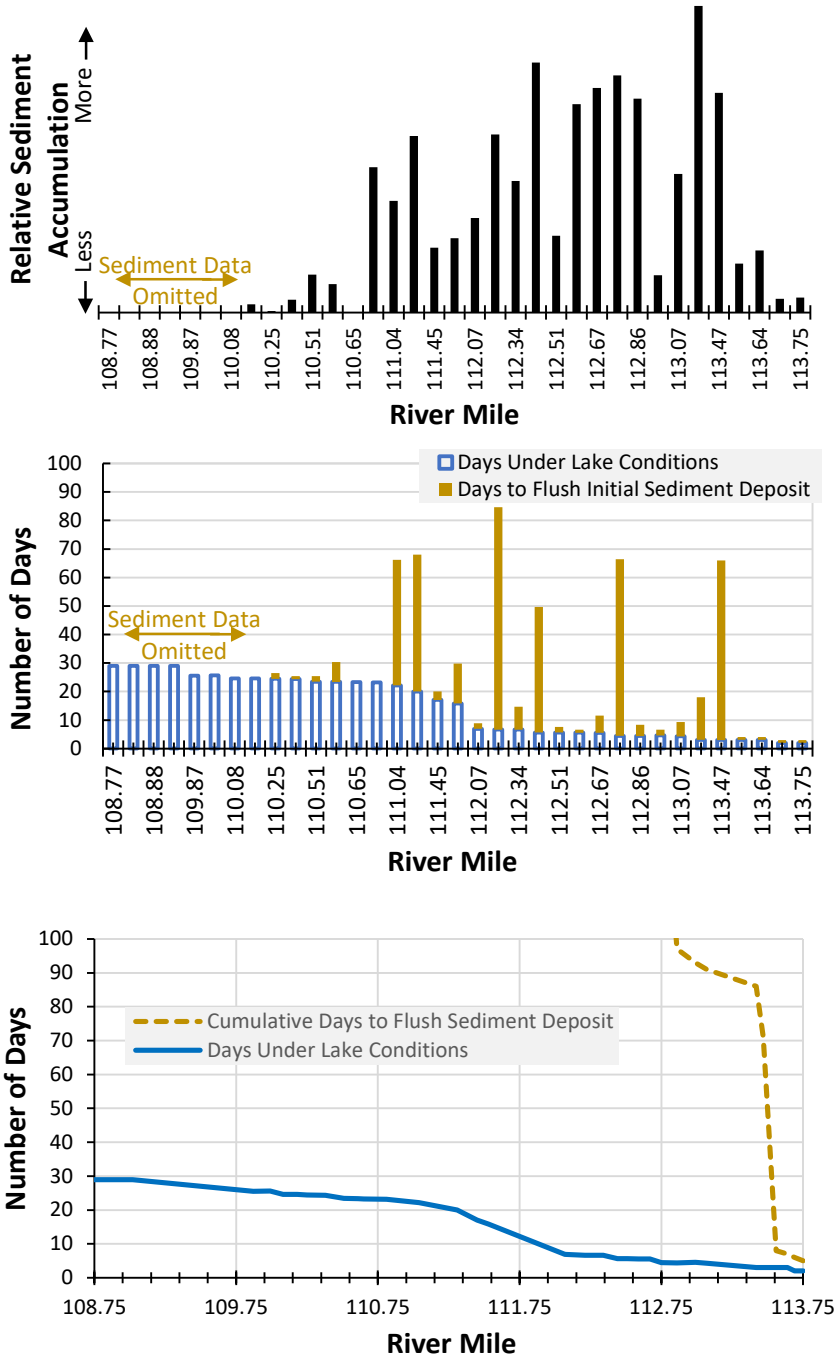

Discussion

The results of the analyses described above can help more specifically identify corresponding impacts and appropriate mitigation measures to avoid or minimize them. The results of this analysis can be compared with studies of sediment flushing in other systems, and against biological habitat requirements to provide more specific context and details regarding potential effects of FRE operations than were presented in the DEISs, where hypothesized impacts of fine sediments were too generalized with respect to describing quantities, timing, duration, and location of impact. As a consequence, the specificity needed to describe and quantify impacts on habitat and ecological functions at the level of species (i.e., Chinook salmon) and life stage (spawning and incubation) was not available from the DEISs. Accordingly, additional information is required to identify appropriate, specific, and actionable mitigation measures to address potential impacts.

Comparison with Other Studies

According to the review by Kondolf et al. (2014), drawdown flushing of reservoirs can be an effective strategy for fine sediment management in systems like the upper Chehalis River basin where the channel is steep and confined with high energy flows, flows are strongly seasonal, the size of the reservoir is relatively small, and the capacity to drain quickly is high. Kondolf et al. (2014) noted the approach is most effective when the ratio of storage volume to mean annual flow volume has been noted to be around 4 percent or less in general, although the critical value for a project will depend on the size of gates relative to high flows. The ratio for the proposed FRE project is around 15 percent, which is indicative that not all accumulated fine sediment might be flushed out before the summer low flow season. Sumi (2008) distinguished between long-term and short-term trapping of sediments and implied the latter to be a key criterion for gate design. With appropriate design, deposition of clays and silts may be minimized so that delayed downstream turbidity impacts may also be minimized. It may be more difficult to design for complete flushing of sand; however, the efficiency of which will depend on the length of time of impoundment and the flushing flow capacity designed for.

A Pacific Northwest analog case study exists for the Fall Creek reservoir located in the Willamette Basin in Oregon, which is managed by the USACE and is located on a high-gradient, bedrock river similar to the upper reaches of the Chehalis River where the proposed FRE facility may be located. The dam is 55 meters (180 feet) high. The reservoir is fully drawn down once annually to provide fish passage for juvenile salmonids, during which time accumulated fine sediments are also flushed (Gibson and Crain 2019; Hamilton et al. 2022). Studies have been performed of the effects of drawdowns on sediment transport characteristics downstream and within the reservoir. For example, six bedload samples were collected downstream of the dam during the first three days of a 6-day drawdown conducted in December 2012 (Schenk and Bragg 2014). Fine to medium sand-sized particles constituted an average of 71 percent of the bedload samples (Schenk and Bragg 2014). The D_{50} of the six bedload samples was less than 0.2 mm, and very little gravel-sized material was present (Schenk and Bragg 2014). As indirect corroboration of the calculations described above for the FRE operations, Schenk and Bragg (2021)

noted subsequently that much of the stored sediment was flushed in the early years of the consecutive drawdowns, indicating that long-term buildup may be precluded where there is sufficient transport capacity. Overall, downstream effects on water quality have not been found to be deleterious to fish, and appear to be mitigatable (Hamilton et al. 2022).

Removal of Marmot Dam on the Sandy River in Oregon presents an extreme case study with impacts that would be substantially greater than can be expected with FRE operations. After the initial, rapid erosion of the gravel and sand deposit that had built up over time behind the dam, suspended sediment levels increased minimally afterward (Cui et al. 2014). Sand materials were transported rapidly through the bedrock gorge downstream and dispersed in the alluvial valley below. Detection of effects related to release of reservoir sediment was challenging in areas of sand deposition because of the high background supply of sand in the river and sediments were transported tens of kilometers downstream to outside of the system (Major et al. 2012; Grant and Lewis 2015).

Biological Implications

Given the projected time frames before accumulated fine sediment is flushed, the primary biological impact of FRE operation on Chinook salmon spawning habitat quality is concluded to be related to incubation conditions as affected by intragravel flow velocities. Temporary fine sediment accumulation and transition to a quiescent lake environment at locations where there is negligible sufficiently oxygenated groundwater flow exchange would be expected to be associated with reduced or zero hydraulic gradients through redds that were constructed in a fluvial environment, and thus reduced delivery of dissolved oxygen and removal of metabolic waste products (Danner 2008; Malcolm et al. 2008). At locations where there is intragravel flow from groundwater, lake level has been noted to be inversely related to intragravel flow velocity (e.g., Decker-Hess and Clancey 1984), such that intragravel conditions could be expected to become less suitable at higher levels of impoundment.

Washload (ultrafine sediment) is not expected to significantly affect survival to emergence in a temporary reservoir because it takes longer to settle and accumulate in significant quantities on the inundated riverbed, and washload-sized particles are rapidly re-entrained at very low velocities (Kondolf et al. 2014). For example, in the case of the Fall Creek drawdown operations, fine sediment concentrations downstream of the dam were composed of almost all suspended silt and clay (Gibson and Crain 2019).

Entombment effects on alevin emergence survival are expected to be increasingly significant moving downstream of Fisk Falls given the estimated residence times of accumulated fine sediments on top of redds, although the shorter length of time for evacuation within the first mile or two below Fisk Falls could be associated with minor entombment effects in that reach. In any case, the effect of potential incubation mortality appears to be the dominant mechanism to address in most of the reach experiencing temporary inundation.

Assessing the potential for primary biological impact accordingly involves two aspects: (i) the water quality conditions within the redd in terms of dissolved oxygen and carbon dioxide concentrations (Danner 2008), and (ii) the length of time that conditions are adverse. Carter's (2005) review of experimental studies indicated that Chinook alevins may show initial signs of stress when dissolved oxygen concentrations fall below approximately 8 milligrams (mg)/Liter (L), and that when levels fall below 6.5 mg/L, embryos become affected at large. Acute mortality was noted at levels around 3 mg/L and below, although at levels around 2.5 mg/L. survival of a large percentage of embryos was still possible albeit with a 6-9 day delay in hatching. However, there can be reduced growth and development rates and depressed survival after hatching. Complete mortality was noted at concentrations of 1.6 mg/L at temperatures between 9.5-11 °C. Salmonid mortality was noted to begin occurring when dissolved oxygen concentrations are below 3 mg/L for periods longer than 3.5 days. Water velocity was noted to be a mitigating factor, where faster intragravel velocities were associated with fewer abnormalities and higher survival rates. The behavior of alevins to move through the gravel to locations with more favorable dissolved oxygen levels was noted.

In subsequent studies, Geist et al. (2006) found that fall Chinook salmon embryos in Hells Canyon of the Snake River took 6 to 10 days longer to hatch when dissolved oxygen levels were around 4 mg/L than at saturation (≥9.6 mg/L), and up to 24 days longer to reach emergence. Mean fork length of alevins decreased and abnormalities increased with decreasing dissolved oxygen concentrations down to 4 mg/L. Overall mortality was not affected at 4 mg/L, although it was considered likely that alevins with abnormalities would be less fit to survive post-emergence. Whitlock (2013) found that groundwater flow and downwelling were more influential on survival than substrate character in Lake Pend Oreille shoreline spawning habitat, and that intragravel dissolved oxygen levels below 4 mg/L were associated with poor to zero survival. Jeric (1996) sampled dissolved oxygen levels in incubation baskets over a range of water depths down to 20 meters in Flaming Gorge Reservoir and found levels decreased with increasing depth. Survival to emergence of kokanee salmon (*O. nerka*) also decreased with increasing depth and were mostly zero percent at depths greater than about 18 meters, and ranged between approximately 0-28 percent at dissolved oxygen levels around 4 mg/L.

It is inferred accordingly that deeper water is associated with lower intragravel velocity and dissolved oxygen concentrations, but the risk of mortality is highly dependent on site-specific groundwater flow gradients. Work by Shumway (1960), Coble (1961), and Silver et al. (1963) indicate that survival is possible at very low intragravel flow velocities, albeit potentially lower than under normal conditions. The weight of evidence above is that as long as oxygen is delivered at levels above 2.5 mg/L (which is not atypical of groundwater quality) and metabolic wastes are transported away, developing embryos and alevins may be able to survive prolonged inundation and fine sediment deposition during FRE operation, and resume pre-flood development rates when throughflow is restored, and can emerge after the fine sediments are removed subsequently. However, whether the emerging alevins are sufficiently fit to then survive in the water column environment is uncertain, and appears to depend on

the level of dissolved oxygen in the groundwater. At locations where groundwater flow gradients are negligible during impoundment, survival should be expected to be negligible.

The above references do not directly indicate the length of time that a developing embryo could withstand reduced dissolved oxygen levels in redds situated in deep, quiescent water. Anecdotal hatchery operations design experience within Kleinschmidt indicates that mortality in egg trays with high densities of incubating embryos may begin to occur within a few hours up to two days when the water supply is interrupted. This is unlikely to be representative of conditions within a natural redd constructed in the inundation zone; however, where egg densities are lower, and a time-varying hydraulic gradient may exist as the water level rises and falls (i.e., as surface water is driven into groundwater during rising stages and then the flow direction reverses during falling stages). The worst case would be that all redds constructed in the impoundment zone would be inundated and covered with fine sediment for long enough without sufficient intragravel flow that survival to emergence and then to smolt stage (as affected by developmental delay and/or abnormalities) becomes negligible for the affected year of spawning. What is 'long enough' for the given site- and operational-specific conditions is uncertain at present.

Implications for Discerning Effects of FRE Operations

The results depicted in Figure 6 and Figure 7 suggest that it does not appear possible to avoid impacts to spawning habitat quality following the operation modeled in the DEISs. The primary Chinook salmon spawning reach in the first two miles below Fisk Falls is predicted to be susceptible to relatively more fine sediment deposition initially, but also to clear of deposited fine sediments most quickly upon resumption of river flow as the temporary impoundment drains. The results imply that effects of FRE operations on survival to emergence during extreme flood events within the potentially impounded reach is smaller within the first two miles below Fisk Falls than farther downstream. These two miles are where spawning habitat is most likely to be found and where accordingly most historic Chinook salmon spawning has occurred in the basin above Pe Ell. Effects increase moving in the downstream direction towards the FRE location. Whether effects are significant at the population level for the Chehalis River Chinook salmon overall is uncertain given that most spawning occurs in tributaries downstream of the South Fork (Litz et al. 2023).

The modeling results suggest that the duration of fine sediments covering redds may be longer for more frequent flood flows. While a larger magnitude, less frequent flood event may transport more sediment during the period the temporary reservoir is filling, the modeling results imply it may also be associated with greater transport capacity after the peak to flush out sediment that has accumulated in a shorter time than would occur during a more frequent, smaller event. Moreover, a faster flow release rate than assumed in the DEISs can be expected to decrease the duration of coverage by fine sediments. The modeling results suggest that it may be feasible to manage releases with the goal of avoiding or minimizing effects (e.g., Auel et al. 2016).

It is possible that deposition of certain sizes of fine sediments may be reduced during filling by outflows sustaining a turbidity current that flows along the bottom to the open outlet gates (Kondolf et al. 2014; Sumi 2015), and that a turbidity current near the bottom could help maintain an intragravel flow gradient while a location is experiencing lake conditions. These potential outcomes could be assessed for feasibility through more detailed analysis that also integrates and evaluates downriver flood management objectives and constraints (if any) posed by landslide risk and debris management.

The possibility also exists for potential effects of fine sediment deposition to be offset by scour mortality that would occur otherwise during extreme events, given the extremely high transport capacity in the channel and reach scale limitations on gravel availability for spawning (Light and Herger 1994; DeVries 2008; Kleinschmidt 2024).

References

Auel, C., S.A. Kantoush, and T. Sumi, 2016. Positive effects of reservoir sedimentation management on reservoir life: Examples from Japan. Pages 4-11 to 4-20 in: International Symposium on "Appropriate technology to ensure proper Development, Operation and Maintenance of Dams in Developing Countries", Johannesburg, South Africa. May.

Carter, K., 2005. The effects of dissolved oxygen on steelhead trout, coho salmon, and chinook salmon biology and function by life stage. California Regional Water Quality Control Board, North Coast Region, 10.

Coble, D.W., 1961. Influence of water exchange and dissolved oxygen in redds on survival of steelhead trout embryos. Transactions of the American Fisheries Society, 90(4): 469-474.

Corps (United States Army Corps of Engineers), 2020. Chehalis River Basin Flood Damage Reduction Project: NEPA Environmental Impact Statement. Seattle District. September.

Corps (United States Army Corps of Engineers), 2023. HEC-RAS 2D sediment technical reference manual. Available online.

Cui, Y., J.K. Wooster, C.A. Braudrick, and B.K. Orr, 2014. Lessons learned from sediment transport model predictions and long-term post-removal monitoring: Marmot Dam removal project on the Sandy River in Oregon. Journal of Hydraulic Engineering, 140(9), p.04014044.

Danner, G.R., 2008. Salmonid embryo development and pathology. Pages 37-58 in: Sear, D. and DeVries, P. [Eds.]. Salmonid spawning habitat in rivers: Physical controls, biological responses, and approaches to remediation. American Fisheries Society Symposium 65. Bethesda MD.

Decker-Hess, J., and P. Clancey. 1984. Impacts of Water Level Fluctuations on Kokanee Reproduction in Flathead Lake, 1984 Annual Report (No. DOE/BP-39641-1). Montana Department of Fish, Wildlife and Parks.

DeVries, P., 2008. Bed disturbance processes and the physical mechanisms of scour in salmonid spawning habitat. Pages 121-147 in Sear, D.A., and P. DeVries, editors. Salmonid spawning habitat in rivers: Physical controls, biological responses, and approaches to remediation. American Fisheries Society, Symposium 65, Bethesda, Maryland.

Ecology (Washington State Department of Ecology), 2020. February 27. State Environmental Policy Act Draft Environmental Impact Statement: Proposed Chehalis River Basin Flood Damage Reduction Project. Publication No.: 20-06-002.

Engelund, F., and E. Hansen, 1967. A monograph on sediment transport in alluvial streams. Teknisk Forlag, Skelbækgade 4, Copenhagen V, Denmark.

Ferguson, J., N. Kendall, and R. Vadas, Jr., 2017. Literature review of the potential changes in aquatic and terrestrial systems associated with a seasonal flood retention only reservoir in the Upper Chehalis Basin. Memorandum to WDFW. March.

Geist, D.R., C.S. Abernethy, K.D. Hand, V.I. Cullinan, J.A. Chandler, and P.A. Groves, 2006. Survival, development, and growth of fall Chinook salmon embryos, alevins, and fry exposed to variable thermal and dissolved oxygen regimes. Transactions of the American Fisheries Society, 135(6), pp.1462-1477.

Gibson, S., and J. Crain, 2019. Modeling Sediment Concentrations during a Drawdown Reservoir Flush: Simulating the Fall Creek Operations with HEC-RAS. U.S. Army Corps of Engineers. ERDC/TN RSM-19-7. August.

Grant, G.E., and S.L. Lewis, 2015. The remains of the dam: what have we learned from 15 years of US dam removals? Pages 31-35 in: In Engineering Geology for Society and Territory-Volume 3: River Basins, Reservoir Sedimentation and Water Resources. Springer International Publishing.

Hamilton, S.K., C.A. Murphy, S.L. Johnson, and A. Pollock, 2022. Water quality ramifications of temporary drawdown of Oregon reservoirs to facilitate juvenile Chinook Salmon passage. Lake and Reservoir Management, 38(2), pp.165-179.

Hill, A. (Anchor QEA), and L. Karpack (Watershed Science & Engineering), 2019. Memorandum to: Bob Montgomery, Anchor QEA. Regarding: Chehalis River Basin Hydrologic Modeling. February 28, 2019.

Jeric, R.J., 1996. Physical factors influencing survival to emergence and time of emergence of shoreslope-spawned kokanee salmon in Flaming Gorge Reservoir, Utah-Wyoming. MS Thesis, Utah State University.

Kleinschmidt (Kleinschmidt Associates), 2024. Chehalis River FRE facility mitigation: Evaluation of potential coarse sediment transport impacts of FRE operations on Chinook Salmon spawning habitat. Technical memorandum prepared for Chehalis River Basin Flood Control Zone District. February.

Kondolf, G.M., Y. Gao, G.W. Annandale, G.L. Morris, E. Jiang, J. Zhang, Y. Cao, P. Carling, K. Fu, Q. Guo, R. Hotchkiss, C. Peteuil, T. Sumi, H. Wang, Z. Wang, Z. Wei, B. Wu, C. Wu, and C.T. Yang, 2014. Sustainable sediment management in reservoirs and regulated rivers: Experiences from five continents. Earth's Future, 2, doi:10.1002/2013EF000184.

Light, J., and L. Herger, 1994. Appendix F: Chehalis headwaters watershed analysis fish habitat assessment. Weyerhaeuser Company. Available: https://fortress.wa.gov/dnr/protectionsa/ApprovedWatershedAnalyses.

Litz, M., T. Seamons, J. Winkowski, D. West, and D. Olson, 2023. Do juvenile Chinook Salmon face a predation gauntlet in the Chehalis River? Presentation at Recreation and Conservation Office Salmon Recovery Conference, Vancouver, Washington. April.

Major, J.J., J.E. O'Connor, C.J. Podolak, M.K. Keith, G.E. Grant, K.R. Spicer, S. Pittman, H.M. Bragg, J.R. Wallick, D.Q. Tanner, A. Rhode, and P.R. Wilcock, 2012. Geomorphic response of the Sandy River, Oregon, to removal of Marmot Dam: U.S. Geological Survey Professional Paper 1792, 64 p.

Malcolm, I., S.M. Greig, A.F. Youngson, and C. Soulsby, 2008. Hyporheic influences on salmon embryo survival and performance. Pages 225-248 in: Sear, D. and DeVries, P. [Eds.]. Salmonid spawning habitat in rivers: Physical controls, biological responses, and approaches to remediation. American Fisheries Society Symposium 65. Bethesda, Maryland.

Parker, G., C.M. Toro-Escobar, M.P. Ramey, and S. Beck, 2003. Effect of floodwater extraction on mountain stream morphology. Journal of Hydraulic Engineering, 129(11), pp.885-895.

Phinney, L.A., P. Bucknell, and R.W. Williams, 1975. A catalog of Washington streams and salmon utilization, Volume 2: Coastal regions. Washington Department of Fisheries.

Ronne L., N. VanBuskirk, and M. Litz, 2020. Spawner Abundance and Distribution of Salmon and Steelhead in the Upper Chehalis River, 2019 and Synthesis of 2013-2019, FPT 20-06 Washington Department of Fish and Wildlife, Olympia, Washington.

Schenk, L., and H. Bragg, 2014. Assessment of Suspended-Sediment Transport, Bedload, and Dissolved Oxygen during a Short-Term Drawdown of Fall Creek Lake, Oregon, Winter 2012-13. U.S. Geological Survey, Open File Report 2014-1114.

Schenk, L., and H. Bragg, 2021. Sediment transport, turbidity, and dissolved oxygen responses to annual streambed drawdowns for downstream fish passage in a flood control reservoir. Journal of Environmental Management, 295, p.113068.

Shumway, D.L., 1960. The influence of water velocity on the development of salmonid embryos at low oxygen levels. M.S. Thesis, Oregon State College. Corvallis, Oregon.

Silver, S.J., C.E. Warren, and P. Doudoroff, 1963. Dissolved oxygen requirements of developing steelhead trout and chinook salmon embryos at different water velocities. Transactions of the American Fisheries Society, 92(4): 327-343.

Sumi, T., 2008. Designing and Operating of Flood Retention 'Dry' Dams in Japan and USA. In: Wang, S. Y. (Ed): ICHE 2008. Proceedings of the 8th International Conference on Hydro-Science and Engineering, September 9-12, 2008, Nagoya, Japan. Nagoya: Nagoya Hydraulic Research Institute for River Basin Management.

Sumi, T., 2015. Comprehensive reservoir sedimentation countermeasures in Japan. Pages 1-20 in: International Workshop on Sediment Bypass Tunnels. Laboratory of Hydraulics, Hydrology and Glaciology, ETH Zurich. April.

WG and Anchor (Watershed GeoDynamics and Anchor QEA, LLC), 2017. Chehalis Basin Strategy: Geomorphology, Sediment Transport, and Large Woody Debris Report – Reducing Flood Damage and restoring Aquatic Species Habitat. June.

Whitlock, S.L., 2013. Kokanee spawning ecology and recruitment response to water level management in Lake Pend Oreille, Idaho. M.S. Thesis, University of Idaho, Moscow Idaho.

ATTACHMENT 1

EXAMPLE CALCULATION OF SEDIMENT DEPOSITION VOLUME AND SUBSEQUENT EVACUATION TIME

River Mile 113.07					
Date & Time	Chan. Vel. (ft/s)	Chan. Bed Shear Stress (lb/sq ft)	W.S. Elev (ft)	Sed. Transport per Timestep (lb)	Comments
1/8/09 0:00	3.37	0.75	553.4	1,666,314	Unimpeded flow increases during rising limb of hydrograph. **(A)**
1/8/09 1:00	3.45	0.78	553.6	1,852,189	
1/8/09 2:00	3.57	0.81	553.9	2,098,791	
1/8/09 3:00	3.81	0.89	554.4	2,753,215	
1/8/09 4:00	3.99	0.93	555.1	3,225,339	
1/8/09 5:00	4.28	1.03	555.7	4,325,622	
1/8/09 6:00	4.57	1.15	556.2	5,818,142	
1/8/09 7:00	4.8	1.24	556.5	7,186,546	
1/8/09 8:00	5.07	1.35	557.0	9,107,974	
1/8/09 9:00	5.31	1.46	557.5	11,236,305	Backwater effects occur as water begins to be impounded downstream of the transect. **(B)**
1/8/09 10:00	5.41	1.5	557.7	12,146,093	
1/8/09 11:00	5.48	1.53	557.8	12,838,180	
1/8/09 12:00	5.59	1.57	558.0	13,886,036	
1/8/09 13:00	5.65	1.6	558.2	14,594,259	
1/8/09 14:00	5.66	1.61	558.2	14,783,486	
1/8/09 15:00	5.63	1.6	558.1	14,491,120	
1/8/09 16:00	5.66	1.61	558.2	14,783,486	
1/8/09 17:00	5.66	1.61	558.2	14,783,486	
1/8/09 18:00	5.71	1.63	558.3	15,327,058	
1/8/09 19:00	5.82	1.68	558.5	16,661,538	
1/8/09 20:00	5.88	1.7	558.6	17,311,441	
1/8/09 21:00	5.94	1.73	558.9	18,136,239	
1/8/09 22:00	5.87	1.68	559.0	16,949,048	

River Mile 113.07						
Date & Time	Chan. Vel. (ft/s)	Chan. Bed Shear Stress (lb/sq ft)	W.S. Elev (ft)	Sed. Transport per Timestep (lb)	Cum. Sed. Transport (lb)	Comments
1/8/09 23:00	5.72	1.57	559.4	14,539,408		
1/9/09 0:00	5.35	1.34	560.2	10,029,285		
1/9/09 1:00	4.98	1.12	561.4	6,640,349		
1/9/09 2:00	4.5	0.88	562.9	3,776,193		
1/9/09 3:00	4.03	0.67	564.7	2,011,998		
1/9/09 4:00	3.44	0.47	566.7	861,329		
1/9/09 5:00	2.87	0.32	568.5	336,817		
1/9/09 6:00	2.46	0.22	570.3	141,062		
1/9/09 7:00	2.1	0.16	571.9	63,756		
1/9/09 8:00	1.82	0.12	573.5	31,104		
1/9/09 9:00	1.58	0.09	575.0	15,226		
1/9/09 10:00	1.36	0.06	576.3	6,141		
1/9/09 11:00	1.22	0.05	577.5	3,759		
1/9/09 12:00	1.08	0.04	578.6	2,108		
1/9/09 13:00	0.96	0.03	579.6	1,082		
1/9/09 14:00	0.85	0.02	580.5	462		
1/9/09 15:00	0.78	0.02	581.3	389		
1/9/09 16:00	0.7	0.02	582.1	313		
1/9/09 17:00	0.64	0.01	582.8	93	38,460,872	Reservoir has reached the transect and water levels quickly rise due to reservoir filling operations. Sediment accumulates at the upstream end of the reservoir. **(C)**
1/9/09 18:00	0.58	0.01	583.5	76		
1/9/09 19:00	0.54	0.01	584.1	66		
1/9/09 20:00	0.51	0.01	584.7	59		
1/9/09 21:00	0.47	0.01	585.3	50		
1/9/09 22:00	0.43	0.01	585.8	42		
1/9/09 23:00	0.41	0.01	586.3	38		
1/10/09 0:00	0.23	0	589.8	0		
1/11/09 0:00	0.16	0	583.7	0		
1/12/09 0:00	0.23	0	573.7	0		
1/13/09 0:00	0.38	0.01	563.7	783		Stagnant water covers the transect as the reservoir water level reaches its maximum elevation above the channel bottom. **(D)**
1/14/09 0:00	1.17	0.09	553.8	200,379		
1/15/09 0:00	2.36	0.49	551.3	10,357,014		
1/16/09 0:00	2.21	0.46	551.1	8,261,097		
1/17/09 0:00	2.14	0.44	550.9	7,246,412		
1/18/09 0:00	2.07	0.43	550.8	6,550,279		
1/19/09 0:00	2.01	0.42	550.7	5,961,870	38,577,050	Reservoir recedes allowing a return to unimpeded flow. Sediment transported downstream. **(E)**

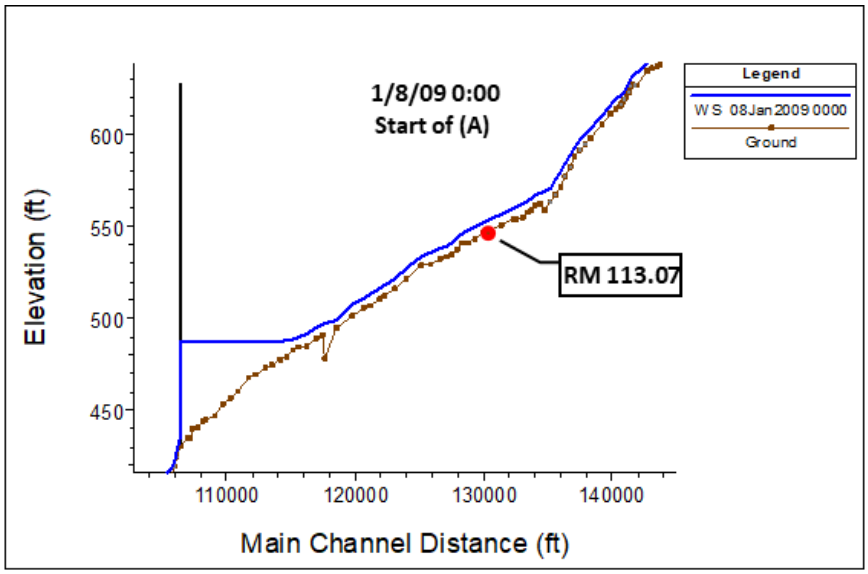
1/8/09 0:00
Start of (A)
RM 113.07
Legend
WS 08Jan2009 0000
Ground
Elevation (ft)
600
550
500
450
110000
120000
130000
140000
Main Channel Distance (ft)

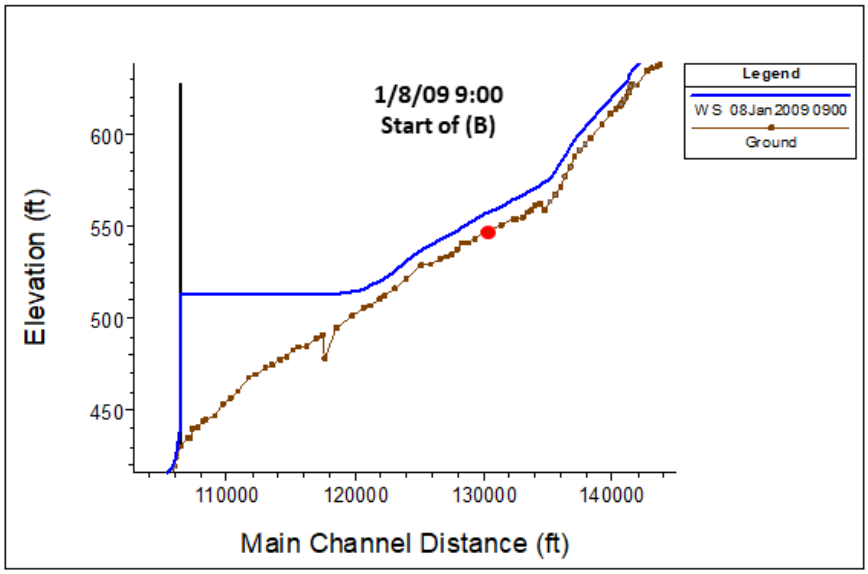
1/8/09 9:00
Start of (B)
Legend
WS 08Jan2009 0900
Ground
Elevation (ft)
600
550
500
450
110000
120000
130000
140000
Main Channel Distance (ft)

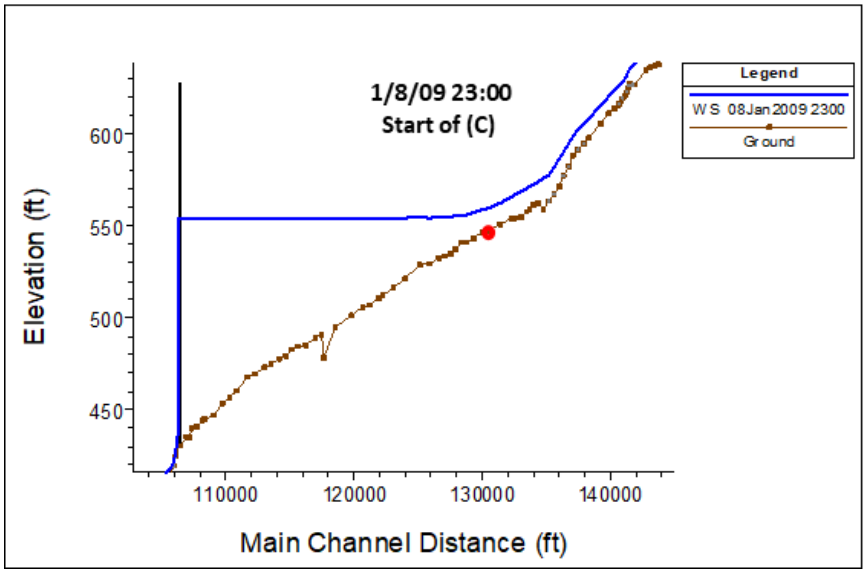
1/8/09 23:00
Start of (C)
Legend
WS 08Jan2009 2300
Ground
Elevation (ft)
600
550
500
450
110000
120000
130000
140000
Main Channel Distance (ft)

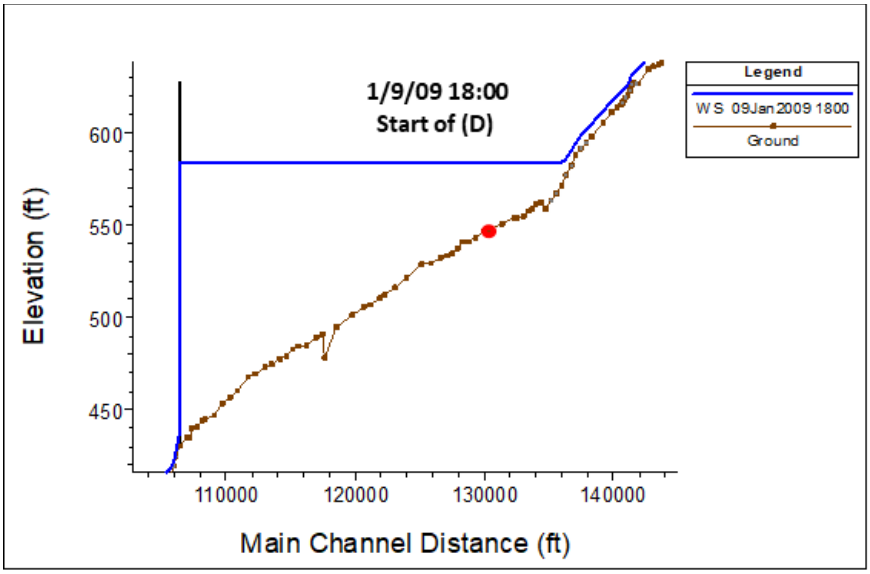
1/9/09 18:00
Start of (D)
Legend
WS 09Jan2009 1800
Ground
Elevation (ft)
600
550
500
450
110000
120000
130000
140000
Main Channel Distance (ft)

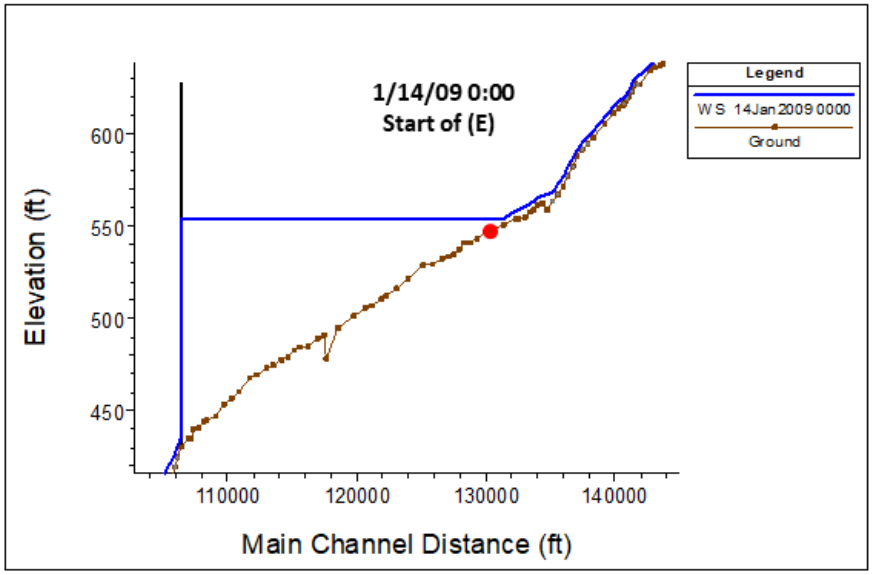
1/14/09 0:00
Start of (E)
Legend
WS 14Jan2009 0000
Ground
Elevation (ft)
600
550
500
450
110000
120000
130000
140000
Main Channel Distance (ft)

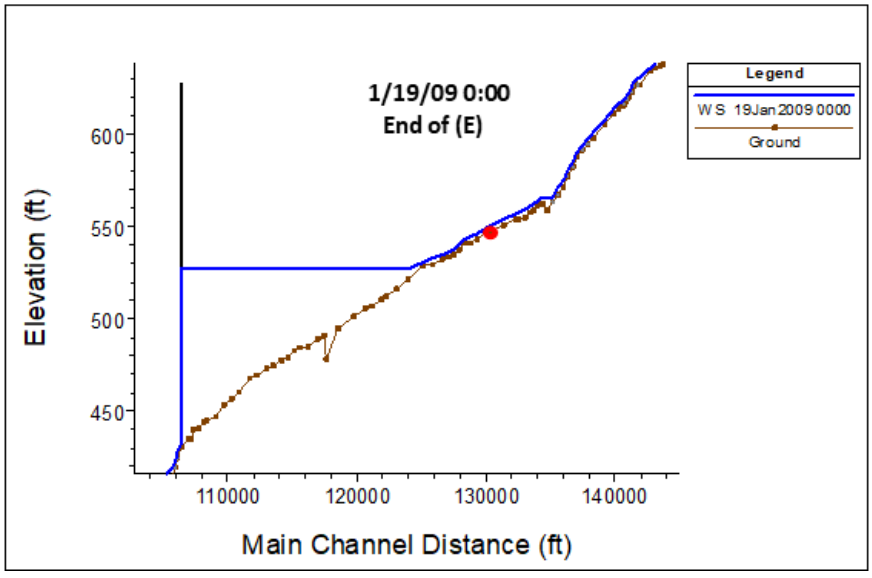
1/19/09 0:00
End of (E)
Legend
WS 19Jan2009 0000
Ground
Elevation (ft)
600
550
500
450
110000
120000
130000
140000
Main Channel Distance (ft)